İZMİR KÂTİP ÇELEBİ ÜNİVERSİTESİ
2010
GRADUATE SCHOOL OF NATURAL AND APPLIED SCIENCES

Control of Robotic Systems Used for Support in Cochlear Microrobot Operations

Submitted to the Graduate School of Natural and Applied Sciences in partial fulfillment of the requirements for the degree of

Master of Science

in Robotics Engineering

by

Goncagül Karayaman

ORCID 0000-0003-2570-6440

July, 2022

This is to certify that we have read the thesis **Control of Robotic Systems Used for Support in Cochlear Microrobot Operations** submitted by **Goncagül Karayaman**, and it has been judged to be successful, in scope and in quality, at the defense exam and accepted by our jury as a MASTER'S THESIS.

APPROVED BY:

Advisor: **Assoc. Prof. Dr. Barış Bıdıklı**
İzmir Kâtip Çelebi University

Committee Members:

Prof. Dr. Enver Tatlıcıoğlu
Ege University

Assoc. Prof. Dr. Erkin Gezgin
İzmir Kâtip Çelebi University

Date of Defense: July 21, 2022

Declaration of Authorship

I, **Goncagül Karayaman**, declare that this thesis titled **Control of Robotic Systems Used for Support in Cochlear Microrobot Operations** and the work presented in it are my own. I confirm that:

- This work was done wholly or mainly while in candidature for the Master's degree at this university.
- Where any part of this thesis has previously been submitted for a degree or any other qualification at this university or any other institution, this has been clearly stated.
- Where I have consulted the published work of others, this is always clearly attributed.
- Where I have quoted from the work of others, the source is always given. This thesis is entirely my own work, with the exception of such quotations.
- I have acknowledged all major sources of assistance.
- Where the thesis is based on work done by myself jointly with others, I have made clear exactly what was done by others and what I have contributed myself.

Date: 21.07.2022

Control of Robotic Systems Used for Support in Cochlear Microrobot Operations

Abstract

The rapid development of robot technology has started to be emphasized medical robotics increasingly. The potential of robotic systems to facilitate the work of healthcare workers, minimize human errors, restore function to lost limbs, and enable operations that cannot be performed due to distance or other factors have made this field increasingly popular.

Surgical robotics applications are the trend subfield of medical robotics. In these applications, it is aimed to reach the desired task with certain precision and accuracy. Therefore, performance of the control system is very crucial for the efficiency of robotic systems used in medical applications. Within the scope of this study, control of robotic systems used as supportive systems in surgical cochlear microrobot operations is studied.

This study is carried out on two different robotic systems serving identical purpose, one of which contains dual serial robot manipulators that must work in coordination and the other one contains a parallel robot manipulator, which are planned to be used as supportive systems in surgical cochlear microrobot operations. Two robust adaptive nonlinear controllers are designed for each of these robotic systems. One of the mentioned control designs is realized in the joint space, while the other one is designed in task space. Lyapunov based arguments are utilized for the theoretical analysis of designed controllers. For the performance demonstration of the designed

controllers simulation and experimental studies are utilized. Dynamic models of robotic systems, whose prototypes produced within the scope of the project in which this study is included, are needed for the simulation studies. To meet this necessity, dynamic modeling of mentioned robotic systems is realized via Newton-Euler and the Lagrangian formulations as a part of this study. After demonstrating the performance of the designed controllers in the simulation environment by using these dynamic models, experimental verification is realized by applying the designed controllers to prototypes of robotic systems.

Keywords: Robotic systems, cochlear microrobot operations, nonlinear control, joint space control, task space control, robust adaptive control.

Koklear Mikrorobot Operasyonlarında Destek için Kullanılan Robotik Sistemlerin Kontrolü

Öz

Robot teknolojisinin hızlı gelişimi ile birlikte medikal robotiğe ağırlık verilmeye başlanmıştır. Robotik sistemlerin sağlık çalışanlarının işini kolaylaştırma, insan hatalarını en aza indirme, işlevini yitirmiş uzuvlara işlev kazandırma, mesafe ya da başka etmenlerden dolayı gerçekleştirilemeyecek operasyonları mümkün kılma gibi potansiyelleri bu alanın popülaritesini arttırmıştır.

Cerrahi robotik uygulamaları medikal robotiğin popüler alt alanıdır. Bu uygulamalarda istenilen göreve belirli bir hassasiyet içerisinde ulaşılması hedeflenir. Bu nedenle, medikal uygulamalarda kullanılan robotik sistemlerin verimliliği için denetim sisteminin başarımı oldukça önemlidir. Bu çalışma kapsamında, cerrahi koklear mikrorobot operasyonlarında destekleyici olarak kullanılan robotik sistemlerin denetimi ile ilgilenilmiştir.

Bu çalışma cerrahi koklear mikrorobot operasyonlarında yardımcı sistem olarak kullanılması planlanan, biri koordine çalışması gereken iki adet seri robot manipülatör diğeri ise paralel bir robot manipülatör içeren aynı amaca hizmet eden iki farklı robotik sistem üzerinden yürütülmektedir. Söz konusu robotik sistemlerin her biri için iki dayanıklı uyarlamalı doğrusal olmayan denetleyici tasarlanmıştır. Bahsedilen denetim tasarımlarından biri eklem uzayında gerçekleştirilirken diğeri

görev uzayı için tasarlanmıştır. Tasarlanan denetleyicilerin başarım gösterimleri için benzetim ve deney çalışmalarından faydalanılmıştır. Benzetim çalışmaları için, prototipleri bu çalışmanın dahil olduğu proje kapsamında üretilen robotik sistemlerin, dinamik modellerine ihtiyaç duyulmuştur. Bu gerekliliği karşılamak için, bahsedilen robotik sistemlerin dinamik modellemesi, Newton-Euler ve Lagrangian formülasyonları aracılığıyla, çalışmanın bir parçası olarak gerçekleştirilmiştir. Tasarlanan denetleyicilerin başarımları bu dinamik modeler kullanılarak benzetim ortamında gösterildikten sonra, deneysel doğrulama tasarlanan denetleyiciler robotik sistemlerin prototiplerine uygulanalarak gerçekleştirilmiştir.

Anahtar Kelimeler: Robotik sistemler, koklear mikrorobot operasyonları, doğrusal olmayan kontrol, eklem uzayı kontrolü, görev uzayı kontrolü, dayanıklı uyarlamalı kontrol

To my family

Acknowledgment

I would like to express my deepest gratitude to my advisor Assoc. Prof. Dr. Barış BIDIKLI for his valuable support and patience at all steps of my thesis. I would like to thank to Assoc. Prof. Dr. Erkin GEZGİN, whose support I feel at every stage, and to the Medical Robotics Laboratory team that I am happy to be a part of, to the KABA Family and to my precious family who raised me and supported me to the end in every decision.

I would like to express my endless thanks BERKAY BURAK KABA for his understanding, confidence and support.

Additionally, I would like to thank The Scientific and Technological Research Council of Turkey for supporting this thesis by Project No: 218E055.

Table of Contents

List of Figures

List of Tables

List of Abbreviations

CTC	Computed Torque Control
DoF	Degrees of Freedom
LQR	Linear Quadratic Regulator
PD	Proportional-Derivative
PID	Proportional-Integral-Derivative

List of Symbols

θ	Joint Position [Deg]
$\dot{\theta}$	Joint Velocity [Deg/S]
$\ddot{\theta}$	Joint Acceleration [Deg/S^2]
τ	Control Input Torque [Nm]
$M(\theta)$	Inertia Matrix
$C(\theta, \dot{\theta})$	Centripetal-Coriolis Matrix
$G(\theta)$	Gravitational Forces
θ_s	Joint Position of the Serial Manipulator [Deg]
$\dot{\theta}_s$	Joint Velocity of the Serial Manipulator [Deg/S]
$\ddot{\theta}_s$	Joint Acceleration of the Serial Manipulator [Deg/S^2]
x_s	End Effector Position of the Serial Manipulator [Deg]
$\dot{x}_s$	End Effector Velocity of the Serial Manipulator [Deg/S]
$\ddot{x}_s$	End Effector Acceleration of the Serial Manipulator [Deg/S^2]
$J_s(\theta_s)$	Jacobian Matrix of the Serial Manipulator
τ_s	Control Input Torque of the Serial Manipulator [Nm]
$M_s(\theta_s)$	Inertia Matrix of the Serial Manipulator
$C_s(\theta_s, \dot{\theta}_s)$	Centripetal-Coriolis Matrix of the Serial Manipulator
$G_s(\theta_s)$	Gravitational Forces of the Serial Manipulator
$V_s(\theta_s, \dot{\theta}_s)$	Combination of C_s and G_s for the Serial Manipulator
e_e, e_g, e_p	Tracking Errors
r_e, e_v	Auxiliary Errors

$\tilde{\phi}_e, \tilde{\phi}_g$	Compensation Errors
z_e , z_g	Vector of Combined Errors
τ_v	Virtual Control Input
f_{d_e} , f_g	Auxiliary Terms
$Y_e(\theta, ., \ddot{\theta}_d), Y_g(\theta, \dot{\theta}, x_d, \dot{x}_d, \ddot{x}_d)$	Regression Matrices
ϕ_e, ϕ_g	Vectors of Uncertain System Parameters
$\hat{\phi}_e, \hat{\phi}_g$	Adaptive Compensations
α_e , G_e, G_g, G_a, K_p	Positive Definite, Constant, Diagonal Gain Matrices
V_e , V_v, V_g	Lyapunov Functions
$\lambda_{min}(\cdot)$	Minimum Eigenvalue of a Matrix
β_e , β_g	Positive Constant Terms
θ_p	Joint Position of the Parallel Manipulator
$\dot{\theta}_p$	Joint Velocity of the Parallel Manipulator
$\ddot{\theta}_p$	Joint Acceleration of the Parallel Manipulator
x_p	End Effector Position of the Parallel Manipulator
$\dot{x}_p$	End Effector Velocity of the Parallel Manipulator
$\ddot{x}_p$	End Effector Acceleration of the Parallel Manipulator
x_N	New System State
$J_p(\theta_p)$	Jacobian Matrix of the Parallel Manipulator
τ_p	Control Input Torque of the Parallel Manipulator [Nm]
$M_p(\theta_p)$	Inertia Matrix of the Parallel Manipulator
$C_p(\theta_p, \dot{\theta}_p)$	Centripetal-Coriolis Matrix of the Parallel Manipulator
$G_p(\theta_p)$	Gravitational Force of the Parallel Manipulator
$V_p(\theta_p, \dot{\theta}_p)$	Combination of $C_p$and G_p for the Parallel Manipulator
e_f, e_d	Tracking Errors
r_f	Auxiliary Error Term

z_f	Vector of Combined Error
$\tilde{\phi}_f$, $\tilde{\phi}_d$	Compensation Errors
A	An Auxiliary Matrix
α_f, G_f, G_d	Constant Gain Matrices
f_{d_f}, f_{g_d}	Auxiliary Terms
$Y_f(\theta, \dot{\theta}, \dot{\theta}_d, \ddot{\theta}_d)$	Regression Matrix
$Y_d(\theta, \dot{\theta}, x_{N_d}, \dot{x}_{N_d})$	Regression Matrix
ϕ_f, ϕ_d	Vectors of Uncertain System Parameters
$\hat{\phi}_f$, $\hat{\phi}_d$	Adaptive Compensations
V_f, V_d	Lyapunov Functions
β_f	Positive Constant
R	Rotation Matrix
K	Kinetic Energy
U	Potential Energy
Γ_i	Constraint Functions
λ_i	Lagrange Multipliers
$\dot{\rho}_{miu}, \dot{\rho}_{miv}$	Linear Velocities u and v Compenent of i^{th} Link of the Parallel Manipulator
ω_{p_i}	Angular Velocity of the i^{th} Link of the Parallel Manipulator
${}^{i}\hat{Z}_i$	A Unit Vector Pointing Along the i
${}^{i+1}\omega_{s_{i+1}}$	Angular Velocity
${}^{i+1}\dot{\omega}_{s_{i+1}}$	Angular Acceleration
l_s , l_p	Link Lengths
m_s, m_p	Link Masses

Chapter 1

Introduction

Technological developments deeply affect every aspects of life. Robotic systems have been commonly used in many areas with the rapidly developing technology. Medical robotics is one of the most popular among these areas. Robotic systems find a wide area of use in the subfields of medical robotics such as physical therapy, rehabilitation and surgical robotics. Considering that, it facilitates the work of healthcare professionals, minimizes human error, restores basic function to disabled limbs, and can perform operations that cannot be performed due to distance or various reasons, robotic systems that can be used efficiently in medical applications are very important. In addition to these, the desired task can be achieved with certain precision and accuracy with the help of robotic systems. However, supporting the robotic system with a suitable control design is an absolute necessity for an efficient and precise implementation of the mentioned applications. As a result of these, control design for the robotic systems used as supporting systems in medical operations has become an attractive topic in the research area of control.

In [1], a robust controller design was proposed for a robotic tendon actuator developed to use in their implementation to human gait assistance. In [2] a control system design for a robotic assisted surgical operation with haptic feedback was presented. Li et al. proposed a nonlinear disturbance observer based control design that uses a fuzzy logic approach to perform power increasing tasks of a robotic exoskeleton [3]. C. H. Guzman et al. designed a robust generalized proportional integration controller for a robotic system used for hip joint rehabilitation to reduce the physical workload of physiotherapists [4]. In [5], an adaptive controller was proposed to compensate friction for trajectory tracking control of industrial medical robots. In [6], an adaptive fuzzy propotional-integral-derivative (PID) force control

for robot-assisted ultrasound, which is used to improve guidance performance for anatomical or pathological structures of the lung under free breathing, was presented. H. Kolbari et al. introduced an adaptive controller design for a robot-assisted remote surgical intervention [7]. Cortesão et al. developed a task space controller for a robotic-assisted minimally invasive surgical operations with haptic feedback [8]. In [9], a durable H_∞ loop shaping controller was proposed to improve the performance of the robotic system used to improve the oscillation structure of the human lower limb system. In [10], to control a flexible medical robot arms that plays an important role in protecting health workers from disease during the Covid-19 pandemic, three control methods were proposed to investigate the robust control method for controlling the position of a manipulator. These methods are linear quadratic regulator (LQR), pole placement and PID control.

Wang et al. presented an external load control of a continuum robotic system used in surgical operations [11]. In the mentioned study, the load control was performed via a hybrid adaptive controller design. Hyun et al. presented that assistive robotic manipulation assistance algorithm has potential to enable users who are currently unable to use an assistive robotic manipulator, which is kinova assistive robotic arm, to use it by using a low cost 3-dimensional depth sensing camera and an improving inverse kinematic algorithm and providing an autonomous or semi-autonomous robotic manipulation assistance [12]. In [13], a motion control algorithm for a parallel robot in the field of laparoscopic surgery and micro surgery operations was proposed. In [14], a control method was proposed to compensate nonlinearities by implementing a position inverse kinematic model in flexible bending instruments used in medical endoscopic systems.

Ozkul et al. developed an exoskeleton-type robot-assisted rehabilitation system for rehabilitation purposes [15]. In the mentioned study an admittance control with inner robust position control loop was proposed to reach the main purpose of the study. A robust controller design was proposed for vascular interventional surgical robot system developed to the implementation to more accurately, safely and stably [16]. In [17], a robust feedback controller design was proposed for electromagnetic steering microrobots used in various biomedical applications. In [18], a Lyapunov based robust control design for 2 degrees of freedom (DoF) lower limb rehabilitation

robot to perform specified passive exercises without the physiotherapist was presented. Sajadi et al. designed a Lyapunov based control method to improve the accuracy of the monitoring procedure for a surgical manipulator to follow a specific reference under the effect of external disturbance [19].

In [20], a robust adaptive control design is proposed for a class of 5 DoF upper limb exoskeleton robot to deal with the problems caused from robust output feedback control design applied on this system. Yang et al. proposed a robust adaptive control design that uses a fuzzy optimal gain design approach for the control of a 2 DoF lower limb exoskeleton robot [21]. Zhang et al. designed a robust adaptive controller for a single link joint driven by pneumatic artificial muscles to deal with its parametric uncertainty and unmodeled dynamics [22].

In [23], the proportional-integral-derivative (PID) controller's performance was introduced in trajectory control of medical robot that has two-link robotic manipulator. Seyfi and Khalaji proposed a robust motion controller with a variable-structure compensator to track the desired trajectories of upper and lower limbs in a cable-driven rehabilitation robot [24]. In [25], force training mode was proposed for position/force control of medical robots interacting to control the deformation of human soft tissues. In [26], three feedback loop controllers were selected and implemented, in which the computed torque control (CTC), the proportional derivative (PD) control and the PID were presented. In the mentioned study, performance of the CTC technique in terms of trajectory tracking of the surgical robot was compared with the each other techniques. A force control design for robotic-assisted beating heart surgery was introduced by Moreira et al. in [27]. A robust force control for the rehabilitation robot that assists with the straight leg lift exercise was proposed by Lee and Oh [28]. In [29], CTC method was introduced for the trajectory tracking of a surgical robot that is the ex-vivo laceration.

From all of the aforementioned studies and other studies in the literature two main observations can be made;

1. Serial and parallel robot manipulators are widely used as supportive systems in medical robotic applications.

2. Robust control approach is commonly preferred into this field by considering its ability to deal with possible parameter uncertainties and external disturbances.

From these observations it is reached that serial and/or parallel manipulators supported with robust control approaches can be considered as feasible supportive systems for medical robotic applications. Moreover, when the literature is examined, it is seen that this type of control design approaches are frequently preferred for the control of many robotic systems in the field of medical robotics.

In [30], a haptic system improved to use in medical applications was controlled via a robust control design. Shang and Cong introduced a new robust nonlinear controller to increase the tracking accuracy for a planar 2 DoF parallel manipulator [31]. In the mentioned study, the proposed controller was designed by combining a nonlinear PD controller with a Lyapunov based robust dynamic compensation approach. Fateh proposed the voltage control strategy for robust tracking control of a three-joint articulated flexible-joint electrically driven robot [32]. A robust backstepping controller was designed to the tracking desired speed trajectory for four-bar linkage mechanism [33]. Okur et al. proposed a robust position control of tendon-driven robot manipulators with full-state feedback to deal with parametric uncertainty in system dynamics [34]. Soltanpour et al. designed a robust controller that is able to overcome uncertainties in robot dynamics and kinematics for trajectory tracking of robot manipulator in task space [35]. In [36], a Lyapunov based robust controller design in task space for dual robot manipulator system used for support in cochlear microrobot operations was presented. A robust nonlinear task space control for parallel manipulator is proposed by Kim et al. [37]. Jin et al. introduced a robust motion control strategy that allows to compansate nonlinear terms in robot dynamics including friction for a robot manipulator [38]. In [39], a robust controller was introduced for position and orientation tracking control of underactuated quadrotor aerial robot.

In the most of the robust control designs it is assumed that all of the dynamics and parameters of the controlled system are completely uncertain. As a result of this situation, robust controllers generally have a structure that works according to the worst case scenario. It can be seen as the main disadvantage of robust controllers since it may cause unnecessarily high control effort. In general, supporting the robust

control designs with adaptive parts that try to compensate the uncertainties in the system dynamics are seen as a feasible solution to cope with this issue.

A Lyapunov based robust adaptive controller design was proposed for the trajectory tracking of robotic manipulators with uncertain external disturbances [40]. In [41], a robust adaptive control design was proposed for the trajectory tracking of a 6-DoF parallel robot. In [42] a robust adaptive control strategy was used for trajectory tracking control of an industrial robot. In the mentioned study the control design was realized in the task space and the parametric variations and uncertain disturbances were coped with owing to the robust structure of the designed controller. Chen et al. designed a robust adaptive controlller for the trajectory tracking of a two-link direct-drive robot manipulator [43]. In [44], different robust adaptive controllers were utilized for the trajectory tracking of the direct drive selective compliance assembly robot arm. In the mentioned study different type of robust adaptive controllers were examined in a comparative manner and it was observed that the proposed adaptive controllers have better tracking performance than their robust counterparts. Dou and Wang designed a robust adaptive motion controller for synchronization of multiple two link robot manipulator [45]. Yin and Pan designed a robust adaptive tracking controller for the trajectory tracking of a 6 DoF industrial robot to deal with parametric uncertainties, external disturbances and uncertain nonlinearities [46]. In [47], a robust adaptive control method was introduced for the control of mechanical manipulators. In the mentioned study, adaptive feedback linearization control strategy was used in accordance with adaptive sliding mode control to overcome unmodeled dynamics and noise. A robust adaptive tracking control was designed for robotic manipulators by taking the actuator faults, disturbance, uncertain dynamics and joint velocity measurement uncertainty [48]. Ahanda et al. proposed a Lyapunov based robust adaptive control of an electrically driven three link flexible joint robot manipulator to deal with uncertainty and joint space constraints [49].

Cochlear microrobot operations, a sub-field of medical robotics, are operations that must be carried out with high precision. One of the most effective ways to ensure high precision is to efficiently control the robotic systems used as supportive systems in these operations. When the related literature is examined it is decided that supporting these systems with robotic systems include serial and parallel

manipulators and providing the control of these systems via robust adaptive control strategies is seen one of the most feasible ways to reach the mentioned purpose. As a result of these, all this study is devoted to realize appropriate control designs for the system used as supportive systems in cochlear microrobot operations.

This study seeks to introduce control approaches of the supportive robotic system designed to provide the use of medical microrobots in cochlear workspaces. The system, designed for inner ear stem cell applications, aims to enable a microrobot placed in the inner ear cochlea region to be moved in tetherless way within the cochlea ducts. This non-contact movement is carried out thanks to the permanent magnets located at the end effectors of the robotic surgical system. The system consists of a macro-micro robot manipulator structure that aims to move the micro robot that can move without connection in the cochlea. In this structure, the macro manipulator is responsible for performing the rough movements of the system, and the micro manipulator mounted on the macro manipulator endpoint is responsible for performing fragile movements. In applications where this structure is used, speed and wide working volume characteristics are obtained owing to the macro manipulator and owing to the micro-manipulator carried by the macro manipulator to the task space, it is ensured that it can work more precisely locally.

The supportive system aims to carry out the movement of the microrobot within the cochlea ducts in a tetherless way. Since it is planned to use serving this purpose two different robotic systems one of which contains serial and the other one contains parallel robot manipulators as supportive systems, control designs are realized by considering these specific systems. First of all dynamic models of the mentioned robotic systems are obtained via recursive Newton-Euler and Lagrangian formulations. Then, two robust adaptive nonlinear controllers are designed for each of the mentioned robotic systems by considering the structures of the obtained system models. At this point some important aspects about control designs should be noted. Since the mentioned controllers are robust adaptive, none of the model parameters are needed. The dynamic models are used to observe the performance of the designed controllers in the simulation environment. Moreover, one of the mentioned controllers are designed for joint space while the remaining one is designed for task space. Lyapunov-based arguments are utilized for the related

theoretical analysis. Performance of the designed controllers is observed in simulation and experimental studies for both of the mentioned systems.

The rest of the study is organized in the following manner. In Chapter 2 modeling and structure of the experimental setups used in this study are introduced. In Chapter 3, four different robust adaptive control designs, two of which are designed for the system containing seral robot manipulators and the other two are designed for the parallel manipulator system. At this point it should be noted that for each of the mentioned systems, one control design is made in the joint space and the other one is realized in the task space. Related analysis, simulation and experimental studies of each controller are presented in a detailed manner in Chapter 3. Finally, the study is concluded by giving conclusions and possible future works in Chapter 4.

Chapter 2

Structure and Modeling of Serial and Parallel Robotic Systems

In this chapter, dynamic modeling of the systems that are thought to be used as supportive systems in surgical microrobot operations is given. Obtaining system models that give an idea about the systems' structures and provide an opportunity to test the performance of the designed controllers in the simulation environment the main objective of the studies conducted in this chapter.

Considering the structure of the microrobot, whose movement in the cochlea must be ensured precisely for a successful operation, two different supportive robotic systems are designed. The main purpose of these systems is to produce an electromagnetic field between two independent end effectors in which the microrobot can continue its movement in a spherical workspace centered on the cochlea with radius R_m. The radius R_m is determined approximately according to the cochlear region and the dimensions of the head region which is the biggest obstacle in the working volume. To achieve this goal, first of all, a robotic system including two independent three link revolute joint serial manipulators operating on the same plane is designed and constructed. Each of the mentioned robot manipulators has 3 DoF. General structure of the first system can be seen in Figure 2.1. The permanent magnets are located in the end effector of the robotic surgery system, for this serial system is the C_s and C_s' as seen in figure 2.1. Maintaining the distance between the two end effectors and operating on a cochlea-centered circle with a radius greater than R_m and are their exposure to each other on the same axis the main working principles of the serial robotic system. In Figure 2.2 the produced prototype of the serial robotic system is shown.

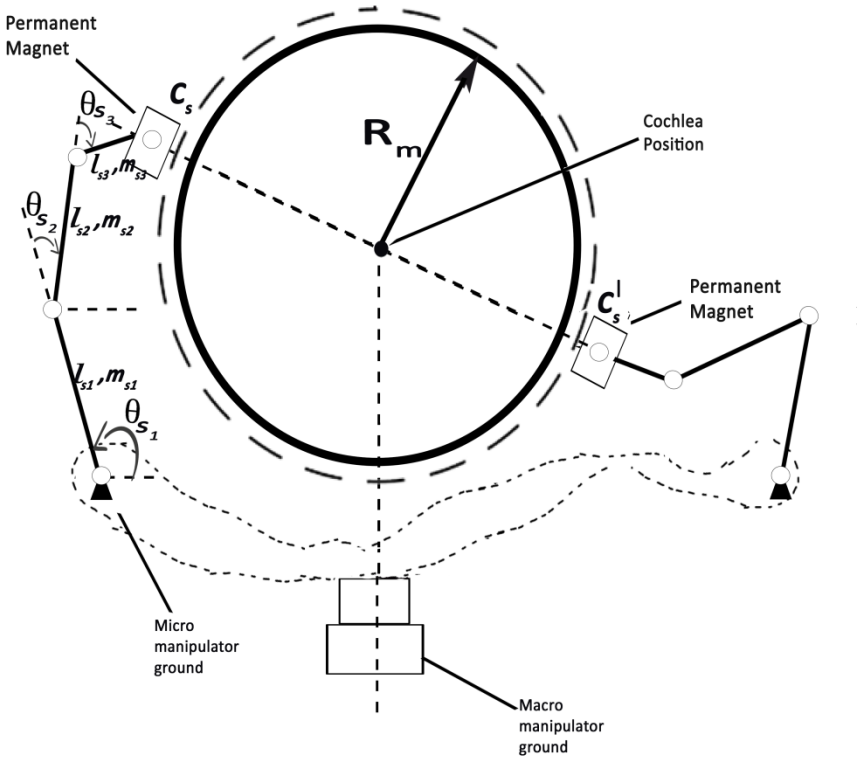

Figure 2.1: Serial manipulator system

(a)

(b)

Figure 2.2: Serial robotic RRR system, (a) Top view, (b) Front view

The second robotic system considered as the supportive system includes a parallel manipulator structure having 5 DoF and containing double-end effectors. General structure of this system can be seen in Figure 2.3. The parallel robot manipulator also operates on a cochlea-centered circle whose radius is greater than R_m. However, due to its structure, it works differently from the serial robotic system, that is, the two end effectors of the parallel system operate in the area where the cochlea is close to the head region on a cochlea-centered circle whose radius is greater than R. In the parallel system, the end effectors keep their distance to the cochlea and the orientation of the magnet in the end effectors constant. The electromagnetic actuator is located in the end effector of the robotic surgery system, for this parallel system is the C_p and C_p' as seen in Figure 2.3. In Figure 2.4 the produced prototype of the serial robotic system is shown.

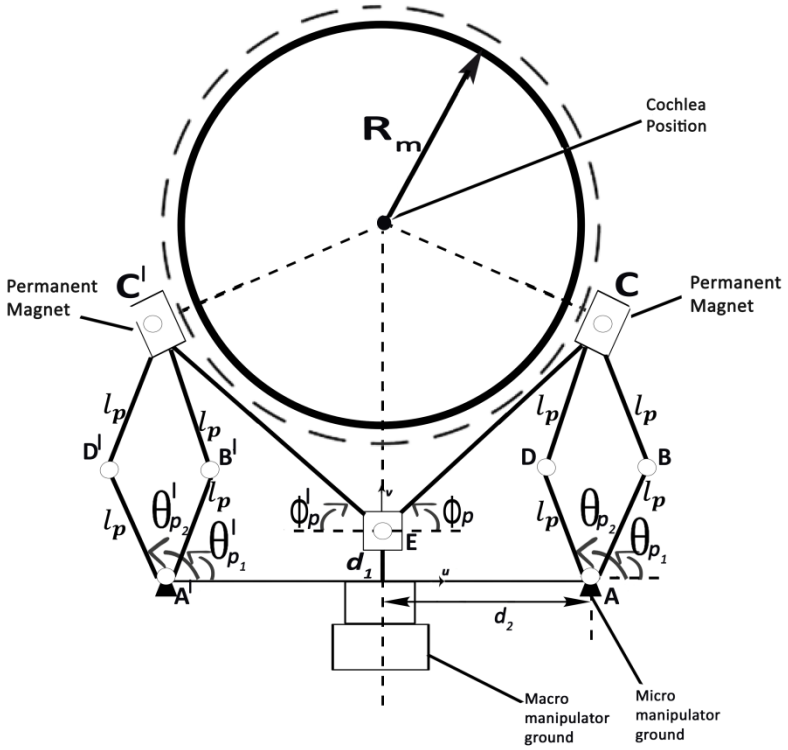

Figure 2.3: Parallel manipulator system

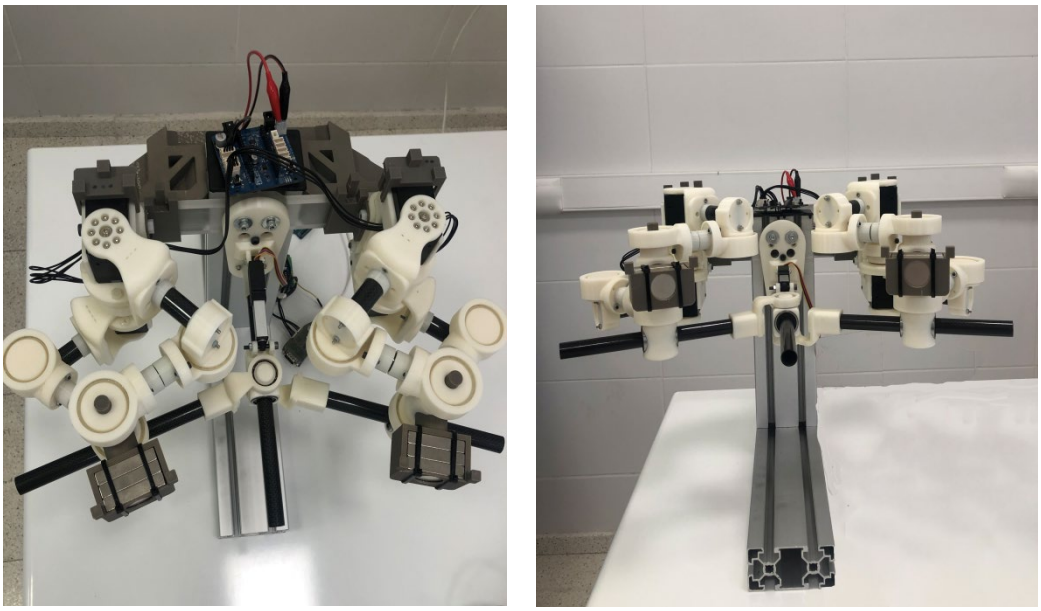

(a) (b)

Figure 2.4: Parallel robotic system, (a) Top view, (b) Front view

In the following sections of this chapter dynamic modeling of the aforementioned systems are given in a detailed manner.

2.1 Dynamic Model of Robot Manipulators

The mathematical model of a robot manipulator is given as [50]

$$M(\theta)\ddot{\theta} + C\left(\theta, \dot{\theta}\right)\dot{\theta} + G(\theta) + F_f\dot{\theta} = \tau \tag{2.1}$$

where $M(\theta) \in \mathbb{R}^{n\times n}$ represents the positive-definite and symmetric inertia matrix. $C\left(\theta, \dot{\theta}\right) \in \mathbb{R}^{n\times n}$ represents the centripetal-coriolis matrix, $G(\theta) \in \mathbb{R}^n$ denotes vector of gravitational forces and $F_f \in \mathbb{R}^{n\times n}$ denotes the friction matrix. In (2.1) the control input torque is represented by $\tau \in \mathbb{R}^n$ while $\theta, \dot{\theta}, \ddot{\theta} \in \mathbb{R}^n$ denote the joint position, velocity and acceleration, respectively. Moreover it should be noted that $n \in \mathbb{R}$ denotes the total DoF of the robot manipulator in the dynamic model. Obtaining each parameters of the dynamic models that are specified from (2.1) according to the structures of the systems used in this study is the main purpose of this chapter. Newton-Euler and Lagrangian formulations can be utilized to achieve this goal.

2.2 Modeling of Serial Robotic System

Since the serial robotic system includes three link revolute joint robot manipulators, this chapter is based on dynamic modeling of 3 DoF RRR robot manipulators. The Newton-Euler formulation is used to obtain the dynamic model, and the modeling steps and the mathematical equations obtained for each step are given in a detailed manner. At this point it should be noted that all dynamic models are presented parametrically in the following chapters. Obtaining a model structure where the possible changes in the parameters of robot manipulators (link masses, used material, link lengths and etc.) can easily be applied is the main purpose of this presentation.

2.2.1 Newton-Euler Formulation

Newton-Euler formulation, which explains the relationship between the force acting on the center of mass of each link and the link inertia and acceleration, is used to obtain the dynamic model terms. The force acting on the center of mass of the link is obtained by Newton's Equation given as

$$F = m_s \dot{v}_{s_c} \tag{2.2}$$

where $m_s \in \mathbb{R}$ denotes mass of link, $\dot{v}_{s_c} \in \mathbb{R}$ denotes acceleration of the center of mass of link. The formula used to find inertia moment exerted at the center of mass of link is given as

$$N = {}^{c}I\dot{\omega}_s + \omega_s \times {}^{c}I_s\omega_s \tag{2.3}$$

where ω_s and $\dot{\omega}_s \in \mathbb{R}$ represent angular velocity and angular acceleration of the link, respectively while ${}^{c}I_s \in \mathbb{R}$ denotes inertia of the link about its center of mass.

The force and torque expressions acting on the centers of the mass of each link are found by calculating the following forward computation equations for $i = 0, \cdots, (n-1)$

$$
\begin{aligned}
{}^{i+1}\omega_{s_{i+1}} &= {}^{i+1}_{i}R\ {}^{i}\omega_{s_i} + \dot{\theta}_{s_{i+1}}\,{}^{i+1}\hat{Z}_{i+1} \\
{}^{i+1}\dot{\omega}_{s_{i+1}} &= {}^{i+1}_{i}R\ {}^{i}\dot{\omega}_{s_i} + {}^{i+1}_{i}R\,{}^{i}\omega_{s_i} \times \dot{\theta}_{s_{i+1}}\,{}^{i+1}\hat{Z}_{i+1} + \ddot{\theta}_{s_{i+1}}\,{}^{i+1}\hat{Z}_{i+1} \\
{}^{i+1}\dot{v}_{s_{i+1}} &= {}^{i+1}_{i}R\left({}^{i+1}\dot{\omega}_{s_{i+1}} \times {}^{i}P_{i+1} + {}^{i}\omega_{s_i} \times ({}^{i}\omega_{s_i} \times {}^{i}P_{i+1}) {}^{i}\dot{v}_{s_i}\right) \\
{}^{i+1}\dot{v}_{s_{c_{i+1}}} &= {}^{i+1}\dot{\omega}_{s_{i+1}} \times {}^{i+1}P_{c_{i+1}} \\
&\quad + {}^{i+1}\omega_{s_{i+1}} \times \left({}^{i+1}\omega_{s_{i+1}} \times {}^{i+1}P_{c_{i+1}}\right) + {}^{i+1}\dot{v}_{s_{i+1}} \\
{}^{i+1}F_{i+1} &= m_{s_{i+1}}\,{}^{i+1}\dot{v}_{s_{c_{i+1}}} \\
{}^{i+1}N_{i+1} &= {}^{c_{i+1}}I_{s_{i+1}}\,{}^{i+1}\dot{\omega}_{s_{i+1}} + {}^{i+1}\omega_{s_{i+1}} \times {}^{c_{i+1}}I_{s_{i+1}}\,{}^{i+1}\omega_{s_{i+1}}
\end{aligned}
\tag{2.4}
$$

where $\dot{\theta}_{s_{i+1}} \in \mathbb{R}$ and $\ddot{\theta}_{s_{i+1}} \in \mathbb{R}$ represent velocity, and acceleration of the $(i+1)^{\text{th}}$ joint, ${}^{i}\hat{Z}_i \in \mathbb{R}^n$ denotes a unit vector pointing along the i^{th} joint axis, ${}^{i+1}\omega_{s_{i+1}} \in \mathbb{R}^n$ angular velocity exerted on other link by $(i+1)^{\text{th}}$ link, ${}^{i+1}\dot{\omega}_{s_{i+1}} \in \mathbb{R}^n$ represents angular acceleration exerted on other link by $(i+1)^{\text{th}}$ link, ${}^{i+1}_{i}R \in \mathbb{R}^{n\times n}$ denotes rotation matrix, ${}^{i+1}\dot{v}_{s_{i+1}} \in \mathbb{R}^n$ represents linear acceleration of $(i+1)^{\text{th}}$ link frame, ${}^{i}P_{i+1} \in \mathbb{R}^n$ denotes position vector of frame $(i+1)$ with respect to frame (i), ${}^{i+1}\dot{v}_{s_{c_{i+1}}} \in \mathbb{R}^n$ represents linear acceleration of the center of mass of $(i+1)^{\text{th}}$ link and ${}^{i+1}P_{c_{i+1}} \in \mathbb{R}^n$ position vector of the center of mass.

Actuator torques or forces are obtained by utilizing the following backward computation equations for $i = n, \cdots, 1$

$$
\begin{aligned}
{}^{i}f_i &= {}^{i}_{i+1}R\,{}^{i+1}\omega_{s_{i+1}} + {}^{i}F_i \\
{}^{i}n_i &= {}^{i}N_i + {}^{i}_{i+1}R\,{}^{i+1}n_{i+1} + {}^{i}P_{c_i} \times {}^{i}F_i + {}^{i}P_{i+1} \times {}^{i}R_{i+1}\,{}^{i+1}f_{i+1} \\
\tau_{s_i} &= {}^{i}n_i^T\hat{Z}_i
\end{aligned}
\tag{2.5}
$$

where ${}^{i}f_i \in \mathbb{R}^n$ denotes force exerted on $(i-1)^{\text{th}}$ link by i^{th} link , ${}^{i}n_i \in \mathbb{R}^n$ denotes moment exerted on $(i-1)^{\text{th}}$ link by i^{th} link and $\tau_{s_i} \in \mathbb{R}$ represents the torque required for the i^{th} joint.

2.2.2 Derivation of the Dynamic Model of 3 DoF RRR Robot Manipulator via Newton-Euler Formulation

To obtain the dynamic model of 3 DoF revolute joint robot manipulator, it is assumed that the links are at the midpoints of the centers of mass. This situation can mathematically be expressed as

$$
\begin{aligned}
{}^{1}P_{c_1} &= \begin{bmatrix} \frac{l_{s1}}{2} & 0 & 0 \end{bmatrix}^T \\
{}^{2}P_{c_2} &= \begin{bmatrix} \frac{l_{s2}}{2} & 0 & 0 \end{bmatrix}^T \\
{}^{3}P_{c_3} &= \begin{bmatrix} \frac{l_{s3}}{2} & 0 & 0 \end{bmatrix}^T
\end{aligned} \tag{2.6}
$$

where l_{si} represents length of i^{th} link. The following assumptions can be made for the angular velocity and angular acceleration since the base coordinate system of the robot arms does not move

$$
\begin{aligned}
{}^{0}\omega_{s_0} &= [0 \quad 0 \quad 0]^T \\
{}^{0}\dot{\omega}_{s_0} &= [0 \quad 0 \quad 0]^T.
\end{aligned} \tag{2.7}
$$

Gravity is on the z-axis in the main coordinate system. This situation is mathematically expressed as

$$
{}^{0}\dot{v}_{s_0} = g\hat{Z}_0 = [0 \quad 0 \quad g]^T \tag{2.8}
$$

where $g \in \mathbb{R}$ represents the gravitational acceleration. The rotation between consecutive link axes is expressed by the rotation matrices given below

$$
\begin{aligned}
{}^{i}_{i+1}R &= \begin{bmatrix} cos\,\theta_{s_{i+1}} & sin\,\theta_{s_{i+1}} & 0 \\ -sin\,\theta_{s_{i+1}} & cos\,\theta_{s_{i+1}} & 0 \\ 0 & 0 & 1 \end{bmatrix} \\
{}^{i+1}_{i}R &= \begin{bmatrix} cos\,\theta_{s_{i+1}} & -sin\,\theta_{s_{i+1}} & 0 \\ sin\,\theta_{s_{i+1}} & cos\,\theta_{s_{i+1}} & 0 \\ 0 & 0 & 1 \end{bmatrix}.
\end{aligned} \tag{2.9}
$$

Forward computation equations for each joint can be calculated as follows by substituting (2.6)-(2.9) in (2.4)

For the first joint

$$
\begin{aligned}
{}^{1}\omega_{s_1} &= \begin{bmatrix} 0 & 0 & \dot{\theta}_{s_1} \end{bmatrix}^T \\
{}^{1}\dot{\omega}_{s_1} &= \begin{bmatrix} 0 & 0 & \ddot{\theta}_{s_1} \end{bmatrix}^T \\
{}^{1}\dot{v}_{s_1} &= [0 \quad 0 \quad g]^T \\
{}^{1}\dot{v}_{s_{c_1}} &= \begin{bmatrix} -\frac{l_{s1}}{2}\dot{\theta}_{s_1}^2 & \frac{l_{s1}}{2}\ddot{\theta}_{s_1} & g \end{bmatrix}^T \\
{}^{1}F_1 &= \begin{bmatrix} -m_{s1}\frac{l_{s1}}{2}\dot{\theta}_{s_1}^2 & m_{s1}\frac{l_{s1}}{2}\ddot{\theta}_{s_1} & gm_{s1} \end{bmatrix}^T \\
{}^{1}N_1 &= \begin{bmatrix} 0 & 0 & \frac{m_{s1}l_{s1}^2}{12}\ddot{\theta}_{s_1} \end{bmatrix}^T
\end{aligned} \tag{2.10}
$$

For the second joint

$$
\begin{aligned}
{}^{2}\omega_{s_2} &= \begin{bmatrix} 0 & 0 & \dot{\theta}_{s_{12}} \end{bmatrix}^T \\
{}^{2}\dot{\omega}_{s_2} &= \begin{bmatrix} 0 & 0 & \ddot{\theta}_{s_{12}} \end{bmatrix}^T \\
{}^{2}\dot{v}_{s_2} &= \begin{bmatrix} l_{s1}\ddot{\theta}_{s_1} \sin\theta_{s_2} - l_{s1}\dot{\theta}_{s_1}^2 \cos\theta_{s_2} \\ l_{s1}\ddot{\theta}_1 \sin\theta_2 + l_{s1}\dot{\theta}_{s_1}^2 \cos\theta_{s_2} \\ g \end{bmatrix} \\
{}^{2}\dot{v}_{s_{c_2}} &= \begin{bmatrix} \frac{-l_{s2}}{2}\left(\dot{\theta}_{s_{12}}\right)^2 + l_{s1}\ddot{\theta}_{s_1} \sin\theta_{s_2} - l_{s1}\dot{\theta}_{s_1}^2 \cos\theta_{s_2} \\ \frac{l_{s2}}{2}\ddot{\theta}_{s_{12}} + l_{s1}\ddot{\theta}_{s_1} \sin\theta_{s_2} + l_{s1}\dot{\theta}_{s_1}^2 \cos\theta_{s_2} \\ g \end{bmatrix} \\
{}^{2}F_2 &= \begin{bmatrix} -m_{s2}\frac{l_{s2}}{2}\left(\dot{\theta}_{s_{12}}\right)^2 + m_{s2}l_{s1}\ddot{\theta}_{s_1} sin\,\theta_{s_2} - m_{s2}l_{s1}\dot{\theta}_{s_1}^2 cos\theta_{s_2} \\ m_{s2}\frac{l_{s2}}{2}\ddot{\theta}_{s_{12}} + m_{s2}l_{s1}\ddot{\theta}_{s_1} sin\,\theta_{s_2} + m_{s2}l_{s1}\dot{\theta}_{s_1}^2 cos\,\theta_{s_2} \\ g m_{s2} \end{bmatrix} \\
{}^{2}N_2 &= \begin{bmatrix} 0 & 0 & \frac{m_{s2}l_{s2}^2}{12}\ddot{\theta}_{s_{12}} \end{bmatrix}^T
\end{aligned}
\tag{2.11}
$$

For the third joint

$$
\begin{aligned}
{}^{3}\omega_{s_3} &= \begin{bmatrix} 0 & 0 & \dot{\theta}_{s_{123}} \end{bmatrix}^T \\
{}^{3}\dot{\omega}_{s_3} &= \begin{bmatrix} 0 & 0 & \ddot{\theta}_{s_{123}} \end{bmatrix}^T \\
{}^{3}\dot{v}_{s_3} &= \begin{bmatrix} {}^{3}\dot{v}_{s_{3x}} & {}^{3}\dot{v}_{s_{3y}} & g \end{bmatrix}^T \\
{}^{3}\dot{v}_{s_{3x}} &= l_{s1}\ddot{\theta}_{s_1} \sin\left(\theta_{s_{23}}\right) + l_{s2}\ddot{\theta}_{s_{12}} \sin\theta_{s_3} - l_{s1}\,\dot{\theta}_{s_1}^2 cos(\theta_{s_{23}}) \\
&\quad - l_{s2}\cos\theta_{s_3}\left(\dot{\theta}_{s_{12}}\right)^2 \\
{}^{3}\dot{v}_{s_{3y}} &= l_{s1}\ddot{\theta}_{s_1} cos(\theta_{s_{23}}) + l_{s2}\left(\dot{\theta}_{s_{12}}\right)^2 sin\,\theta_{s_3} + l_{s2}\ddot{\theta}_{s_{12}} cos\,\theta_{s_3} \\
&\quad + l_{s1}\dot{\theta}_{s_1}^2 sin\left(\theta_{s_{23}}\right) \\
{}^{3}\dot{v}_{s_{c_3}} &= \begin{bmatrix} {}^{3}\dot{v}_{s_{c_{3x}}} & {}^{3}\dot{v}_{s_{c_{3y}}} & g \end{bmatrix}^T \\
{}^{3}\dot{v}_{s_{c_{3x}}} &= -\frac{l_{s3}}{2}\left(\dot{\theta}_{s_{123}}\right)^2 + l_{s1}\,\ddot{\theta}_{s_1} sin\left(\theta_{s_{23}}\right) - l_{s2}\left(\dot{\theta}_{s_{12}}\right)^2 cos\,\theta_{s_3} \\
&\quad - l_{s1}\dot{\theta}_{s_1}^2 cos\left(\theta_{s_{23}}\right) + l_{s2}\ddot{\theta}_{s_{12}} sin\,\theta_{s_3} \\
{}^{3}\dot{v}_{s_{c_{3y}}} &= \frac{l_{s3}}{2}\ddot{\theta}_{s_{123}} + l_{s1}\ddot{\theta}_{s_1} cos\left(\theta_{s_{23}}\right) + l_{s2}\left(\dot{\theta}_{s_{12}}\right)^2 sin\,\theta_{s_3} \\
&\quad + l_{s1}\dot{\theta}_{s_1}^2 sin\left(\theta_{s_{23}}\right) + l_{s2}\,\ddot{\theta}_{s_{12}} cos\,\theta_{s_3} \\
{}^{3}\mathrm{F}_3 &= \begin{bmatrix} m_{s3}\,{}^{3}\dot{v}_{s_{c_{3x}}} & m_3\,{}^{3}\dot{v}_{s_{c_{3y}}} & g m_{s3} \end{bmatrix}^T \\
{}^{3}\mathrm{N}_3 &= \begin{bmatrix} 0 & 0 & \frac{m_{s3}l_{s3}^2}{12}\ddot{\theta}_{s_{123}} \end{bmatrix}^T
\end{aligned}
\tag{2.12}
$$

where $m_{s_i} \in \mathbb{R}$ represents mass of i^{th} link, $\theta_{s_{i\cdots j}} = \left(\theta_{s_i} + \cdots + \theta_{s_j}\right) \in \mathbb{R}$ represents sum of joint angle, $\dot{\theta}_{s_{i\cdots j}} = \left(\dot{\theta}_{s_i} + \cdots + \dot{\theta}_{s_j}\right) \in \mathbb{R}$ represents sum of joint velocity and $\ddot{\theta}_{s_{i\cdots j}} = \left(\ddot{\theta}_{s_i} + \cdots + \ddot{\theta}_{s_j}\right) \in \mathbb{R}$ represents sum of joint acceleration.

Backward computation equations for each joint are calculated as follows by substituting (2.10)-(2.12) in (2.5).

For the third joint

$$
\begin{aligned}
&{}^3f_3 = {}^3F_3 \\
&{}^3n_3 = \begin{bmatrix} 0 & \dfrac{1}{2gm_{s3}l_{s3}} & {}^3n_{3z} \end{bmatrix}^T \\
&{}^3n_{3z} = \frac{1}{3}l_{s3}{}^2 m_{s3}\ddot{\theta}_{s_{123}} + \frac{1}{2}l_{s2}l_{s3}m_{s3}\ddot{\theta}_{s_1}\cos\theta_{s_3} \\
&\qquad + \frac{1}{2}l_{s1}l_{s3}m_{s3}\ddot{\theta}_{s_1}\cos\theta_{s_{23}} + \frac{1}{2}l_{s2}l_{s3}m_{s3}\ddot{\theta}_{s_2}\cos\theta_{s_3} \\
&\qquad + \frac{1}{2}l_{s2}l_{s3}m_{s3}\dot{\theta}_{s_1}^2\sin\theta_{s_3} + \frac{1}{2}l_{s1}l_{s3}m_{s3}\dot{\theta}_{s_1}^2\sin\theta_{s_{23}} \\
&\qquad + \frac{1}{2}l_{s2}l_{s3}m_{s3}\dot{\theta}_{s_2}^2\sin\theta_{s_3} + l_{s2}l_{s3}m_{s3}\dot{\theta}_{s_1}\dot{\theta}_{s_2}\sin\theta_{s_3}.
\end{aligned}
\tag{2.13}
$$

For the second joint

$$
\begin{aligned}
&{}^2f_2 = \begin{bmatrix} {}^2f_{2x} & {}^2f_{2y} & -g(m_{s2}+m_{s3}) \end{bmatrix}^T \\
&{}^2f_{2y} = (l_{s1}m_{s3} + l_{s1}m_{s2})\ddot{\theta}_{s_1}\cos\theta_{s_2} - \frac{1}{2}l_{s3}m_{s3}\ddot{\theta}_{s_{123}}\cos\theta_{s_3} \\
&\qquad - (l_{s1}m_{s3} + l_{s1}m_{s2})\,\dot{\theta}_{s_1}^2\sin\theta_{s_2} \\
&\qquad - \frac{1}{2}l_{s3}m_{s3}\left(\dot{\theta}_{s_{123}}\right)^2\sin\theta_{s_3} \\
&\qquad - (l_{s2}m_{s3} + \frac{1}{2}l_{s2}m_{s2})\left(\dot{\theta}_{s_{12}}\right)^2 \\
&{}^2n_2 = \begin{bmatrix} -\dfrac{1}{2}gm_{s3}l_{s3}\sin\theta_{s_3} \\ g(l_{s2}m_{s3} + \dfrac{1}{2}l_{s3}m_{s3}\cos\theta_{s_3} + \dfrac{1}{2}m_{s2}l_{s2}) \\ {}^2n_{2z} \end{bmatrix} \\
&{}^2n_{2z} = \frac{1}{2}\big(l_{s1}l_{s3}m_{s3}\cos\theta_{s_{23}} + l_{s1}l_{s2}m_{s2}\cos\theta_{s_2} \\
&\qquad + 2l_{s1}l_{s2}m_{s3}\cos\theta_{s_2}\big)\ddot{\theta}_{s_1} + l_{s2}l_{s3}m_{s3}\,\ddot{\theta}_{s_2}\cos\theta_{s_3} \\
&\qquad + (\frac{1}{3}l_{s2}^2m_{s2} + l_{s2}^2m_{s3})\ddot{\theta}_{s_{12}} + \frac{1}{3}l_{s3}^2m_{s3}\ddot{\theta}_{s_{123}} \\
&\qquad + \frac{1}{2}l_{s2}l_{s3}m_{s3}\ddot{\theta}_{s_3}\cos\theta_{s_3} - \frac{1}{2}l_{s2}l_{s3}m_{s3}\dot{\theta}_{s_3}^2\sin\theta_{s_3} \\
&\qquad + \frac{1}{2}(l_{s2}^2m_{s2}\sin\theta_{s_2} + l_{s1}l_{s3}m_{s3}\sin\theta_{s_{23}})\dot{\theta}_{s_1}^2 \\
&\qquad - l_{s2}l_{s3}m_{s3}(\dot{\theta}_{s_1}\dot{\theta}_{s_3} + \dot{\theta}_{s_2}\dot{\theta}_{s_3})\,\sin\theta_{s_3}
\end{aligned}
\tag{2.14}
$$

For the first joint

$$
\begin{aligned}
{}^1f_1 &= \begin{bmatrix} {}^1f_{1x} & {}^1f_{1y} & -g(m_{s1}+m_{s2}+m_{s3}) \end{bmatrix}^T \\
{}^1f_{1x} &= -(l_{s2}m_{s3}+\frac{1}{2}l_{2s}m_{s2})sin\theta_{s_2}\ddot{\theta}_{s_{12}} - \frac{1}{2}l_{s3}m_{s3}\,\ddot{\theta}_{s_{123}}sin(\theta_{s_{23}}) \\
&\quad - \frac{1}{2}l_{s3}m_{s3}\dot{\theta}^2_{s_{123}}\cos\theta_{s_3} \\
&\quad - (\frac{1}{2}l_{s2}m_{s2}+l_{s2}m_{s3})\,\dot{\theta}^2_{s_{12}}\cos\theta_{s_2} \\
&\quad - \Big(\frac{1}{2}l_{s1}m_{s1}+l_{s2}m_{s2}+l_{s1}m_{s3}\,sin(\theta_{s_{23}})^2 \\
&\quad - l_{s1}m_{s3}cos(\theta_{s_{23}})^2\Big)\dot{\theta}^2_{s_1} \\
{}^1f_{1y} &= \frac{1}{2}l_{s1}m_{s1}\ddot{\theta}_{s_1} + (l_{s2}m_{s3}+\frac{1}{2}l_{s2}m_{s2})\ddot{\theta}_{s_{12}}\cos\theta_{s_2} \\
&\quad + \frac{1}{2}l_{s3}m_{s3}\ddot{\theta}_{s_{123}}cos\theta_{s_{23}} - \frac{1}{2}l_{s3}m_{s3}\,sin\,\theta_{s_3}\,\dot{\theta}^2_{s_{123}} \\
&\quad - (\frac{1}{2}l_{s2}m_{s2}+l_{s2}m_{s3})\dot{\theta}^2_{s_{12}}\,sin\,\theta_{s_2} \\
&\quad + \big(2l_{s1}m_{s3}\,sin\,\theta_{s_{23}}cos\theta_{s_{23}}\big)\dot{\theta}^2_1 \\
{}^1n_1 &= \begin{bmatrix} -g\left(\frac{1}{2}m_{s3}l_{s3}\,sin\,\theta_{s_{23}}+l_{s2}m_{s3}\,sin\,\theta_{s_2}+\frac{1}{2}m_{s2}l_{s2}\,sin\,\theta_{s_2}\right) \\ {}^1n_{1y} \\ {}^1n_{1z} \end{bmatrix} \\
{}^1n_{1y} &= g\left(\tfrac{1}{2}m_{s3}l_{s3}\cos\theta_{s_{23}}+l_{s2}m_{s3}\cos\theta_{s_2}+\tfrac{1}{2}m_{s2}l_{s2}\cos\theta_{s_2}\right. \\
&\quad \left. + m_{s1}l_{s1}+(m_{s2}+m_{s3})l_{s1}\right) \\
{}^1n_{1z} &= \big(\tfrac{1}{3}l^2_{s1}m_{s1}+l^2_{s1}m_{s2} \\
&\quad + 2l_{s1}l_{s2}m_{s3}\cos\theta_{s_2}+l_{s1}l_{s2}m_{s2}\cos\theta_{s_2} \\
&\quad + l_{s1}l_{s3}m_{s3}\cos\theta_{s_{23}}+l_{s2}l_{s3}m_{s3}\cos\theta_{s_3}\big)\ddot{\theta}_{s_1} \\
&\quad + \Big(l_{s1}l_{s2}m_{s3}\cos\theta_{s_2}+\tfrac{1}{2}l_{s1}l_{s2}m_{s2}\cos\theta_{s_2} \\
&\quad + \tfrac{1}{2}l_{s1}l_{s3}m_{s3}\cos\theta_{s_{23}}+l_{s2}l_{s3}m_{s3}\cos\theta_{s_3}\Big)\ddot{\theta}_{s_2} \\
&\quad + \tfrac{1}{2}\big(l_{s1}l_{s3}m_{s3}\cos\theta_{s_{23}}+l_{s2}l_{s3}m_{s3}\cos\theta_{s_3}\big)\ddot{\theta}_{s_3} \\
&\quad + (\tfrac{1}{3}l^2_{s2}m_{s2}+l^2_{s2}m_{s3})\ddot{\theta}_{s_{12}}+\tfrac{1}{3}l^2_{s3}m_{s3}\ddot{\theta}_{s_{123}} \\
&\quad + \Big(\tfrac{1}{2}l^2_{s2}m_{s2}\,sin\,\theta_{s_2}+\tfrac{1}{2}l_{s1}l_{s3}m_{s3}\,sin\,\theta_{s_{23}} \\
&\quad - 2l_{s1}l_{s2}m_{s3}\,sin\,\theta_{s_2}-\tfrac{1}{2}l_{s1}l_{s2}m_{s2}\,sin\,\theta_{s_2}\Big)\dot{\theta}^2_{s_1} \\
&\quad - (\tfrac{1}{2}l_{s1}l_{s3}m_{s3}\,sin\,\theta_{s_{23}}+l_1l_2m_3\,sin\,\theta_{s_2} \\
&\quad + \tfrac{1}{2}l_1l_2m_2\,sin\,\theta_{s_2})\dot{\theta}^2_{s_2} \\
&\quad - \tfrac{1}{2}\big(l_{s2}l_{s3}m_{s3}\,sin\,\theta_{s_3}+l_{s1}l_{s3}m_{s3}\,sin\,\theta_{s_{23}}\big)\dot{\theta}^2_{s_3} \\
&\quad - \big(l_{s1}l_{s3}m_{s3}\,sin\,\theta_{s_{23}}+2l_{s1}l_{s2}m_{s3}\,sin\,\theta_{s_2} \\
&\quad + l_{s1}l_{s2}m_{s2}\,sin\,\theta_{s_2}\big)\dot{\theta}_{s_1}\dot{\theta}_{s_2} \\
&\quad - \big(l_{s2}l_{s3}m_{s3}\,sin\,\theta_{s_3}+l_{s1}l_{s3}m_{s3}\,sin\,\theta_{s_{23}}\big)(\dot{\theta}_{s_1}\dot{\theta}_{s_3} \\
&\quad + \dot{\theta}_{s_2}\dot{\theta}_{s_3})
\end{aligned}
\tag{2.15}
$$

Torques that are effective on each joints can be obtained as

$$
\begin{aligned}
\tau_{s_1} = {}^1f_1^T\hat{Z}_1 = {} & \Big(\tfrac{1}{3}l_{s1}^2m_{s1} + l_{s1}^2(m_{s2}+m_{s3}) + \tfrac{1}{3}m_{s3}l_{s3}^2 + \tfrac{1}{3}l_{s2}^2m_{s2} \\
& + l_{s2}^2m_{s3} + l_{s1}l_{s3}m_{s3}\cos\theta_{s_{23}} + 2l_{s1}l_{s2}m_{s3}\cos\theta_{s_2} \\
& + l_{s1}l_{s2}m_{s2}\cos\theta_{s_2} + l_{s2}l_{s3}m_{s3}\cos\theta_{s_3}\Big)\ddot{\theta}_{s_1} \\
& + \Big(\tfrac{1}{3}m_{s3}l_{s3}^2 + \tfrac{1}{3}l_{s2}^2m_{s2} + l_{s2}^2m_{s3} \\
& + \tfrac{1}{2}l_{s1}l_{s3}m_{s3}\cos\theta_{s_{23}} + l_{s1}l_{s2}m_{s3}\cos\theta_{s_2} \\
& + \tfrac{1}{2}l_{s1}l_{s2}m_{s2}\cos\theta_{s_2} + l_{s2}l_{s3}m_{s3}\cos\theta_{s_3}\Big)\ddot{\theta}_{s_2} \\
& + (\tfrac{1}{3}m_{s3}l_{s3}^2 + \tfrac{1}{2}l_{s2}l_{s3}m_{s3}\cos\theta_{s_3} \\
& + \tfrac{1}{2}l_{s1}l_{s3}m_{s3}\cos\theta_{s_{23}})\ddot{\theta}_{s_3} \\
& + \Big(\tfrac{1}{2}l_{s2}^2m_{s2}\,sin\,\theta_{s_2} + \tfrac{1}{2}l_{s1}l_{s3}m_{s3}\,sin\,\theta_{s_{23}} \\
& - 2l_{s1}l_{s2}m_{s3}\,sin\,\theta_{s_2} - \tfrac{1}{2}l_{s1}l_{s2}m_{s2}\,sin\,\theta_{s_2}\Big)\dot{\theta}_{s_1}^2 \\
& - (\tfrac{1}{2}l_{s1}l_{s3}m_{s3}\,sin\,\theta_{s_{23}} + l_1l_2m_3\,sin\,\theta_{s_2} \\
& + \tfrac{1}{2}l_1l_2m_2\,sin\,\theta_{s_2})\dot{\theta}_{s_2}^2 \\
& - \tfrac{1}{2}\big(l_{s2}l_{s3}m_{s3}\,sin\,\theta_{s_3} + l_{s1}l_{s3}m_{s3}\,sin\,\theta_{s_{23}}\big)\dot{\theta}_{s_3}^2 \\
& - \big(l_{s1}l_{s3}m_{s3}\,sin\,\theta_{s_{23}} + 2l_{s1}l_{s2}m_{s3}\,sin\,\theta_{s_2} \\
& + l_{s1}l_{s2}m_{s2}\,sin\,\theta_{s_2}\big)\dot{\theta}_{s_1}\dot{\theta}_{s_2} \\
& - \big(l_{s2}l_{s3}m_{s3}\,sin\,\theta_{s_3} + l_{s1}l_{s3}m_{s3}\,sin\,\theta_{s_{23}}\big)(\dot{\theta}_{s_1}\dot{\theta}_{s_3} \\
& + \dot{\theta}_{s_2}\dot{\theta}_{s_3})
\end{aligned}
\tag{2.16}
$$

$$
\begin{aligned}
\tau_{s_2} = {}^2f_2^T\hat{Z}_2 = {} & \Big(\tfrac{1}{3}m_{s3}l_{s3}^2 + \tfrac{1}{3}l_{s2}^2m_{s2} + l_{s2}^2m_{s3} + \tfrac{1}{2}l_{s1}l_{s3}m_{s3}\cos\theta_{s_{23}} \\
& + l_{s1}l_{s2}m_{s3}\cos\theta_{s_2} + \tfrac{1}{2}l_{s1}l_{s2}m_{s2}\cos\theta_{s_2} \\
& + l_{s2}l_{s3}m_{s3}\cos\theta_{s_3}\Big)\ddot{\theta}_{s_1} \\
& + \Big(\tfrac{1}{3}m_{s3}l_{s3}^2 + \tfrac{1}{3}l_{s2}^2m_{s2} + l_{s2}^2m_{s3} \\
& + l_{s2}l_{s3}m_{s3}\,cos\,\theta_{s_3}\Big)\ddot{\theta}_{s_2} \\
& + \Big(\frac{1}{2}l_{s2}l_{s3}m_{s3}\,cos\,\theta_{s_3} + \tfrac{1}{3}m_{s3}l_{s3}^2\Big)\ddot{\theta}_{s_3} \\
& + \frac{1}{2}\big(l_{s1}l_{s3}m_{s3}\,cos\,\theta_{s_{23}} + l_{s1}l_{s2}m_{s2}\,cos\,\theta_{s_2} \\
& + 2l_{s1}l_{s2}m_{s3}\,cos\,\theta_{s_2}\big)\ddot{\theta}_{s_1} + l_{s2}l_{s3}m_{s3}\,\ddot{\theta}_{s_2}cos\,\theta_{s_3} \\
& + \Big(\frac{1}{3}l_{s2}^2m_2 + l_{s2}^2m_{s3}\Big)\ddot{\theta}_{s_{12}} + \frac{1}{3}l_{s3}^2m_{s3}\ddot{\theta}_{s_{123}} \\
& + \frac{1}{2}l_{s2}l_{s3}m_{s3}\ddot{\theta}_{s_3}cos\theta_{s_3} \\
& + \frac{1}{2}\big(l_{s2}^2m_{s2}\,sin\theta_{s_2} + l_{s1}l_{s3}m_{s3}\,sin\,\theta_{s_{23}}\big)\dot{\theta}_{s_1}^2 \\
& - \frac{1}{2}l_{s2}l_{s3}m_{s3}\dot{\theta}_{s_3}^2sin\theta_{s_3} \\
& - l_{s2}l_{s3}m_{s3}\big(\dot{\theta}_{s_1}\dot{\theta}_{s_3} + \dot{\theta}_{s_2}\dot{\theta}_{s_3}\big)sin\theta_{s_3}
\end{aligned}
\tag{2.17}
$$

$$
\begin{aligned}
\tau_{s_3} = {}^3f_3^T\hat{Z}_3 = {} & \left(\tfrac{1}{3}m_{s3}l_{s3}^2 + \tfrac{1}{2}l_{s2}l_{s3}m_{s3}\cos\theta_{s_3}\right. \\
& \left. + \tfrac{1}{2}l_{s1}l_{s3}m_{s3}\cos\theta_{s_{23}}\right)\ddot{\theta}_{s_1} + \left(\tfrac{1}{3}m_{s3}l_{s3}^2\right)\ddot{\theta}_{s_3} \\
& + \left(\frac{1}{2}l_{s2}l_{s3}m_{s3}\,cos\,\theta_{s_3} + \tfrac{1}{3}m_{s3}l_{s3}^2\right)\ddot{\theta}_{s_2} \\
& + \left(\tfrac{1}{2}l_{s2}l_{s3}m_{s3}\,sin\,\theta_{s_3} + \tfrac{1}{2}l_{s1}l_{s3}m_{s3}\,sin\,\theta_{s_{23}}\right)\dot{\theta}_{s_1}^2 \\
& + \tfrac{1}{2}l_{s2}l_{s3}m_{s3}\,sin\,\theta_{s_3}\,\dot{\theta}_{s_2}^2 + l_{s2}l_{s3}m_{s3}\,sin\,\theta_{s_3}\dot{\theta}_{s_1}\dot{\theta}_{s_2}
\end{aligned}
\tag{2.18}
$$

By substituting (2.16) - (2.18) in (2.1), the dynamic model in (2.1) can be specified for 3 DoF revolute joint robot manipulator as

$$
M_s(\theta_s)\ddot{\theta}_s + V_s\left(\theta_s, \dot{\theta}_s\right)\dot{\theta}_s = \tau_s \tag{2.19}
$$

where $V_s \in \mathbb{R}^{3\times3}$ is a matrix and that is used for the definition given as $V_s\dot{\theta}_s \triangleq C_s\dot{\theta}_s + G_s$. At this point it should be noted that dimensions of the all terms in (2.19) are assumed to be adjusted according to a 3 DoF RRR robot manipulator.

The following computations can be used to reach elements of the inertia matrix M_s and the matrix V_s given in (2.19)

$$
\begin{aligned}
M_{s11} = {} & \tfrac{1}{3}l_{s1}^2m_1 + l_{s1}^2(m_{s2} + m_{s3}) + \tfrac{1}{3}m_{s3}l_{s3}^2 + \tfrac{1}{3}l_{s2}^2m_{s2} + l_{s2}^2m_{s3} \\
& + l_{s1}l_{s3}m_{s3}\cos\theta_{s_{23}} + 2l_{s1}l_{s2}m_{s3}\cos\theta_{s_2} \\
& + l_{s1}l_{s2}m_{s2}\cos\theta_{s_2} + l_{s2}l_{s3}m_{s3}\cos\theta_{s_3} \\
M_{s12} = {} & \tfrac{1}{3}m_{s3}l_{s3}^2 + \tfrac{1}{3}l_{s2}^2m_{s2} + l_{s2}^2m_{s3} + \tfrac{1}{2}l_{s1}l_{s3}m_{s3}\cos\theta_{s_{23}} \\
& + l_{s1}l_{s2}m_{s3}\cos\theta_{s_2} + \tfrac{1}{2}l_{s1}l_{s2}m_{s2}\cos\theta_{s_2} \\
& + l_{s2}l_{s3}m_{s3}\cos\theta_{s_3} \\
M_{s13} = {} & \tfrac{1}{3}m_{s3}l_{s3}^2 + \tfrac{1}{2}l_{s2}l_{s3}m_{s3}\cos\theta_{s_3} + \tfrac{1}{2}l_{s1}l_{s3}m_{s3}\cos\theta_{s_{23}} \\
M_{s22} = {} & \tfrac{1}{3}m_{s3}l_{s3}^2 + \tfrac{1}{3}l_{s2}^2m_{s2} + l_{s2}^2m_{s3} + l_{s2}l_{s3}m_{s3}\cos\theta_{s_3} \\
M_{s23} = {} & \frac{1}{2}l_{s2}l_{s3}m_{s3}\,cos\,\theta_{s_3} + \tfrac{1}{3}m_{s3}l_{s3}^2 \\
M_{s33} = {} & \tfrac{1}{3}m_{s3}l_{s3}^2 \\
V_{s11} = {} & \left(\tfrac{1}{2}l_{s2}^2m_{s2}\,sin\,\theta_{s_2}\right. \\
& + \tfrac{1}{2}l_{s1}l_{s3}m_{s3}\,sin\,\theta_{s_{23}} - 2l_{s1}l_{s2}m_{s3}\,sin\,\theta_{s_2} \\
& \left. - \tfrac{1}{2}l_{s1}l_{s2}m_{s2}\,sin\,\theta_{s_2}\right)\dot{\theta}_{s_1} \\
& - \left(l_{s2}l_{s3}m_{s3}\sin\theta_{s_3} + l_{s1}l_{s3}m_{s3}\sin\theta_{s_{23}}\right)\dot{\theta}_{s_3}
\end{aligned}
\tag{2.20}
$$

$$
\begin{aligned}
V_{s12} = -\dot{\theta}_{s_1}(& l_{s1}l_{s3}m_{s3}\, sin\,\theta_{s_{23}} \\
& + 2l_{s1}l_{s2}m_{s3}\, sin\theta_{s_2} + l_{s1}l_{s2}m_{s2}\, sin\,\theta_{s_2}) \\
& - \left(\tfrac{1}{2}l_{s_1}l_{s_3}m_{s_3}\, sin\theta_{s_{23}} + l_{s1}l_{s2}m_{s3}\, sin\,\theta_{s_2}\right. \\
& \left. + \tfrac{1}{2}l_{s1}l_{s2}m_{s2}\, sin\,\theta_{s_2}\right)\dot{\theta}_{s_2} \\
& - \left(l_{s2}l_{s3}m_{s3}\, sin\,\theta_{s_3} + l_{s1}l_{s3}m_{s3}\, sin\,\theta_{s_{23}}\right)\dot{\theta}_{s_3}
\end{aligned}
$$

$$
V_{s13} = -\frac{1}{2}\left(l_{s2}l_{s3}m_{s3}\, sin\,\theta_{s_3} + l_{s1}l_{s3}m_{s3}\, sin\,\theta_{s_{23}}\right)\dot{\theta}_{s_3}
$$

$$
\begin{aligned}
V_{ss21} = & \tfrac{1}{2}\left(l_{s2}^2 m_{s2}\, sin\,\theta_{s_2} + l_{s1}l_{s3}m_{s3}\, sin\,\theta_{s_{23}}\right)\dot{\theta}_{s_1} \\
& - l_{s2}l_{s3}m_{s3}\, sin\,\theta_{s_3}\,\dot{\theta}_{s_3}
\end{aligned}
$$

$$
V_{s22} = -l_{s2}l_{s3}m_{s3}\, sin\,\theta_{s_3}\,\dot{\theta}_{s_3}
$$

$$
V_{s23} = -\tfrac{1}{2}l_{s2}l_{s3}m_{s3}\, sin\,\theta_{s_3}\,\dot{\theta}_{s_3}
$$

$$
\begin{aligned}
V_{s31} = & \left(\tfrac{1}{2}l_{s2}l_{s3}m_{s3}\, sin\,\theta_{s_3} + \tfrac{1}{2}l_{s1}l_{s3}m_{s3}\, sin\,\theta_{s_{23}}\right)\dot{\theta}_{s_1} \\
& + l_{s_2}l_{s_3}m_{s3}\, sin\,\theta_{s_3}\dot{\theta}_{s_2}
\end{aligned}
$$

$$
V_{s32} = \tfrac{1}{2}l_{s_2}l_{s_3}m_{s_3}\, sin\,\theta_{s_3}\,\dot{\theta}_{s_2}^2
$$

$$
V_{s33} = 0.
$$

At this point it should be noted that, the remaining elements of M can be reached via its symmetry.

2.3 Modeling of Parallel Robotic System

Since the parallel robotic system is a 5 DoF robot manipulator that contains both of revolute and prismatic joints and two independently movable end effectors into its structure, the modeling study presented in this chapter is specified for this type of system. The Lagrange formulation is used to obtain the dynamic model, and the modeling steps and the mathematical equations obtained for each step are given in a detailed manner. At this point it should be noted that all dynamic models are presented parametrically in the following chapters. Obtaining a model structure where the possible changes in the parameters of robot manipulators (link masses, used material, link lengths and etc.) can easily be applied is the main purpose of this presentation.

2.3.1 Lagrange Formulation

The Lagrange formulation used to obtain dynamic model terms is given as

$$\frac{d}{dt}\left(\frac{\partial L}{\partial \dot{\theta}_{p_j}}\right) - \frac{\partial L}{\partial \theta_{p_j}} = \tau_{p_j} + \sum_{i=1}^{k} \lambda_i \frac{\partial \Gamma_i}{\partial \theta_{p_j}}, \tag{2.21}$$

where $i = 1, \cdots, k$ and $j = 1, \cdots, n$. In (2.21), $\theta_{p_j} \in \mathbb{R}$ represent generalized coordinates, $\tau_{p_j} \in \mathbb{R}$ represent actuator torques and forces, $\lambda_i \in \mathbb{R}$ represent Lagrange multipliers and $\Gamma_i \in \mathbb{R}$ represent constraint functions. Manipulator's kinetic energy and potential energy are denoted by K and $U \in \mathbb{R}$, respectively while the definition $L \triangleq K - U$ is utilized. Moreover, $k \in \mathbb{R}$ denotes the total number of constraint functions, and $n \in \mathbb{R}$ denotes the total number of generalized coordinates. The Lagrange formulation in (2.21) can be decomposed into a total of n equation sets that can be expressed as

$$\begin{aligned} \sum_{i=1}^{k} \lambda_i \frac{\partial \Gamma_i}{\partial \theta_{p_j}} &= \frac{d}{dt}\left(\frac{\partial L}{\partial \dot{\theta}_{p_j}}\right) - \frac{\partial L}{\partial \theta_{p_j}} - \tau_{p_j} \\ \tau_{p_j} &= \frac{d}{dt}\left(\frac{\partial L}{\partial \dot{\theta}_{p_j}}\right) - \frac{\partial L}{\partial \theta_{p_j}} - \sum_{i=1}^{k} \lambda_i \frac{\partial \Gamma_i}{\partial \theta_{p_j}}. \end{aligned} \tag{2.22}$$

Kinetic energy of the system is expressed as

$$K = \frac{1}{2}\sum_{i=1}^{n}\left[I_{p_i}{\omega_{p_i}}^2 + m_{pi}\left({\dot{\rho}_{miu}}^2 + {\dot{\rho}_{miv}}^2\right)^2\right] = \frac{1}{2}\dot{\theta}_p^T M \dot{\theta}_p \tag{2.23}$$

where $\dot{\rho}_{miu}$ and $\dot{\rho}_{miv} \in \mathbb{R}$ represent u and v component of linear velocities of i^{th} link respectively and $\omega_{p_i} \in \mathbb{R}$ represents the angular velocity of the i^{th} link.

Potential energy of the system is expressed as

$$U = \sum_{i=1}^{n} m_{pi} g h_{mi} = g {m_v}^T H \tag{2.24}$$

where $h_{mi} \in \mathbb{R}$ is the height of the link centers of gravity with respect to the global reference system, $m_v \triangleq [m_{p1}, m_{p2}, \dots, m_{pn}]^T \in \mathbb{R}^n$ is the vector containing the mass of links, $H \triangleq [h_{m1}, h_{m2}, \dots, h_{mn}]^T \in \mathbb{R}^n$ represents the vector containing the heights.

The part containing the constraint functions in (2.21) is expressed as

$$\sum_{i=1}^{k} \lambda_i \frac{\partial \Gamma_i}{\partial \theta_{p_j}} = \begin{bmatrix} \frac{\partial \Gamma_1}{\partial \theta_{p_1}} & \cdots & \frac{\partial \Gamma_k}{\partial \theta_{p_1}} \\ \vdots & \ddots & \vdots \\ \frac{\partial \Gamma_1}{\partial \theta_{p_j}} & \cdots & \frac{\partial \Gamma_k}{\partial \theta_{p_j}} \end{bmatrix} \begin{bmatrix} \lambda_1 \\ \vdots \\ \lambda_k \end{bmatrix} = \Gamma_c. \tag{2.25}$$

Finally, equation of motion produced according to Lagrange method can be obtained as follows by substituting (2.23)-(2.25) in (2.21)

$$M\ddot{\theta}_p + \dot{M}\dot{\theta}_p - \frac{\partial K}{\partial \theta_p} + \frac{\partial U}{\partial \theta_p} + \begin{bmatrix} \frac{\partial \Gamma_1}{\partial \theta_{p_1}} & \cdots & \frac{\partial \Gamma_k}{\partial \theta_{p_1}} \\ \vdots & \ddots & \vdots \\ \frac{\partial \Gamma_1}{\partial \theta_{p_j}} & \cdots & \frac{\partial \Gamma_k}{\partial \theta_{p_j}} \end{bmatrix} \begin{bmatrix} \lambda_1 \\ \vdots \\ \lambda_k \end{bmatrix} = \tau_p \tag{2.26}$$

2.3.2 Derivation of the Dynamic Model of 5 DoF Revolute Prismatic Joint Robot Manipulator via Lagrange Formulation

To obtain the dynamic model of 5DoF robot manipulator, kinetic energy in (2.23) is rearranged as

$$K = \frac{1}{2}\dot{\theta}_p^T I_{15}\dot{\theta}_p + \frac{1}{2}\dot{\theta}_p^T F^T I_{57} F\dot{\theta}_p + \frac{1}{2}\dot{\theta}_p^T X^T m_v X\dot{\theta}_p + \frac{1}{2}\dot{\theta}_p^T Y^T m_v Y\dot{\theta}_p \tag{2.27}$$

where

$$\dot{\theta}_p \triangleq \left[\dot{\theta}_{p1}, \dot{\theta}_{p2}, \dot{d}_1, \dot{\theta}_{p1}', \dot{\theta}_{p2}'\right]^T$$

$$I_{15} \triangleq \begin{bmatrix} I_{p_1}+I_{p_3} & 0 & 0 & 0 & 0 \\ 0 & I_{p_2}+I_{p_4} & 0 & 0 & 0 \\ 0 & 0 & 0 & 0 & 0 \\ 0 & 0 & 0 & I_{p_1}+I_{p_3} & 0 \\ 0 & 0 & 0 & 0 & I_{p_2}+I_{p_4} \end{bmatrix}$$

$$I_{57} \triangleq \begin{bmatrix} I_{p_5}+I_{p_7} & 0 \\ 0 & I_{p_5}+I_{p_7} \end{bmatrix}$$

$$F \triangleq \begin{bmatrix} \frac{Z_1}{W_1} & \frac{Z_2}{W_1} & \frac{Z_5}{W_1} & 0 & 0 \\ 0 & 0 & \frac{Z_6}{W_2} & \frac{Z_3}{W_2} & \frac{Z_4}{W_2} \end{bmatrix}$$

$$X \triangleq \begin{bmatrix} -\frac{l_p}{2}\sin\theta_{p_1} & 0 & 0 & 0 & 0 \\ -l_p\sin\theta_{p_1} & -\frac{l_p}{2}\sin\theta_{p_2} & 0 & 0 & 0 \\ -\frac{l_p}{2}\sin\theta_{p_1} & -l_p\sin\theta_{p_2} & 0 & 0 & 0 \\ 0 & -\frac{l_p}{2}\sin\theta_{p_2} & 0 & 0 & 0 \\ -l_p\sin\theta_{p_1} & -l_p\sin\theta_{p_2} & 0 & 0 & 0 \\ 0 & -\frac{l_p}{2}\sin\theta_{p_2} & 0 & 0 & 0 \\ Z_7\sin\phi_p & Z_8\sin\phi_p & Z_9\sin\phi_p & 0 & 0 \\ 0 & 0 & 0 & -\frac{l_p}{2}\sin\theta'_{p_1} & 0 \\ 0 & 0 & 0 & -l_p\sin\theta'_{p_2} & -\frac{l_p}{2}\sin\theta'_{p_2} \\ 0 & 0 & 0 & -\frac{l_p}{2}\sin\theta'_{p_2} & -l_p\sin\theta'_{p_2} \\ 0 & 0 & 0 & 0 & -\frac{l_p}{2}\sin\theta'_{p_2} \\ 0 & 0 & 0 & -l_p\sin\theta'_{p_2} & -l_p\sin\theta'_{p_2} \\ 0 & 0 & Z_{10}\sin\phi'_p & Z_{11}\sin\phi'_p & Z_{12}\sin\phi'_p \end{bmatrix} \tag{2.28}$$

$$Y \triangleq \begin{bmatrix} \frac{l_p}{2}\cos\theta_{p_1} & 0 & 0 & 0 & 0 \\ l_p\cos\theta_{p_1} & \frac{l_p}{2}\cos\theta_{p_2} & 0 & 0 & 0 \\ \frac{l_p}{2}\cos\theta_{p_1} & l_p\cos\theta_{p_2} & 0 & 0 & 0 \\ 0 & \frac{l_p}{2}\cos\theta_{p_2} & 0 & 0 & 0 \\ l_p\cos\theta_{p_1} & l_p\cos\theta_{p_2} & 0 & 0 & 0 \\ 0 & \frac{l_p}{2}\cos\theta_{p_2} & 0 & 0 & 0 \\ Z_7\cos\phi_p & Z_8\cos\phi_p & Z_9\cos\phi_p & 0 & 0 \\ 0 & 0 & 0 & \frac{l_p}{2}\cos\theta'_{p_1} & 0 \\ 0 & 0 & 0 & l_p\cos\theta'_{p_2} & \frac{l_p}{2}\cos\theta'_{p_2} \\ 0 & 0 & 0 & \frac{l_p}{2}\cos\theta'_{p_2} & l_p\cos\theta'_{p_2} \\ 0 & 0 & 0 & 0 & \frac{l_p}{2}\cos\theta'_{p_2} \\ 0 & 0 & 0 & l_p\cos\theta'_{p_2} & l_p\cos\theta'_{p_2} \\ 0 & 0 & Z_{10}\cos\phi'_p & Z_{11}\cos\phi'_p & Z_{12}\cos\phi'_p \end{bmatrix}.$$

At this point it should be noted that $W_{1,2}$ and Z_i for $i = 1, \cdots, 12$ are given in a detailed manner in Appendix A.

From (2.23), (2.27) and (2.28) the inertia matrix $M \in \mathbb{R}^{5\times5}$ can be obtained as

$$M_p = I_{15} + F^T I_{57} F + X^T m_v X + Y^T m_v Y \tag{2.29}$$

and the term $\dot{M}_p\dot{\theta}_p$ can be obtained as follows from the time derivative of (2.29)

$$\dot{M}_p\dot{\theta}_p = \begin{bmatrix} \dot{\theta}_p^T \begin{bmatrix} \frac{\partial M_{p11}}{\partial \theta_{p_1}} & \cdots & \frac{\partial M_{p15}}{\partial \theta_{p_1}} \\ \vdots & \ddots & \vdots \\ \frac{\partial M_{p11}}{\partial \theta'_{p_2}} & \cdots & \frac{\partial M_{p15}}{\partial \theta'_{p_2}} \end{bmatrix} \dot{\theta}_p \\ \vdots \\ \dot{\theta}_p^T \begin{bmatrix} \frac{\partial M_{p15}}{\partial \theta_{p_1}} & \cdots & \frac{\partial M_{p55}}{\partial \theta_{p_1}} \\ \vdots & \ddots & \vdots \\ \frac{\partial M_{p15}}{\partial \theta'_{p_2}} & \cdots & \frac{\partial M_{p55}}{\partial \theta'_{p_2}} \end{bmatrix} \dot{\theta}_p \end{bmatrix} \tag{2.30}$$

From (2.27) and (2.29) it can be seen that the term $\frac{\partial K}{\partial \theta_p}$ can be expressed as

$$\frac{\partial K}{\partial \theta_p} = \frac{1}{2}\begin{bmatrix} \dot{\theta}_p^T \begin{bmatrix} \frac{\partial M_{p11}}{\partial \theta_{p_1}} \\ \vdots \\ \frac{\partial M_{p15}}{\partial \theta_{p_1}} \end{bmatrix} & \cdots & \dot{\theta}_p^T \begin{bmatrix} \frac{\partial M_{p15}}{\partial \theta_{p_1}} \\ \vdots \\ \frac{\partial M_{p55}}{\partial \theta_{p_1}} \end{bmatrix} \\ \vdots & \ddots & \vdots \\ \dot{\theta}_p^T \begin{bmatrix} \frac{\partial M_{p11}}{\partial \theta'_{p_2}} \\ \vdots \\ \frac{\partial M_{p15}}{\partial \theta'_{p_2}} \end{bmatrix} & \cdots & \dot{\theta}_p^T \begin{bmatrix} \frac{\partial M_{p15}}{\partial \theta'_{p_2}} \\ \vdots \\ \frac{\partial M_{p55}}{\partial \theta'_{p_2}} \end{bmatrix} \end{bmatrix} \dot{\theta}_p. \tag{2.31}$$

The Centripetal-coriolis matrix $C_p \in \mathbb{R}^{5\times5}$ specified for 5 DoF robot manipulator can be obtained as follows by using (2.29)-(2.31) in (2.26) and considering this result with the general form in (2.1)

$$C_p = \frac{1}{2}\begin{bmatrix} \dot{\theta}_p^T \begin{bmatrix} \frac{\partial M_{p11}}{\partial \theta_{p_1}} \\ \vdots \\ 2\frac{\partial M_{p11}}{\partial \theta'_{p_2}} - \frac{\partial M_{p15}}{\partial \theta_{p_1}} \end{bmatrix} & \cdots & \dot{\theta}_p^T \begin{bmatrix} \frac{\partial M_{p15}}{\partial \theta_{p_1}} \\ \vdots \\ 2\frac{\partial M_{p15}}{\partial \theta'_{p_2}} - \frac{\partial M_{p55}}{\partial \theta_{p_1}} \end{bmatrix} \\ \vdots & \ddots & \vdots \\ \dot{\theta}_p^T \begin{bmatrix} 2\frac{\partial M_{p15}}{\partial \theta_{p_1}} - \frac{\partial M_{p11}}{\partial \theta'_{p_2}} \\ \vdots \\ \frac{\partial M_{p15}}{\partial \theta'_{p_2}} \end{bmatrix} & \cdots & \dot{\theta}_p^T \begin{bmatrix} 2\frac{\partial M_{p55}}{\partial \theta_{p_1}} - \frac{\partial M_{p15}}{\partial \theta'_{p_2}} \\ \vdots \\ \frac{\partial M_{p55}}{\partial \theta'_{p_2}} \end{bmatrix} \end{bmatrix}. \tag{2.32}$$

The vector of gravatitional forces $G_p \in \mathbb{R}^5$ specified for 5 DoF robot manipulator can be obtained as follows by using (2.24) in the general form in (2.1)

$$G_p = \begin{bmatrix} \frac{\partial U}{\partial \theta_{p_1}} & \frac{\partial U}{\partial \theta_{p_2}} & \frac{\partial U}{\partial d_1} & \frac{\partial U}{\partial \theta'_{p_1}} & \frac{\partial U}{\partial \theta'_{p_2}} \end{bmatrix}^{\boldsymbol{T}} \tag{2.33}$$

where the derivative of the constraint equations according to the system actuator variables are zero and Γ_c is the zero vector.

By using (2.27)-(2.32) in (2.26), compact form of the dynamic model of 5 DoF robot manipulator can be obtained as

$$M_p\ddot{\theta}_p + V_p(\theta_p, \dot{\theta}_p)\dot{\theta}_p = \tau_p \tag{2.34}$$

where $V_p \in \mathbb{R}^{5\times5}$ is a matrix that is used for the definition given as $V_p\dot{\theta}_p \triangleq C_p\dot{\theta}_p + G_p = \dot{M}_p\dot{\theta}_p - \frac{\partial K}{\partial \theta_p} + \frac{\partial U}{\partial \theta_p}$. At this point it should be noted that dimensions of the all terms in (2.34) are assumed to be adjusted according to a 5 DoF robot manipulator that contains both revolute and prismatic joints.

The following computations can be used to reach elements of the inertia matrix M_p and the matrix V_p given in (2.34)

$$\begin{aligned}
M_{p11} &= I_{p_1} + I_{p_3} + \frac{\left((I_{p_5} + I_{p_7})(Z_1)^2\right)}{W_1^2} + \frac{l_p^2 m_{p3}}{4} + \frac{l_p^2 m_{p1}}{4} + l_p^2 m_2 \\
&\quad + l_p^2 m_{p5} + \frac{d_3^2 m_{p7}(Z_1)^2}{4\,(W_1)^2} \\
M_{p12} &= \frac{(I_{p_5} + I_{p_7})(Z_1)(Z_2)}{W_1^2} + \frac{l_p^2 m_{p2}\cos(\theta_{p_1} - \theta_{p_2})}{2} \\
&\quad + \frac{l_p^2 m_{p3}\cos(\theta_{p_1} - \theta_{p_2})}{2} + l_p^2\, m_{p5}\cos(\theta_{p_1} - \theta_{p_2}) \\
&\quad + \frac{d_3^2 m_{p7}(Z_1)(Z_2)}{(2W_1)^2} \\
M_{p13} &= -\frac{(I_{p_5} + I_{p_7})\left(d_2 + l_p\cos\theta_{p_1} + \frac{l_p\cos\theta_{p_2}}{W_1}\right)Z_1}{W_1} \\
&\quad - \frac{d_3^2 m_{p7}\sin^2\phi_p\left(d_2 + l_p\cos\theta_{p_1} + \frac{l_p\cos\theta_{p_2}}{W_1}\right)Z_1}{2W_1} \\
M_{p14} &= 0 \\
M_{p15} &= 0 \\
M_{p22} &= I_{p_2} + I_{p_4} + \frac{(I_{p_5} + I_{p_7})(Z_2)^2}{(W_1)^2} + \frac{l_p^2 m_{p2}}{4} + l_p^2 m_{p3} + \frac{l_p^2 m_{p4}}{2} \\
&\quad + 2l_p^2 m_{p5} + \frac{d_3^2 m_{p7}(Z_2)^2}{4(W_1)^2} \\
M_{p23} &= -\frac{(I_{p_5} + I_{p_7})\left(d_2 + l_p\cos\theta_{p_1} + \frac{l_p\cos\theta_{p_2}}{W_1}\right)Z_2}{W_1} \\
&\quad - \frac{\left(d_3^2 m_{p7}\left(d_2 + l_p\cos\theta_{p_1} + \frac{l_p\cos\theta_{p_2}}{W_1}\right)Z_2\right)}{2W_1} \\
M_{p24} &= 0
\end{aligned} \tag{2.35}$$

$$M_{p25} = 0$$

$$M_{p33} = m_{p6} + m_{p7}\left(\frac{d_3 cos\phi_p (d_2 + l_p cos\theta_{p_1} + \frac{l_p cos\theta_{p_2}}{W_1})}{2} - 1\right)^2 + \left(I_{p_5} + I_{p_7}\right)(d_2 + l_p cos\theta_{p_1} + \frac{l_p cos\theta_{p_2}}{W_1})^2 + \frac{d_3^2 m_{p7} sin^2\phi_p (d_2 + l_p cos\theta_{p_1} + \frac{l_p cos\theta_{p_2}}{YW_1})^2}{4}$$

$$M_{p34} = -\frac{\left(I_{p_5} + I_{p_7}\right)\left(l_p cos\theta'_{p_1} - d_2 + l_p cos\theta'_{p_2}\right)Z_4}{W_2^2} - \frac{d_3^2 m_{p7}\left(l_p cos\theta'_{p_1} - d_2 + l_p cos\theta'_{p_2}\right)Z_4}{(2W_2)^2} + \frac{d_3 m_{p7} cos\,\phi'_p Z_4}{2W_2}$$

$$M_{p35} = M_{p53} = -\frac{\left(I_{p_5} + I_{p_7}\right)\left(l_p cos\,\theta'_{p1} - d_2 + l_p cos\,\theta'_{p2}\right)Z_4}{W_2^2} - \frac{d_3^2 m_{p7}\left(l_p cos\,\theta'_{p1} - d_2 + l_p cos\,\theta'_{p2}\right)Z_4}{(2W_2)^2} + \frac{\left(d_3 m_{p7} cos\,\phi'_p\right)Z_4}{2W_2}$$

$$M_{p44} = I_{p_1} + I_{p_3} + \frac{\left(I_{p_5} + I_{p_7}\right)(Z_3)^2}{W_2^2} + \frac{l_p^2 m_{p1}}{4} + l_p^2 m_{p2} + \frac{l_p^2 m_3}{4} + l_p^2 m_{p5} + \frac{d_3^2 m_{p7}(Z_3)^2}{(2W_2)^2}$$

$$M_{p45} = \frac{\left(I_{p_5} + I_{p_7}\right)Z_3 Z_4}{W^2} + \frac{d_3^2 m_{p7} Z_3 Z_4}{4\,(W_2)^2} + \frac{l_p^2 m_{p2}\,cos\left(\theta'_{p_1} - \theta'_{p_2}\right)}{2} + \frac{l_p^2 m_{p_3}\,cos\left(\theta'_{p_1} - \theta'_{p_2}\right)}{2} + l_p^2 m_{p5}\,cos\left(\theta'_{p_1} - \theta'_{p_2}\right)$$

$$M_{p55} = I_{p_2} + I_{p_4} + \frac{\left(I_{p_5} + I_{p_7}\right)(Z_4)^2}{W_2^2} + \frac{l_p^2 m_{p2}}{4} + l_p^2 m_{p3} + \frac{l_p^2 m_{p4}}{4} + l_p^2 m_{p5} + \frac{d_3^2 m_{p7}(Z_4)^2}{(2W_2)^2}$$

$$V_{1i} = v_{p1i}\left(\dot{\theta}_{p_1}, \dot{\theta}_{p_2}, \dot{d}_1, \theta_{p_1}, \theta_{p_2}, d_1\right)$$

$$V_{2i} = v_{p2i}\left(\dot{\theta}_{p_1}, \dot{\theta}_{p_2}, \dot{d}_1, \theta_{p_1}, \theta_{p_2}, d_1\right)$$

$$V_{3i} = v_{p3i}\left(\dot{\theta}_{p_1}, \dot{\theta}_{p_2}, \dot{d}_1, \dot{\theta}'_{p_1}, \dot{\theta}'_{p_2}, \theta_{p_1}, \theta_{p_2}, d_1, \theta'_{p_1}, \theta'_{p_2}\right)$$

$$V_{4i} = v_{p4i}\left(\dot{\theta}'_{p_1}, \dot{\theta}'_{p_2}, \dot{d}_1, d_1, \theta'_{p_1}, \theta'_{p_2}\right)$$

$$V_{5i} = v_{p5i}\left(\dot{\theta}'_{p_1}, \dot{\theta}'_{p_2}, \dot{d}_1, d_1, \theta'_{p_1}, \theta'_{p_2}\right)$$

where j = 1, ⋯ ,5 at this point it should be noted that further detail about the terms in (2.35) can be found in Appendix B.The remaining elements of M_p can be reached via its symmetry.

.

Chapter 3

Controller Design and Analysis for Robotic Systems

In this chapter, control designs realized for both robotic systems, theoretical analysis of these control designs and performance demonstration of the designed controllers in simulation and experimental studies are presented. At this point it should be noted that two different robust adaptive controllers one of which is realized in joint space while the other one is realized in task space are designed for both robotic systems. Theoretical analysis of the designed controllers is realized via Lyapunov based arguments while their efficiency and performance are tested in simulation and experimental studies. Dynamic models obtained in Chapter 2 are utilized to conduct simulation studies while experimental studies are realized on experimental setups produced within the scope of the project in which this study is included. Providing multiple options that can be used for the control of robotic systems used as supportive systems in cochlear microrobot surgical operations is the main reason for the control design in both joint and task space.

It should be noted that the ascept which movement of the joints of both manipulator systems are ensured via current driven direct current motors and there is a linear relationship between torque and current is accepted as valid during the control designs by considering the experimental setup.This relationship was experimentally obtained. All the details about obtaining this relationship are given in the Appendix C.

3.1 Robust Adaptive Control Design for Serial Robotic System

In this chapter, two different control designs are presented for the serial robotic system that contains two independent 3 DoF RRR serial robot manipulators. The main objective of this system is to control the position of the microrobot by utilizing the magnetic field created with the help of magnets located at the end effectors of the mentioned robot manipulators. However, to ensure the permanence of the created magnetic field and its effectiveness on the microrobot, the movements of robot manipulators must be continued so that the distance between their end effectors is always protected. The successful operation of the system is possible with the synchronous control of the positions of the end effectors. To achieve this goal, the main control objective is determined as the end effector of one of the two structurally identical robot manipulators to follow the desired trajectory, and the end effector of the other to operate synchronously with respect to the first end effector by keeping the distance between the two end effectors.

From the control purpose, it can be reached that the main task is determined in the space of end effector and this space is called as task space. There are two possible approaches to realize a trajectory tracking in the task space. In the common approach frequently encountered in the literature trajectory of the joint space is obtained according to the desired trajectory of the task space via inverse kinematic and the control design is realized in the joint space. In another approach that has recently been encountered in the literature, the control design is directly realized in the task space. All approaches are presented in this chapter. Robust control design is preferred to take the advantage of the structure that is able to cope with parameter uncertainties, parameter changes and external disturbances. To deal with possible high control effort necessity of the robust controllers its structure is supported via adaptive compensations and as a result of these robust adaptive control designs are realized for both joint space and task space controllers. At this point it should be noted that the robot manipulators in the robotic system are primarily modeled and their models are completely known. However, in the future, control designs independent of model knowledge are aimed due to the possible negative effects that

situations such as possible changes in experimental systems, system dynamics that cannot be modeled, disturbances and etc. can cause in the control signal and process. For this purpose, robust adaptive control designs are proposed for both cases.

The following items are accepted as valid during the control designs by considering the experimental setup:

- The angular position and angular velocity of all joints are measurable.
- The position and velocity of the end effectors of both robot manipulators are measurable.
- All measurable system states are known by the other robot manipulator.
- The control input signal is sent to both robot manipulators via the same computer with an equal amount of time delay.

In the following subsections, control designs, related analyses and performance verifications of designed controllers are presented in a detailed manner. The most important thing to consider here is that, although the control objectives are common, the two controller structures are different completely different it and realizing a performance comparison between them is not an appropriate approach. Obtaining more than one controller designs that are available for the experimental system and are suitable for achieving the control objective is the main aim of realizing the trajectory tracking in both joint space and task space.

3.1.1 Joint Space Control of 3 DoF RRR Serial Manipulator

The main purpose of the joint space control is to reach the tracking trajectory in the joint space by using inverse kinematics in order to find the equivalent of the tracking trajectory determined in the task space. And then, a control design that makes the difference between the angular positions of the joints and the determined trajectory to zero is proposed. Robust control design approach is preferred to cope with parametric uncertainties. However, as can be seen from the literature, the biggest challenge of this type of control design is the possibility of needing a higher control effort. To overcome this issue, the designed robust controller is supported with adaptive compensations, which is a frequently preferred approach in the literature.

3.1.1.1 Model Properties

The dynamic model in (2.19) is used with the following skew-symmetry and boundedness properties that are valid for all robot manipulators having an identical structure with robot manipulators used in this study

$$h^T \left(\frac{1}{2}\dot{M}_s - V_s\right) h = 0, \forall \mathrm{h} \in \mathbb{R}^3. \tag{3.1}$$

At this point it should be noted that, the robotic system consists of two robot manipulators having the identical structure. Since the proposed control design is independent from system parameters, it is a valid control design for all structurally identical robot manipulators. For this reason, the control purpose can be achieved by applying the control design made on the model given in this chapter to both robot manipulators. Owing to this issue the control designs proposed in this chapter are given by considering the general structure given in (2.19) and at the end of the control design process a controller that can be used for the control of both robot manipulators included in the serial robotic system. The only notation specification is made in the simulation sections to show the control gains of two robot manipulators separately.

3.1.1.2 Error System Development

The tracking error is defined as the difference between the desired trajectory obtained via inverse kinematics from the desired of the end effector and the measured positions of the joint angles. The mathematical expression of the tracking error is given as

$$e_e \triangleq \theta_{s_d} - \theta_s \tag{3.2}$$

where $\theta_{s_d} \in \mathbb{R}^3$ denotes second order differentiable, bounded, and sufficiently smooth desired trajectory. Boundedness of the desired trajectory and its first and second order time derivatives are other properties that are utilized in the control design. An auxiliary error term denoted by $r_e \in \mathbb{R}^3$ is defined as

$$r_e \triangleq \dot{e}_e + \alpha_e e_e \tag{3.3}$$

where $\alpha_e \in \mathbb{R}^{3\times3}$ is a positive definite, diagonal and constant gain matrix. The following expression can be obtained by premultiplying the time derivative of (3.3) is with M_s and and adding the term $V_s r_e$ to the both sides of the resulting equation

$$M_s \dot{r}_e = f_{d_e} - \tau_s - V_s r_e - e_e \tag{3.4}$$

where (2.19) and (3.2) are utilized. An auxiliary term $f_{d_e} \in \mathbb{R}^3$ is defined as

$$f_{d_e} \triangleq M_s \ddot{\theta}_{s_d} + V_s \dot{\theta}_s + V_s r_e + M_s \alpha_e \dot{e}_e + e_e. \tag{3.5}$$

For the following steps of the controller design and analysis, this auxiliary can be decomposed as

$$f_{d_e} = Y_e\left(\theta_s, \dot{\theta}_s, \dot{\theta}_{s_d}, \ddot{\theta}_{s_d}\right)\phi_e \tag{3.6}$$

where $Y_e\left(\theta_s, \dot{\theta}_s, \dot{\theta}_{s_d}, \ddot{\theta}_{s_d}\right) \in \mathbb{R}^{3\times n}$ denotes the regression matrix containing the certain and measurable terms while $\phi_e \in \mathbb{R}^n$ indicates the uncertain constant vector containing the system parameters. To cope with the mentioned uncertainty, an adaptive

compensation terms $\hat{\phi}_e \in \mathbb{R}^n$ is utilized and the adaptive compensation error $\tilde{\phi}_e \in \mathbb{R}^n$ is defined as

$$\tilde{\phi}_e \triangleq \phi_e - \hat{\phi}_e. \tag{3.7}$$

By substituting the (3.6) and (3.7) into (3.4), the open loop error system can be obtained as

$$M_s \dot{r}_e = Y_e\left(\theta_s, \dot{\theta}_s, \ddot{\theta}_{sd}\right)\tilde{\phi}_e + Y_e\left(\theta_s, \dot{\theta}_s, \ddot{\theta}_{sd}\right)\hat{\phi}_e - \tau_s - V_s r_e - e_e \tag{3.8}$$

3.1.1.3 Control Design

Control input is designed as

$$\tau_s = Y_e \hat{\phi}_e + G_e r_e \tag{3.9}$$

where $G_e \in \mathbb{R}^{3\times3}$ denotes the positive definite, constant and diagonal control gain matrix. The closed loop error system required for stability analysis can be obtained as follows by substituting the designed controller in (3.8)

$$M_s \dot{r}_e = Y_e\left(\theta_s, \dot{\theta}_s, \ddot{\theta}_{s_d}\right)\tilde{\phi}_e - V_s r_e - G_e r_e - e_e. \tag{3.10}$$

After that point the analysis can be continued with the stability analysis.

3.1.1.4 Stability Analysis

Theorem 1: *The global asymptotic stability of the closed loop error system mathematically expressed as*

$$\|e_e(t)\|_{i_\infty} \; and \; \|r_e(t)\|_{i_\infty} \to 0 \; as \; t \to 0 \tag{3.11}$$

can be provided via the control design in (3.9) .

Proof: The nonnegative Lyapunov function candidate $V_e\left(\mathrm{e_e}, \mathrm{r_e}, \widetilde{\Phi}_\mathrm{e}\right) \in \mathbb{R}$ is selected as

$$V_e = \frac{1}{2}\left(e_e^T e_e + r_e^T M_s r_e + \tilde{\phi}_e{}^T \tilde{\phi}_e\right). \tag{3.12}$$

Time derivative of the Lyapunov function can be obtained as

$$\begin{aligned} \dot{V}_e = {} & e_e^T(r_e - \alpha_e e_e) - r_e^T G_e r_e + \tilde{\phi}_e{}^T\left[-\dot{\hat{\phi}}_e + Y_e^T r_e\right] \\ & + r_e^T\left(\frac{1}{2}\dot{M}_s - V_s\right) r_e - r_e^T e_e \end{aligned} \tag{3.13}$$

where (3.3), time derivative of (3.7) and (3.10) are utilized.

If the adaptive compensation $\hat{\phi}_e$ is updated according to the following rule

$$\dot{\hat{\phi}}_e = Y_e^T r_e \tag{3.14}$$

and the skew-symmetry property in (3.1) are utilized, (3.13) can be upper bounded as

$$\dot{V}_e \leq -\beta_e \|z_e\| \tag{3.15}$$

where $\beta_e \in \mathbb{R}$ denotes the positive constant defined as

$$\beta_e \triangleq -\min\{\lambda_{min}(\alpha_e), \lambda_{min}(G_e)\} \tag{3.16}$$

and the vector of combined error $z_e \in \mathbb{R}^6$ is (3.16) is defined as

$$z_e \triangleq [e_e^T \quad r_e^T]^T. \tag{3.17}$$

In (3.16), $\lambda_{min}(\cdot)$ denotes the minimum eigenvalue of the matrix.

The boundedness of $V_e(\mathrm{e_e}, \mathrm{r_e}, \widetilde{\Phi}_\mathrm{e})$ can be reached from (3.12) and (3.15) and it can be utilized to guarantee the boundedness of $z_e(t)$ and its elements (i.e., $z_e(t)$, $e_e(t)$ and $r_e(t) \in \mathcal{L}_\infty$). Standard signal chasing arguments can be utilized to show the boundedness of the all of the remaining closed-loop operation signals. The boundedness of $r_e(t)$ and $e_e(t)$ can be utilized along with (3.3) to show the boundedness of $\dot{e}(t)$ (i.e., $\dot{e}_e(t) \in \mathcal{L}_\infty$) and this results can be used to shown that $e_e(t)$ is a uniformly continuous signal. Finally, it can be shown that $z_e(t) \in \mathcal{L}_2$ from the integration of both sides of (3.15) and it proves that $e_e(t)$ and $z_e(t) \in \mathcal{L}_2$. The

asymptotic tracking result in Theorem 1 can be obtained when all of these boundedness statements are considered with the Barbalat's Lemma [61].

3.1.1.5 Simulation Studies

The following link lengths and masses that were selected in accordance with the experimental setup were used in the dynamic model in (2.19) for the simulation studies

$$l_{s1} = l_{s2} = 0.105\ m, l_{s3} = 0.04\ m$$
$$m_{s1} = 95.18\ g, m_{s2} = 78.78\ g, m_{s3} = 11.19\ g. \tag{3.18}$$

At this point it should be noted that the dimensions given in (3.18) are same for both of the robot manipulators in the serial robotic system. The desired trajectory of the first robot manipulator denoted by $\theta_{s_{d_{m_1}}} \in \mathbb{R}^3$ was determined in the joint space as follows, and the desired trajectory of the second robot manipulator was adjusted to follow position changes in the first robot manipulator while maintaining the distance between the end effectors

$$\theta_{s_{d_{m_1}}}(t) = \begin{bmatrix} 81.14 - 3.007\,cos(0.632t\,) - 0.129\,sin(0.632t) \\ 71.02 - 7.082cos(0.632t\,) + 0.09566\sin(0.632t) \\ 117.8 - 4.074cos(0.632t\,) + 0.03005sin(0.632t) \end{bmatrix} [deg] \tag{3.19}$$

The initial position of the first robot manipulator was selected as $\theta_{s_{m_1}}(0) = [73 \quad 83 \quad 110]^T[deg]$, and the initial position of the second robot manipulator was selected as $\theta_{s_{m_2}}(0) = [110 \quad -128 \quad 100]^T[deg]$. Controller gains were selected as follows via trial-and-error method for both robot manipulators

$$\alpha_{e_{1,2}} = diag\{5, 4, 3\}$$
$$G_{e_{1,2}} = diag\{\,0.05, 0.04, 0.003\} \tag{3.20}$$

where α_{e_i} and $G_{e_i} \in \mathbb{R}^{3\times3}$ denotes the gain values adjusted for i^{th} robot manipulator for $i = 1$ and 2.

Desired trajectories and actual positions are shown in Figures 3.1 and 3.2 for the first and second robot manipulators, respectively. Tracking errors are shown in Figures 3.3 and 3.4 for the first and second robot manipulators, respectively. From Figures 3.1-3.4, it can be seen that the control objective was met. Torques applied to the joints of the first and second robot manipulators are shown in Figures 3.5 and 3.6, respectively.

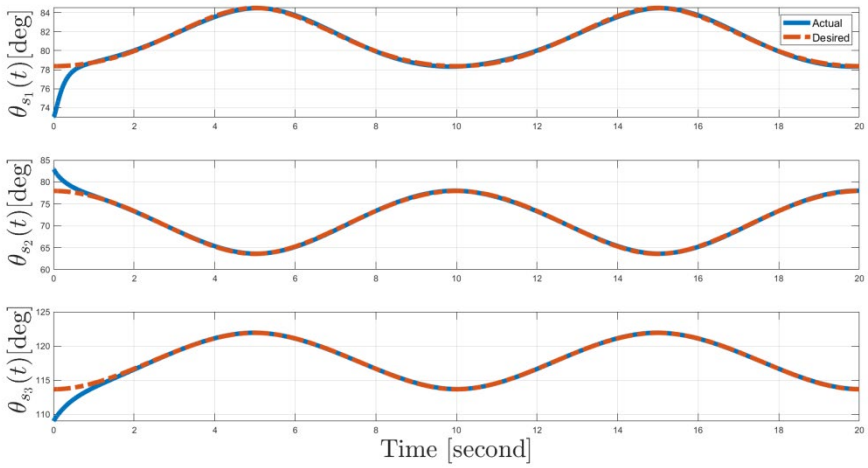

Figure 3.1: Desired vs. actual positions of the first robot manipulator's joints

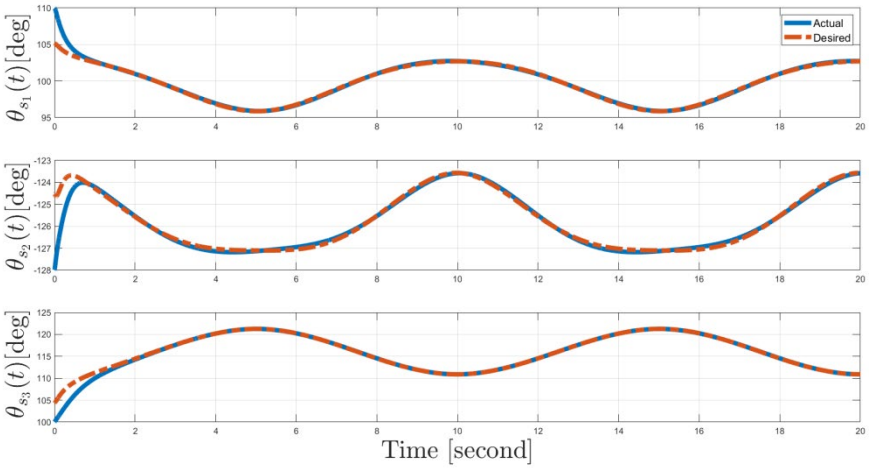

Figure 3.2: Desired vs. actual positions of the second robot manipulator's joints

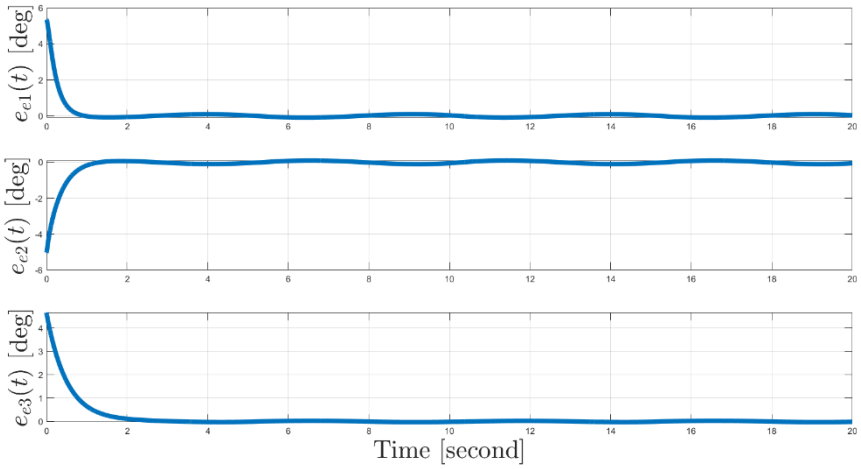

Figure 3.3: Tracking error of the first robot manipulator's joints

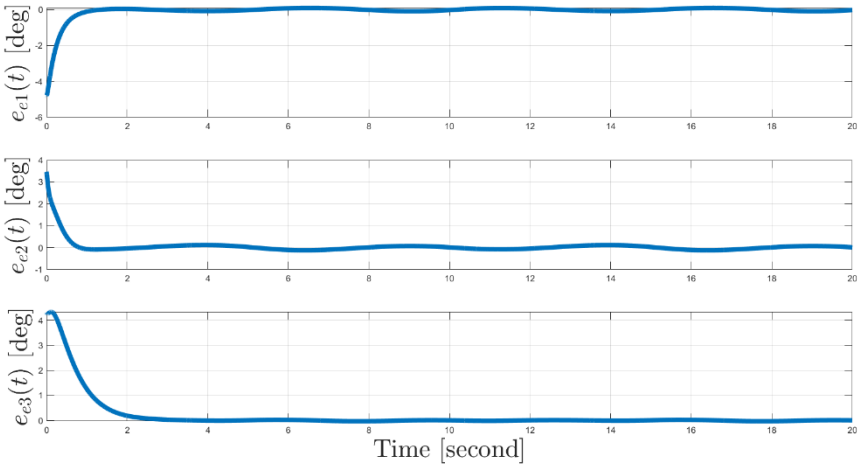

Figure 3.4: Tracking error of the second robot manipulator's joints

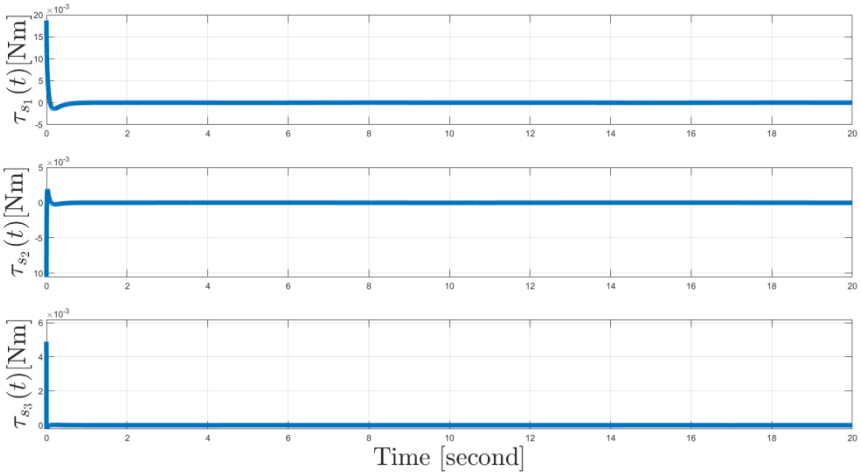

Figure 3.5: Control input torques for the first robot manipulator joints

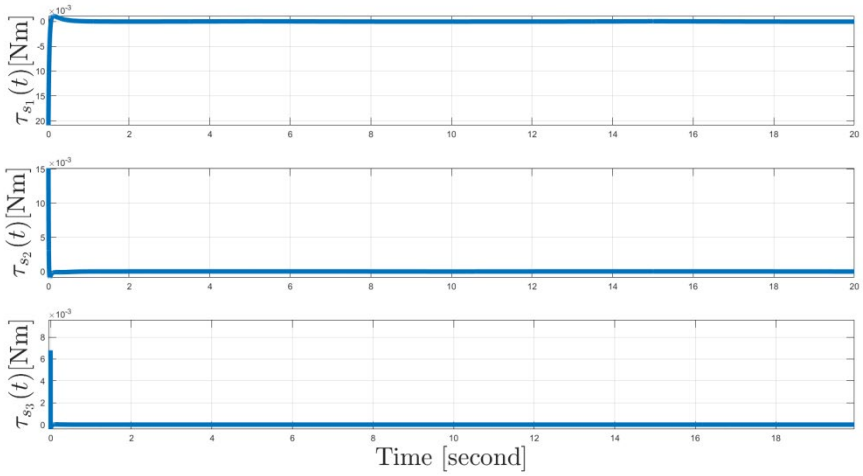

Figure 3.6: Control input torques for the second robot manipulator joints

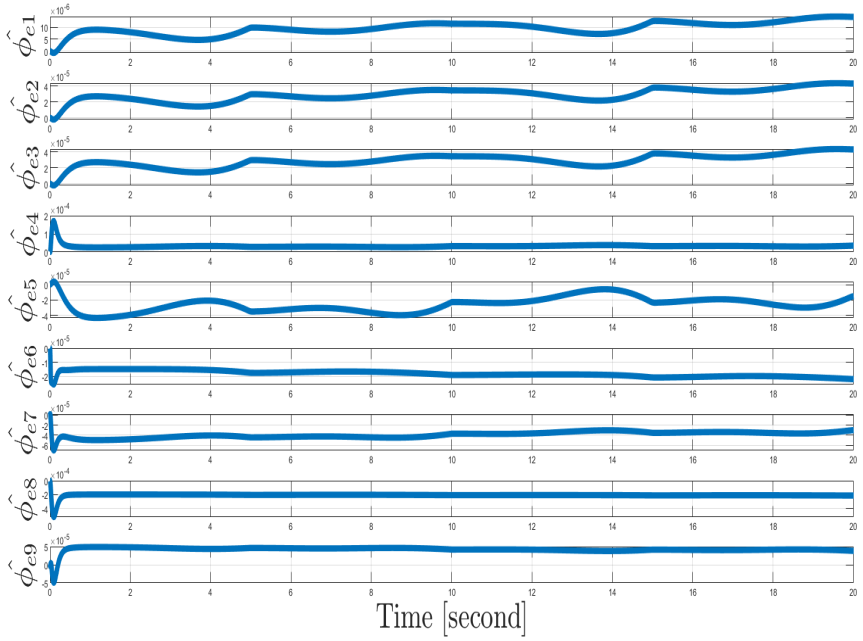

Figure 3.7: Adaptive compensation terms for the first robot manipulator

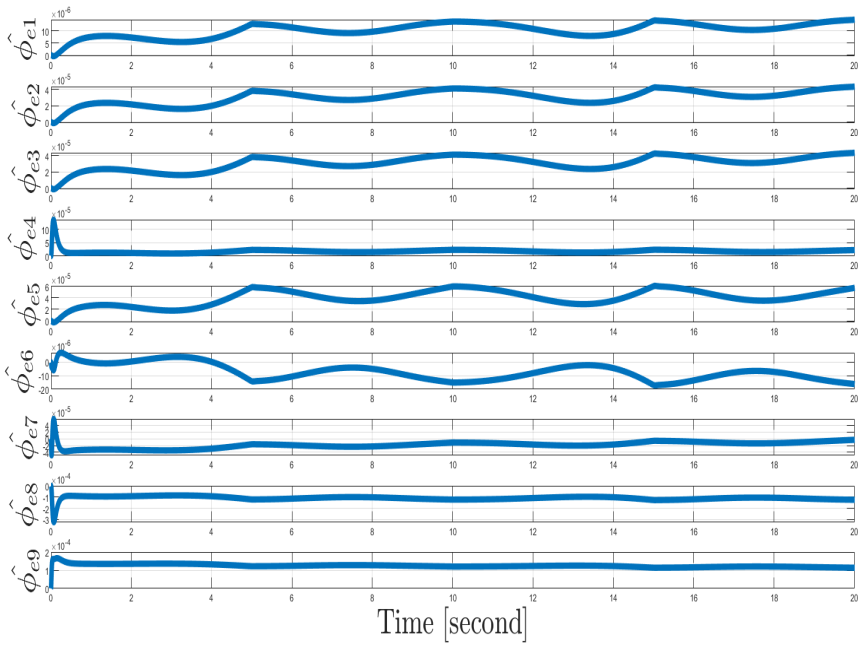

Figure 3.8: Adaptive compensation terms for the second robot manipulator

3.1.1.6 Experimental Results

Performance of the designed controller was tested on the experimental setup by keeping the desired trajectory, initial positions and control gains identical with the simulation studies presented in Chapter 3.1.1.5.

Desired trajectories and actual positions are shown in Figures 3.9 and 3.10 for the first and second robot manipulators, respectively. Tracking errors are shown in Figures 3.11 and 3.12 for the first and second robot manipulators, respectively. From Figures 3.9-3.12, it can be seen that the control objective was met. Torques applied to the joints of the first and second robot manipulators are shown in Figures 3.13 and 3.14, respectively.

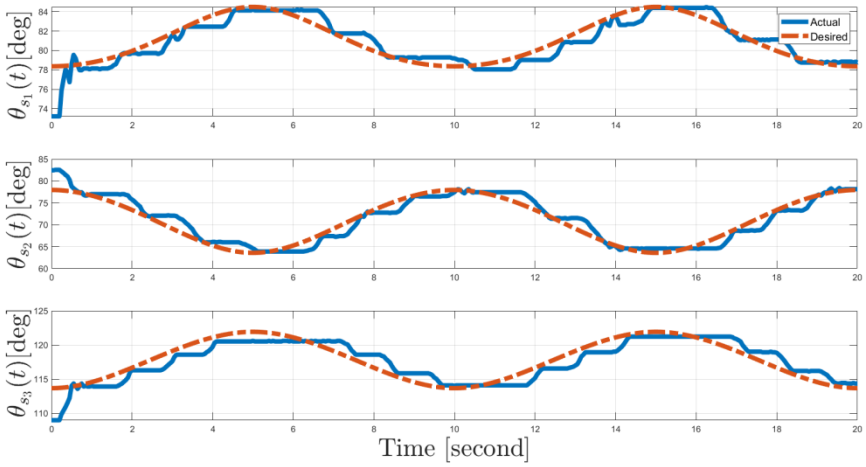

Figure 3.9: Desired vs. actual positions of the first robot manipulator's joints

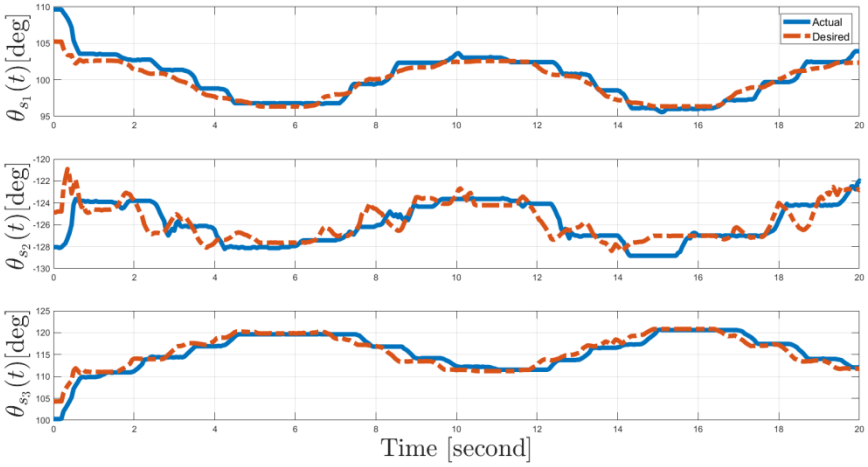

Figure 3.10: Desired vs. actual positions of the second robot manipulator's joints

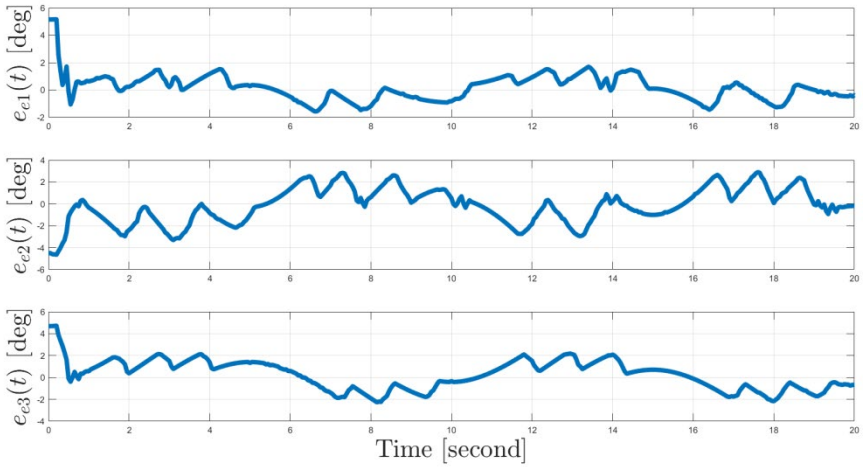

Figure 3.11: Tracking error of the first robot manipulator's joints

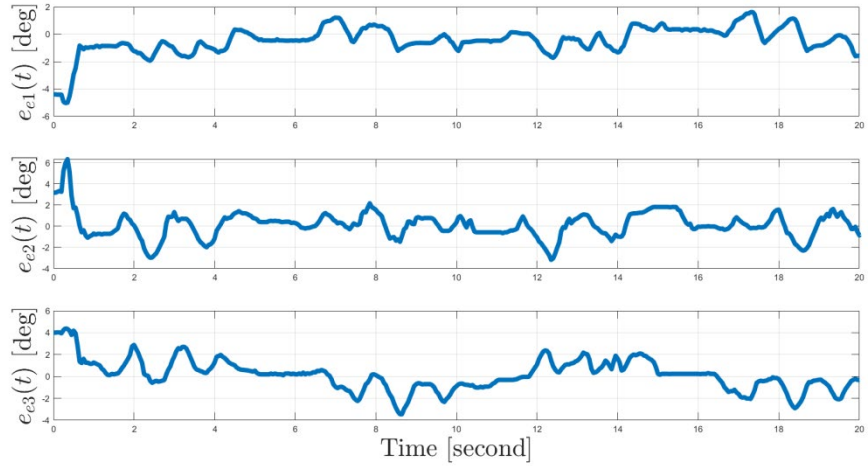

Figure 3.12: Tracking error of the second robot manipulator's joints

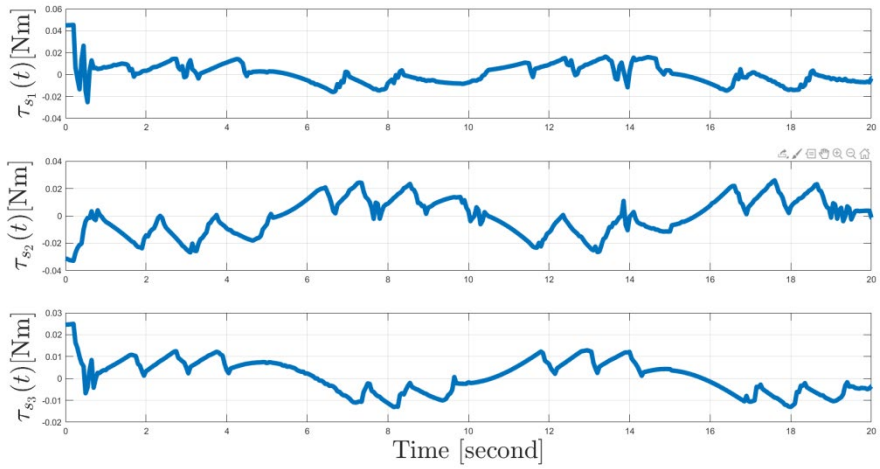

Figure 3.13: Control input torques for the first robot manipulator's joints

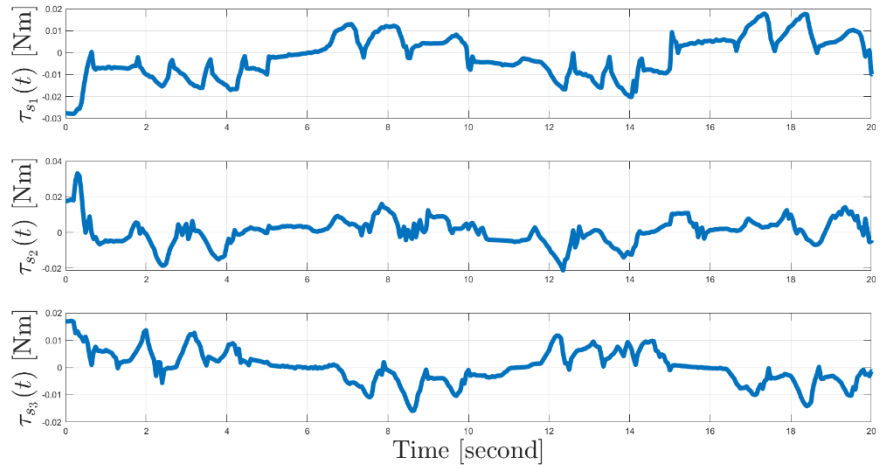

Figure 3.14: Control input torques for the second robot manipulator's joints

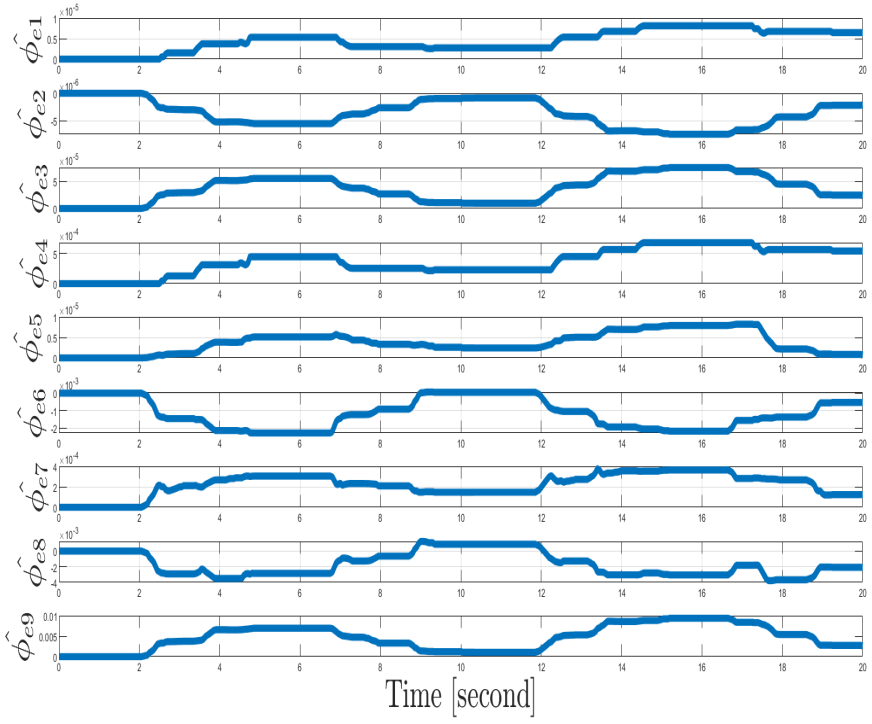

Figure 3.15: Adaptive compensation terms for the first robot manipulator

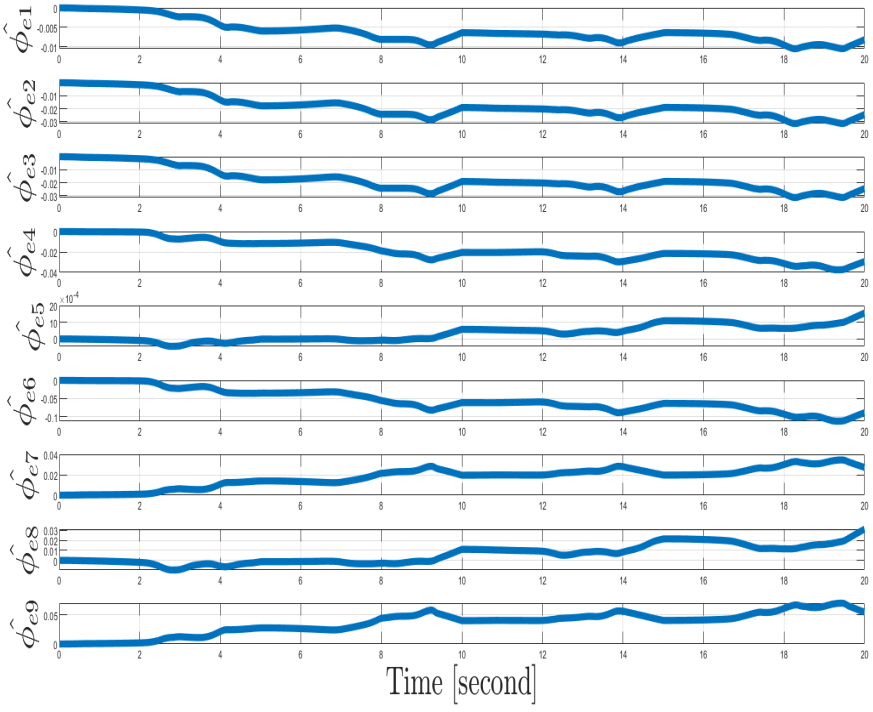

Figure 3.16: Adaptive compensation terms for the second robot manipulator

3.1.2 Task Space Control of 3 DoF RRR Serial Manipulator

Different from the joint space control the desired trajectory of the first manipulator can directly be determined in terms of position of the end effector. Owing to this issue, inverse kinematic can be avoided and the control purpose can directly be determined in the space where the main study is realized. To determine the control purpose in the task space, the task space must also be included in the dynamic model. This situation is possible by using a two-stage model whose first stage is the dynamic model given in (2.19) and second stage is another dynamic equation that give the transition between joint and task spaces. In this chapter, the backstepping control design approach is used, considering the suitability of the approach for the control of systems with multiple stage models. In accordance with the purpose of the mentioned approach, a virtual control input is designed to obtain the zero convergence of the tracking error defined in the task space, and it is shown that the control objective can be achieved when the designed controller is substituted with one of the system states. Then, the control signal is designed to make the error between the virtual control input and the system state used to instead of this input zero.

3.1.2.1 Model Properties

To include the task space into the dynamic model of 3 DoF revolute joint serial robot manipulator, the dynamic model in (2.19) is used with the forward kinematic model given as

$$x_s = f(\theta_s) \tag{3.21}$$

where $x_s \in \mathbb{R}^3$ represents end position of the end effector in Cartesian coordinate systems and forward kinematics model is given with the function denoted as $f: \mathbb{R}^3 \rightarrow \mathbb{R}^3$. Time derivative of (3.21) can be expressed with Jacobian matrix $J_s(\theta_s) \in \mathbb{R}^{3\times3}$

$$\dot{x}_s = J_s(\theta_s)\dot{\theta}_s \tag{3.22}$$

where the Jacobian matrix of the each of the robot manipulators is defined as

$$J_s(\theta_s) \triangleq \begin{bmatrix} -l_{s_1}\sin\theta_{s_1} - l_{s_2}\sin\theta_{s_{23}} - l_{s_3}\sin\theta_{s_{123}} & -l_{s_2}\sin\theta_{s_{23}} - l_{s_3}\sin\theta_{s_{123}} & -l_{s_3}\sin\theta_{s_{123}} \\ l_{s_1}\cos\theta_{s_1} + l_{s_2}\cos\theta_{s_{23}} + l_{s_3}\cos\theta_{s_{123}} & l_{s_2}\cos\theta_{s_{23}} + l_{s_3}\cos\theta_{s_{123}} & l_{s_3}\cos\theta_{s_{123}} \\ 1 & 1 & 1 \end{bmatrix} \quad (3.23)$$

The two stage dynamic model, whose stages are given in (2.19) and (3.22), respectively, are used for the control design presented in this chapter. Moreover, skew-symmetry property given in (3.1) and the availability of the Jacobian matrix in (3.23) are utilized. At this point it should be noted that, availability of the Jacobian matrix is commonly preferred approach in the task space control design of robot manipulators and since the Jacobian matrix just contain measurable angular positions and link lengths it doesn't disrupt the robustness of the designed controller. Invertibility of the Jacobian matrix for all system states is another property that is used in the control design.

3.1.2.2 Error System Development

The tracking error is defined as the difference between measured position of the end effector and the tracking trajectory.

$$e_g \triangleq x_s - x_{s_d} \quad (3.24)$$

where $x_{s_d} \in \mathbb{R}^3$represents one times differentiable, bounded, and smooth enough tracking trajectory. Boundedness of the desired trajectory and its first order time derivative are other properties that are utilized in the control design. The difference between virtual control input and angular velocity is defined as an auxiliary error term that is given as

$$e_v \triangleq \dot{\theta}_s - \tau_v \quad (3.25)$$

where $\tau_v \in \mathbb{R}^3$ represents virtual control input. The following result can be obtained when (3.22) is substituted in the time derivative of (3.24)

$$\dot{e}_g = J_s\dot{\theta}_s - x_{s_d} \quad (3.26)$$

The virtual control input is designed as

$$\tau_v = J_s^{-1}(\dot{x}_{s_d} - G_g e_g) \tag{3.27}$$

where $G_g \in \mathbb{R}^{3\times3}$ is a positive definite, constant and diagonal gain matrix. If the virtual control input in (3.27) is substituted with $\dot{\theta}_s$ in (3.26) the following result is obtained

$$\dot{e}_g = -G_g e_g \tag{3.28}$$

The error system in (3.27) can be considered as a closed loop error system and a preliminary Lyapunov-like analysis can be realized onto it. For this analysis, a non-negative Lyapunov function candidate defined as

$$V_v \triangleq \frac{1}{2} e_g^T e_g \tag{3.29}$$

Time derivative of (3.29) is obtained as

$$\dot{V}_v = -e_g^T G_g e_g \tag{3.30}$$

where (3.28) is utilized. This result is enough to show that, so that the control objective is met. However, to make the analysis in (3.29) and (3.30) a valid analysis, zero convergence of the auxiliary error term defined in (3.25) must be obtained. After this point, necessary analysis is made to guarantee this situation.

The time derivative of (3.25) is premultiplying with M_s and (2.19) and (3.24) are utilized in the resulting equation to obtain the open loop error system given as

$$M_s \dot{e}_v = f_g + \tau_s - V_s e_v \tag{3.31}$$

where $V_s e_v$ is added to both sides. The auxiliary term $f_g\left(\theta_s, \dot{\theta}_s, x_{s_d}, \dot{x}_{s_d}, \ddot{x}_{s_d}\right) \in \mathbb{R}^3$ is defined as

$$f_g = -V_s \dot{\theta}_s + V_s e_v - M_s[\dot{J}_s^{-1}\left(\dot{x}_{s_d} - G_g e_g\right) + J_s^{-1}(\ddot{x}_{s_d} - G_g \dot{e}_g)] \tag{3.32}$$

The auxiliary term in the above equation can be decomposed as

$$f_g = Y_g\left(\theta_s, \dot{\theta}_s, x_{s_d}, \dot{x}_{s_d}, \ddot{x}_{s_d}\right)\phi_g \tag{3.33}$$

In equation (3.32) $Y_g\left(\theta_s, \dot{\theta}_s, \ddot{\theta}_{s_d}\right) \in \mathbb{R}^{3\times m}$ structure shows the regression matrix containing the fully known only measurable terms and the trajectory, while $\phi_g \in \mathbb{R}^m$ indicates the uncertain vector containing the constant system parameters. To cope with the mentioned uncertainty, adaptive compensation of uncertainty is used and adaptive compensation error $\tilde{\phi}_g \in \mathbb{R}^m$ is defined as

$$\tilde{\phi}_g \triangleq \phi_g - \hat{\phi}_g \tag{3.34}$$

By substituting the equations (3.33) and (3.34) into (3.31), the open loop error system can be obtained as

$$M_s\dot{e}_v = Y_g(\theta_s, \dot{\theta}_s, \ddot{\theta}_{s_d})\tilde{\phi}_g + Y_g(\theta_s, \dot{\theta}_s, \ddot{\theta}_{s_d})\hat{\phi}_g + \tau_s - V_s e_v \tag{3.35}$$

3.1.2.3 Control Design

Control input is designed as follows

$$\tau_s = -Y_g\hat{\phi}_g - G_a e_v \tag{3.36}$$

where $G_a \in \mathbb{R}^{3\times 3}$ denotes the positive definite, constant and diagonal control gain matrix. The closed loop error system required for stability analysis can be obtained as follows by substituting the designed controller in (3.35)

$$M_s\dot{e}_v = -Y_g\tilde{\phi}_g - G_a e_v - V_s e_v. \tag{3.37}$$

After that point the stability analysis can be continued with the stability analysis.

3.1.2.4 Stability Analysis

Theorem 2: *The global asymptotic stability of the closed loop error system mathematically expressed as*

$$\left\|e_g(t)\right\|_{i_\infty} and \ \|e_v(t)\|_{i_\infty} \to 0 \ as \ t \to 0 \tag{3.38}$$

can be provided via the control design in (3.36) .

Proof: The non-negative Lyapunov function candidate $V_g\left(e_v, e_g, \tilde{\phi}_g\right) \in \mathbb{R}$ is selected as

$$V_g = V_v + \frac{1}{2}\left(e_v^T M_s e_v + \tilde{\phi}_g{}^T \tilde{\phi}_g\right) \tag{3.39}$$

Time derivative of the Lyapunov function can be obtained as

$$\begin{aligned} \dot{V}_g = -e_g^T G_g \, e_g - e_v^T G_a e_v + \tilde{\phi}_g{}^T \left[-\dot{\hat{\phi}}_g + Y_g^T e_v\right] \\ + e_v^T \left(\frac{1}{2}\dot{M}_s - V_s\right) e_v \end{aligned} \tag{3.40}$$

where (3.30), time derivative of (3.34) and (3.37) are utilized.

If the adaptive compensation $\hat{\phi}_g$ is updated according to the following rule

$$\dot{\hat{\phi}}_g = Y_g^T e_v \tag{3.41}$$

and the skew-symmetry property in (3.1) are utilized, (3.40) can be upper bounded as

$$\dot{V}_g \leq -\beta_g \left\|z_g\right\| \tag{3.42}$$

where $\beta_g \in \mathbb{R}$ denotes the positive constant defined as

$$\beta_g \triangleq -\min\left\{\lambda_{min}\left(G_g\right), \lambda_{min}(G_a)\right\} \tag{3.43}$$

and $z_g \in \mathbb{R}^6$ is the vector of combined error defined as

$$z_g \triangleq \left[e_g^T \quad e_v^T\right]^T. \tag{3.44}$$

The boundedness of $V_g(\mathrm{e_e}, \mathrm{r_e}, \widetilde{\Phi}_\mathrm{e})$ can be reached from (3.39) and (3.42) and it can be utilized to guarantee the boundedness of $z_g(t)$ and its elements (i.e., $z_g(t)$, $e_g(t)$ and $e_v(t) \in \mathcal{L}_\infty$). Standard signal chasing arguments can be utilized to show the boundedness of the all of the remaining closed loop operation signals. Finally, it can be shown that $z_g(t) \in \mathcal{L}_2$ from the integration of both sides of (3.42) and it proves that $e_g(t)$ and $z_g(t) \in \mathcal{L}_2$. The asymptotic tracking result in Theorem 2 can be obtained when all of these boundedness statements are considered with the Barbalat's Lemma [61].

3.1.2.5 Simulation Studies

Dimensions of the robot manipulators were used as given in (3.18). The desired trajectory of the first robot manipulator was determined in the task space as follows, and the desired trajectory of the second robot manipulator was adjusted to follow position changes in the first robot manipulator while maintaining the distance between the end effectors

$$\mathrm{x}_{\mathrm{s_{d_{m_1}}}} = \begin{bmatrix} 0.03cos(a_1) \\ 0.03sin(a_1) \\ -90 \end{bmatrix} \begin{bmatrix} m \\ m \\ \mathrm{deg} \end{bmatrix} \tag{3.45}$$

where

$$a_1 = 0.2625 - 0.2587\,cos(0.6285t\,) - 0.00023\,sin(0.6285t) \tag{3.46}$$

The initial position of the first robot manipulator was selected as $\mathrm{x}_{\mathrm{s_{m_1}}}(0) = [0.028 \quad 0.01 \quad -103]^T [m\ m\ deg]$, and the initial position of the second robot manipulators was selected as $\mathrm{x}_{\mathrm{s_{m_2}}}(0) = [-0.0356 \quad 0.00083 \quad 92]^T$ $[m\ m\ deg]$. Control gains were selected as follows for the first robot manipulator via trial-and-error method

$$\begin{aligned} G_{g_1} &= diag\{2, 2, 3\} \\ G_{a_1} &= diag\{0.06, 0.06, 0.007\} \end{aligned} \tag{3.47}$$

Control gains were selected as follows for the first robot manipulator via trial-and-error method

$$\begin{aligned} G_{g_2} &= diag\{1.5, 1, 1\} \\ G_{a_2} &= diag\{0.1, 0.05, 1\} \end{aligned} \tag{3.48}$$

Desired trajectories and actual positions of end effectors of the first and second robot manipulators are shown in Figures 3.17 and 3.18 against time, respectively. The movements of the end effectors in Cartesian coordinate system can be seen in Figures 3.19 and 3.20 with their desired movements in Cartesian coordinate system. Tracking errors for the tracking of end effectors are shown in Figures 3.21 and 3.22 for the first and second robot manipulator, respectively. From Figures 3.17-3.20, it can be seen that the control objective was met. Torques applied to the joints of the first and second robot manipulators are shown in Figures 3.23 and 3.24, respectively. Adaptive compensation of the first and second robot manipulators are shown in Figures 3.25 and 3.26, respectively.

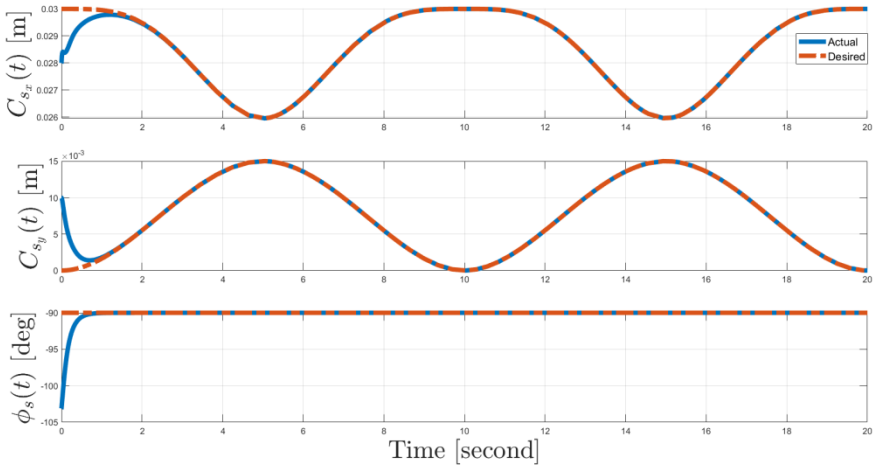

Figure 3.17: Desired vs. actual positions of the first robot manipulator's end effector

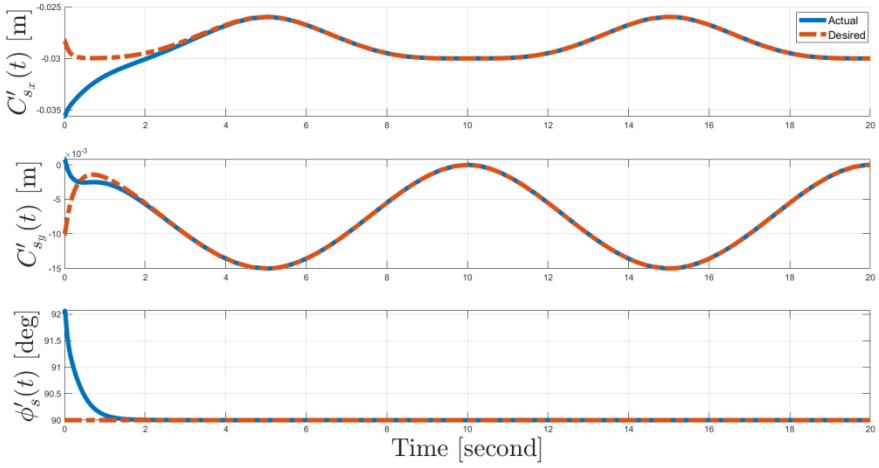

Figure 3.18: Desired vs. actual positions of the second robot manipulator's end effector

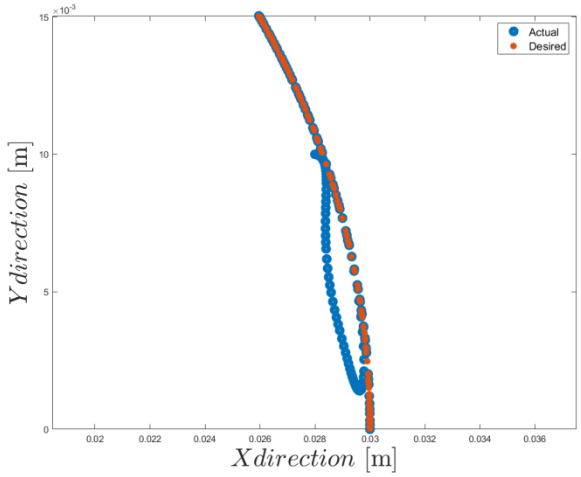

Figure 3.19: Desired vs. actual positions of the first robot manipulator's end effector

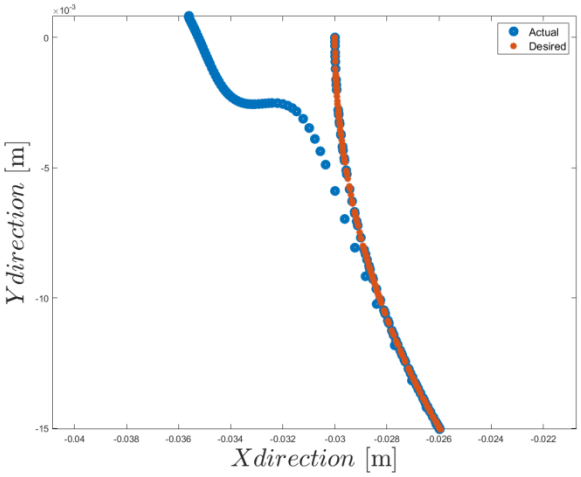

Figure 3.20: Desired vs. actual positions of the second robot manipulator's end effector

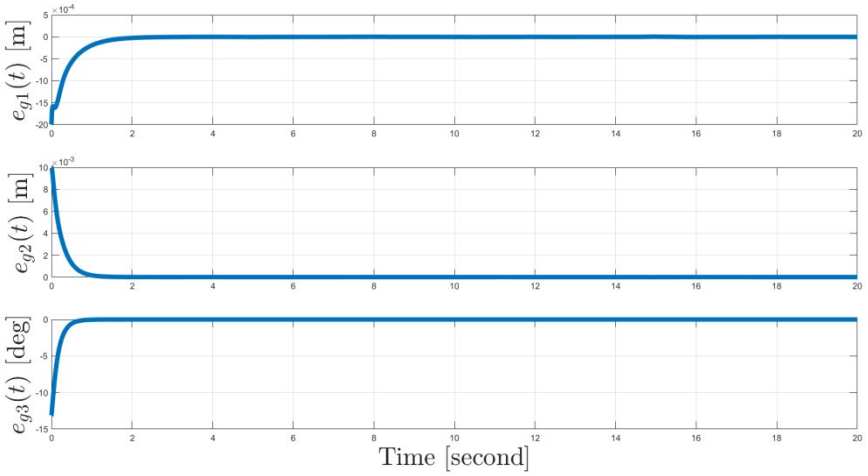

Figure 3.21: Tracking error of the first robot manipulator's end effector

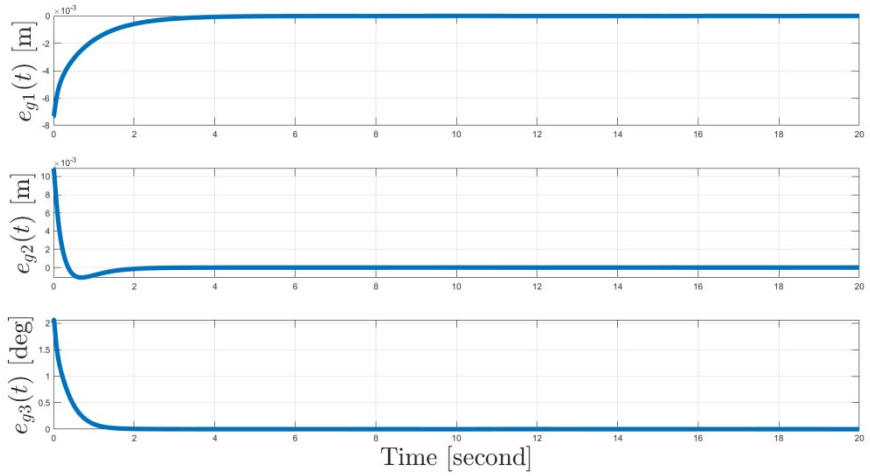

Figure 3.22: Tracking error of the second robot manipulator's end effector

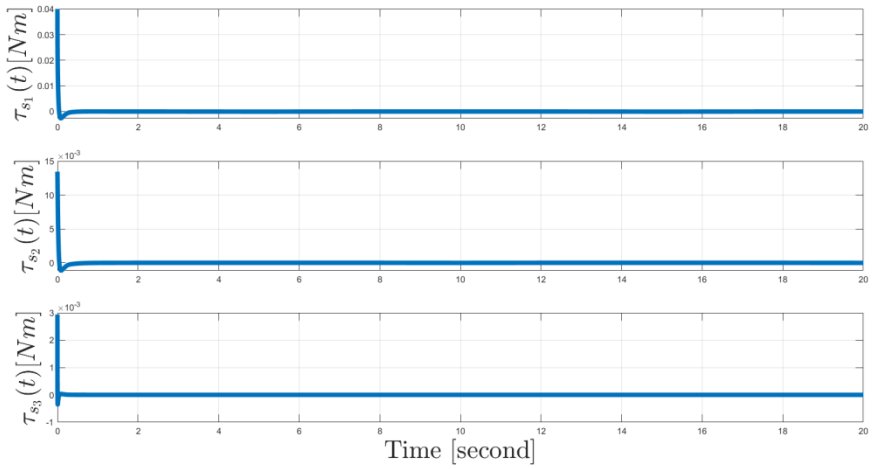

Figure 3.23: Control input torques for the first robot manipulator's joints

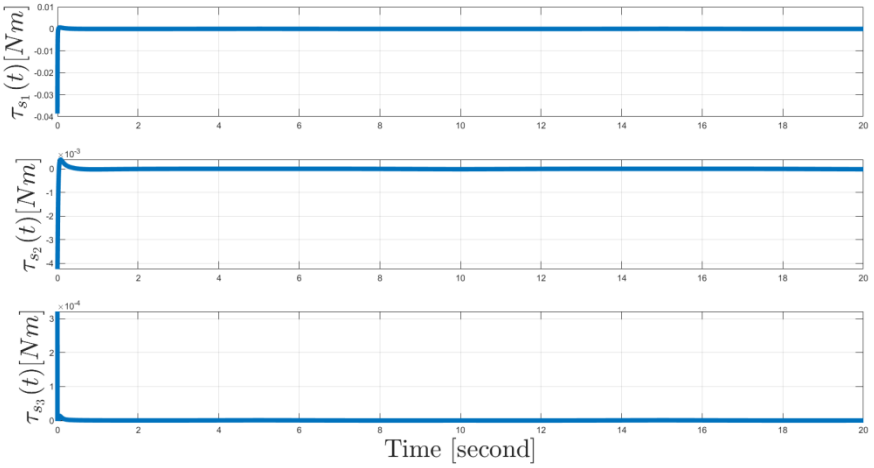

Figure 3.24: Control input torques for the second robot manipulator's joints

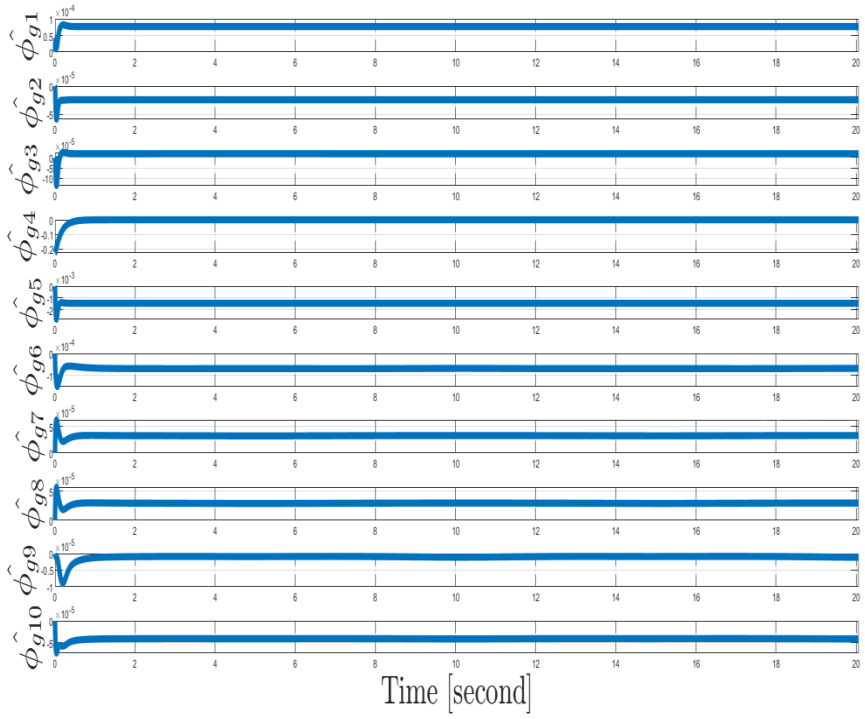

Figure 3.25: Adaptive compensation terms for the first robot manipulator

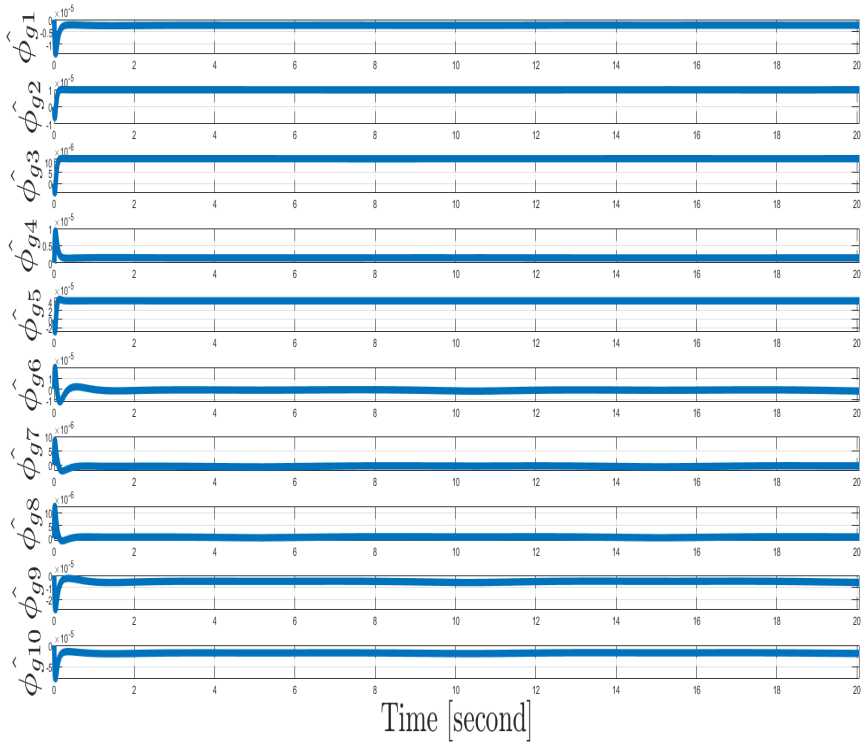

Figure 3.26: Adaptive compensation terms for the second robot manipulator

3.1.2.6 Experimental Results

Performance of the designed controller was tested on the experimental setup by keeping the desired trajectory, initial positions and control gains identical with the simulation studies presented in Chapter 3.1.2.5.

Desired trajectories and actual positions of end effectors of the first and second robot manipulators are shown in Figures 3.27 and 3.28 against time, respectively. The movements of the end effectors in Cartesian coordinate system can be seen in Figures 3.29 and 3.30 with their desired movements in Cartesian coordinate system. Tracking errors for the tracking of end effectors are shown in Figures 3.31 and 3.32 for the first and second robot manipulator, respectively. From Figures 3.27-3.32, it can be seen that the control objective was met. Torques applied to the joints of the first and second robot manipulators are shown in Figures 3.33 and 3.34, respectively. Adaptive compensation of the first and second robot manipulators are shown in Figures 3.35 and 3.36, respectively.

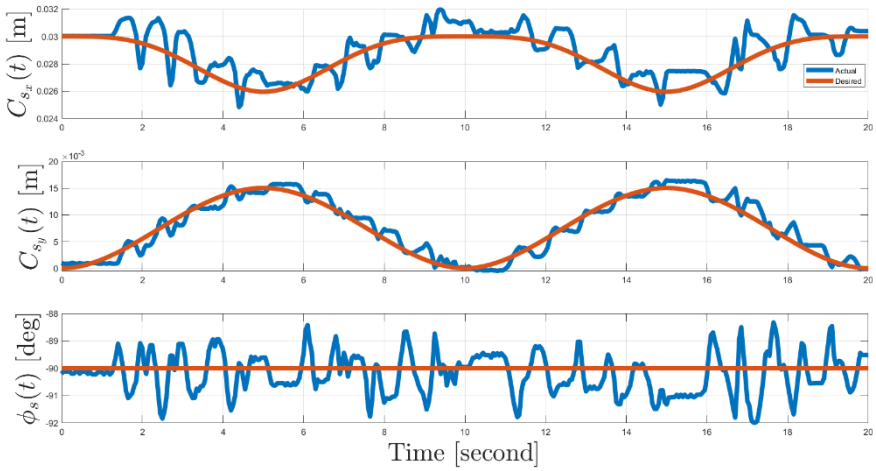

Figure 3.27: Desired vs. actual positions of the first robot manipulator's end effector

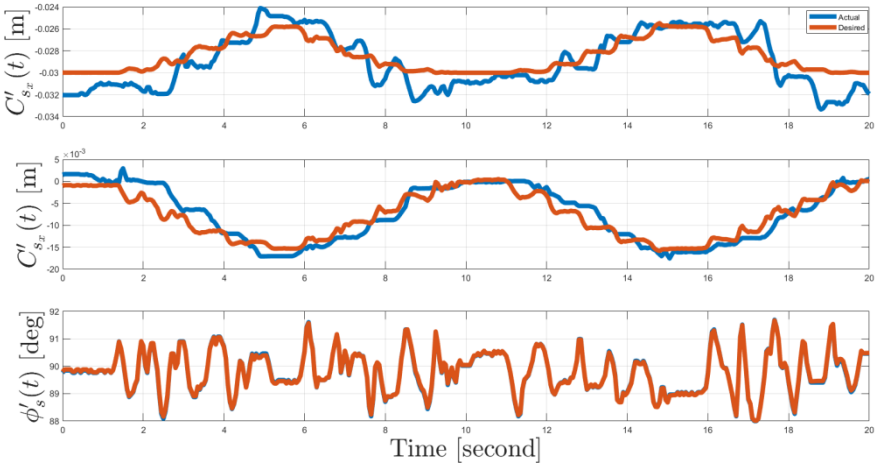

Figure 3.28: Desired vs. actual positions of the second robot manipulator's end effector

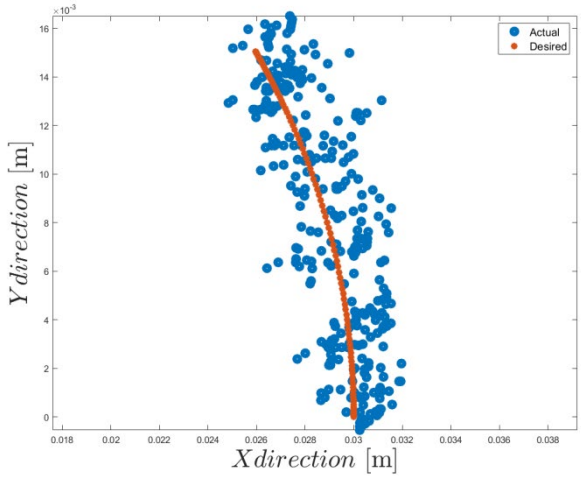

Figure 3.29: Desired vs. actual positions of the first robot manipulator's end effector

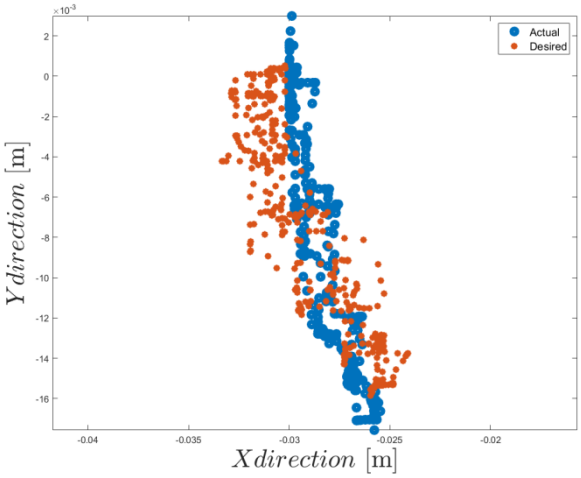

Figure 3.30: Desired vs. actual positions of the second robot manipulator's end effector

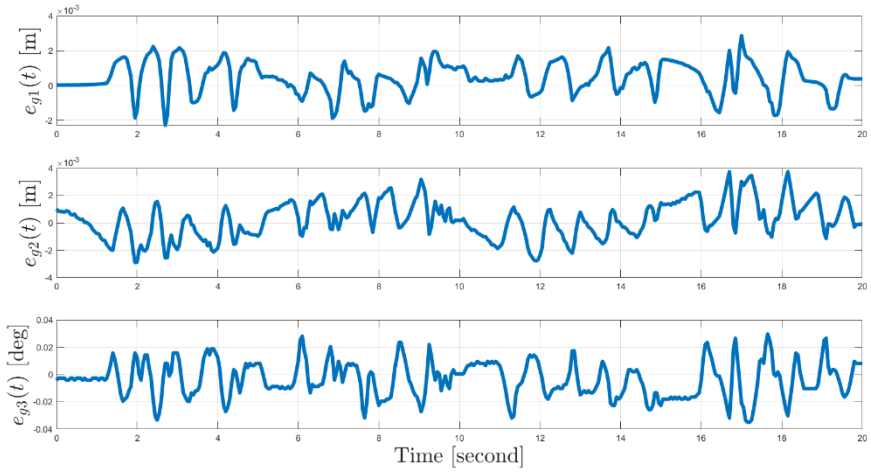

Figure 3.31: Tracking error of the first robot manipulator's end effector

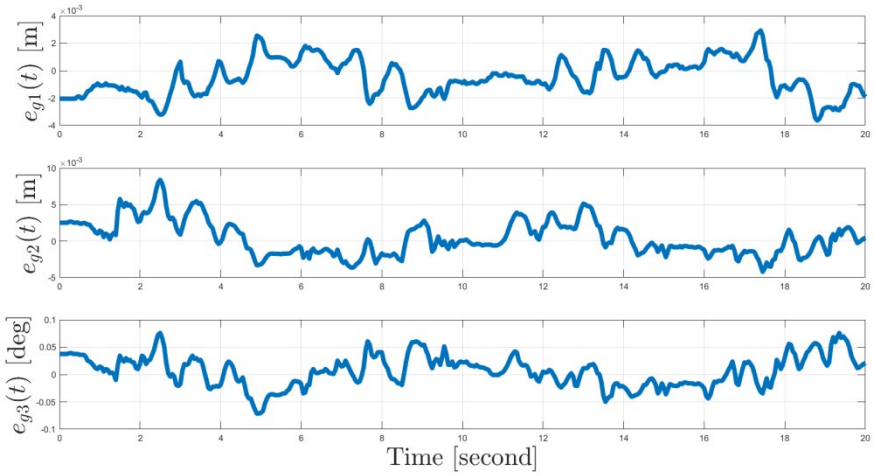

Figure 3.32: Tracking error of the second robot manipulator's end effector

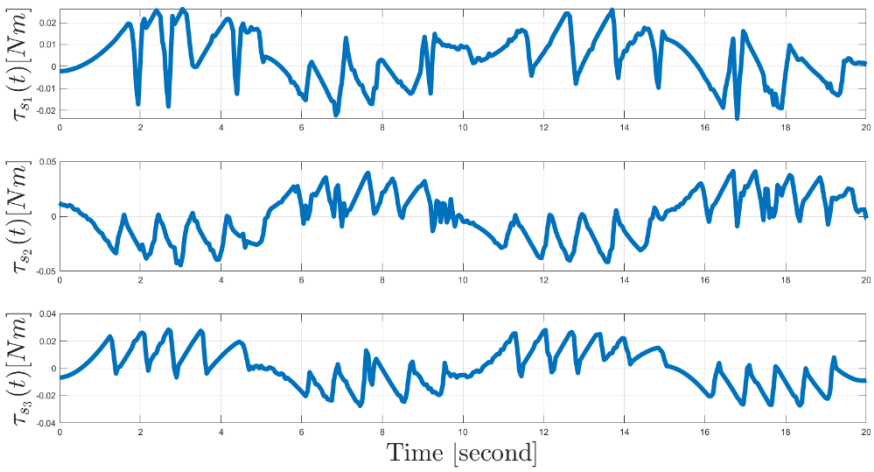

Figure 3.33: Control input torques for the first robot manipulator's joints

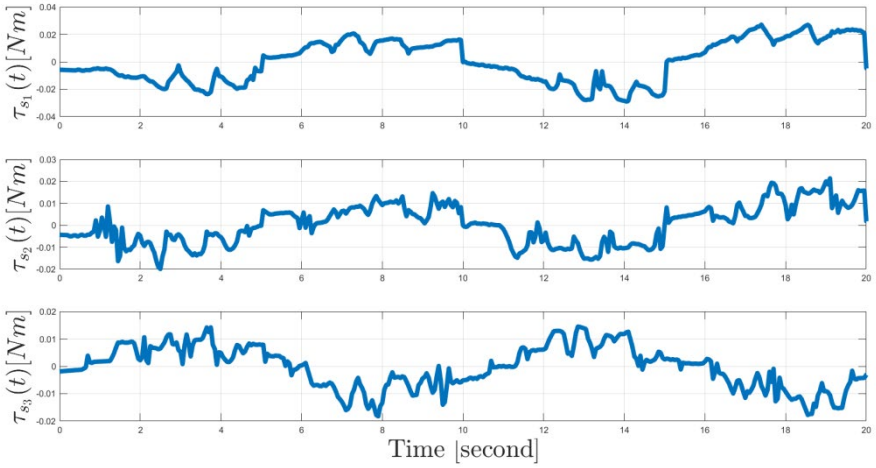

Figure 3.34: Control Input Torques for the Second Robot Manipulator's Joints

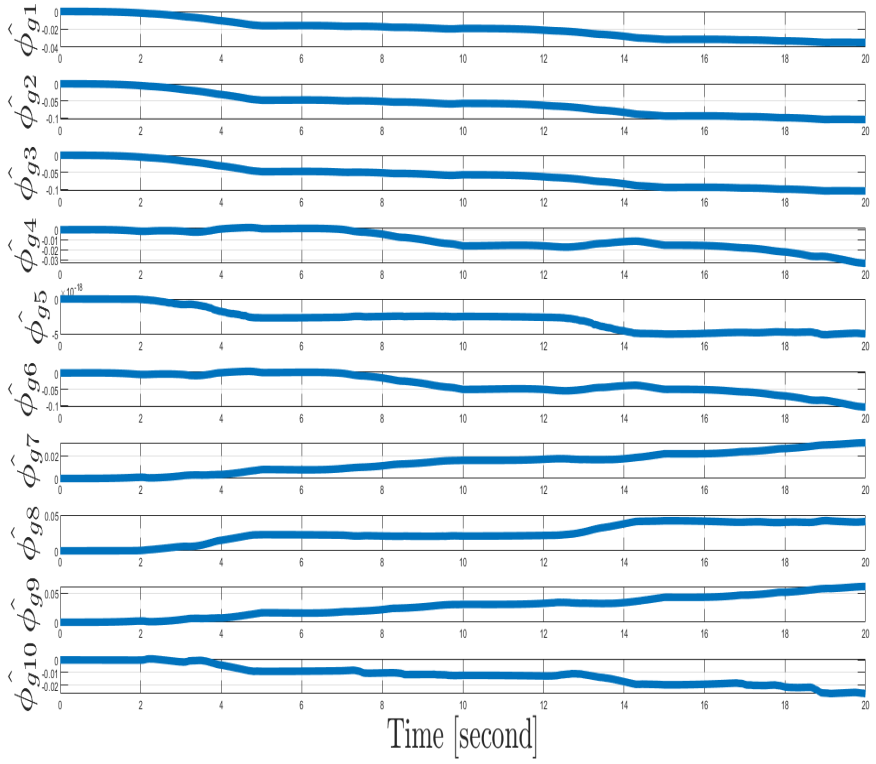

Figure 3.35: Adaptive compensation terms for the first robot manipulator

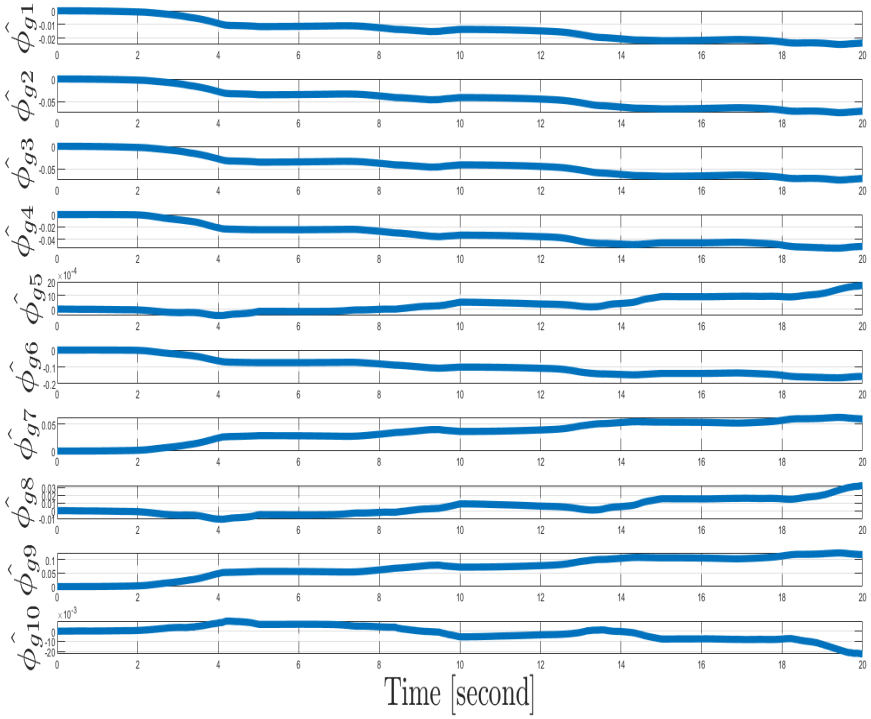

Figure 3.36: Adaptive compensation terms for the second robot manipulator

3.2 Robust Adaptive Control Design for Parallel Robotic System

In this chapter, two different control designs are presented for the parallel robotic system that contains a 5 DoF robot manipulator that contain both of revolute and prismatic joints and two independently movable end effectors into its structure. The main objective of this system is to control the position of the microrobot by utilizing the magnetic field created with the help of magnets located at the mentioned end effectors. However, to ensure the permanence of the created magnetic field and its effectiveness on the microrobot, the movements of the end effectors must be continued so that the distance between them must always be protected in a tracking rule. The successful operation of the system is possible with a feasible control design. As it can be seen from the dynamic model in (2.38), the structure of the parallel robotic system is considered as a 5 DoF integrated structure and the control problem must be solved by considering this issue.

Similar with the serial robotic system it can be considered that the main task is determined in the space of end effectors and this space is called as task space and, similar to control designs realized for the serial robotic system, a task determined in this main space can be realized via joint space or directly in the task space. Each of approaches is presented in this chapter. Robust control design is preferred to take the advantage of the structure that is able to cope with parameter uncertainties, parameter changes and external disturbances. To cope with possible high control effort necessity of the robust controllers its structure is supported via adaptive compensations and as a result of these robust adaptive control designs are realized for both joint space and task space controllers. At this point it should be noted that the robot manipulators in the robotic system are primarily modeled and their models are completely known. However, in the future, control designs independent of model knowledge are aimed due to the possible negative effects that situations such as possible changes in experimental systems, system dynamics that cannot be modeled, disturbances and etc. can cause in the control signal and process. For this purpose, robust adaptive control designs are proposed for both cases.

The following items are accepted as valid during the control designs by considering the experimental setup:

- The angular position and angular velocity of all joints are measurable.
- The position and velocity of the end effectors are measurable.

In the following subsections, control designs related analyzes and performance verifications of designed controllers are presented in a detailed manner. The most important thing to consider here is that, although the control objectives are common, the two controller structures are completely different it and realizing a performance comparison between them is not an appropriate approach. Obtaining more than one controller designs that are available for the experimental system and are suitable for achieving the control objective is the main aim of realizing the trajectory tracking in both joint space and task space.

3.2.1 Joint Space Control of 5 DoF Parallel Robot Manipulator

The main purpose of the joint space control is to reach the desired trajectory in the joint space by using inverse kinematics to find the equivalent of the desired trajectory determined in the task space. And then, a control design that makes the difference between the angular positions of the joints and the determined trajectory to zero is proposed. Robust control design approach is preferred to cope with parametric uncertainties. However, as can be seen from the literature, the biggest challenge of this type of control design is the possibility of needing a higher control effort. To overcome this issue, the designed robust controller is supported with adaptive compensations, which is a frequently preferred approach in the literature.

3.2.1.1 Model Properties

The dynamic model in (2.34) is used with the following skew-symmetry property that is valid for all robot manipulators having an identical structure with robot manipulators used in this study

$$h^T \left(\frac{1}{2} \dot{M}_p - V_p \right) h = 0 \; \forall h \in \mathbb{R}^5. \tag{3.49}$$

3.2.1.2 Error System Development

The tracking error is defined as the difference between the desired trajectory obtained via inverse kinematics from the desired trajectory of the end effector and the measured positions of the joints. The mathematical expression of the tracking error is given as

$$e_f \triangleq \theta_{p_d} - \theta_p \tag{3.50}$$

where $\theta_{p_d} \in \mathbb{R}^5$ denotes a second order differentiable and sufficiently smooth desired trajectory. Boundedness of the desired trajectory and its first and second order time derivatives are other properties that are utilized in the control design. An auxiliary error term denoted by $r_f \in \mathbb{R}^5$ is defined as

$$r_f \triangleq \dot{e}_f + \alpha_f e_f \tag{3.51}$$

where $\alpha_f \in \mathbb{R}^{5\times5}$ is a positive definite, diagonal and constant gain matrix. The following expression can be obtained by premultiplying the time derivative of (3.51) is with *M* and and adding the term $V_p r_f$ to the both sides of the resulting equation

$$M_p \dot{r}_f = f_{d_f} - \tau_p - V_p r_f \tag{3.52}$$

where (2.34) and (3.50) are utilized. An auxiliary term $f_{d_f} \in \mathbb{R}^5$ is defined as

$$f_{d_f} \triangleq M_p \ddot{\theta}_{p_d} + V_p \dot{\theta}_p + V_p r_f + M_p \alpha_f \dot{e}_f. \tag{3.53}$$

For the following steps of the controller design and analysis, this auxiliary term can be decomposed as

$$f_{d_f} = Y_f\left(\theta_p, \dot{\theta}_p, \dot{\theta}_{pd}, \ddot{\theta}_{p_d}\right)\phi_f \tag{3.54}$$

where $Y_f\left(\theta_p, \dot{\theta}_p, \dot{\theta}_{pd}, \ddot{\theta}_{p_d}\right) \in \mathbb{R}^{5\times n}$ structure shows the regression matrix containing the fully known only measurable terms and the trajectory, while $\phi_f \in \mathbb{R}^n$ indicates the uncertain vector containing the constant system parameters. To cope with the

mentioned uncertainty, adaptive compensation of uncertainty is used and adaptive compensation error $\tilde{\phi}_f \in \mathbb{R}^n$ is defined as

$$\tilde{\phi}_f \triangleq \phi_f - \hat{\phi}_f \tag{3.55}$$

By substituting (3.54) and (3.55) into (3.52), the open loop error system can be obtained as

$$M_p \dot{r}_f = Y_f\left(\theta_p, \dot{\theta}_p, \ddot{\theta}_{pd}\right)\tilde{\phi}_f + Y_f\left(\theta_p, \dot{\theta}_p, \ddot{\theta}_{pd}\right)\hat{\phi}_f - \tau_p - V_p r_f \tag{3.56}$$

3.2.1.3 Control Design

Control input is designed as follows

$$\tau_p = Y_f \hat{\phi}_f + G_f r_f \tag{3.57}$$

where $G_f \in \mathbb{R}^{5\times5}$ denotes the positive definite, constant and diagonal control gain matrix. The closed loop error system required for stability analysis can be obtained as follows by substituting the designed controller in (3.56)

$$M_p \dot{r}_f = Y_f\left(\theta_p, \dot{\theta}_p, \ddot{\theta}_{p_d}\right)\tilde{\phi}_f - V_p r_f - G_f r_f. \tag{3.58}$$

After that point the analysis can be continued with the stability analysis.

3.2.1.4 Stability Analysis

Theorem 3: *The semi-global asymptotic stability of the closed loop error system mathematically expressed as*

$$\left\|e_f(t)\right\|_{i_\infty} \text{ and } \left\|r_f(t)\right\|_{i_\infty} \to 0 \text{ as } t \to 0 \tag{3.59}$$

can be provided via the control design in (3.57) for the selection of control gains $\lambda_{min}(\alpha_f)$ *and* $\lambda_{min}\left(G_f\right) > \frac{1}{2}$.

Proof: The nonnegative Lyapunov function candidate $V_f(\mathrm{e_f}, \mathrm{r_f}, \widetilde{\Phi}_\mathrm{f}) \in \mathbb{R}$ is selected as

$$V_f = \frac{1}{2}\left(e_f^T e_f + r_f^T M_p r_f + \tilde{\phi}_f{}^T \tilde{\phi}_f\right) \tag{3.60}$$

Time derivative of the Lyapunov function can be obtained as

$$\begin{aligned}\dot{V}_f = {} & e_f^T(r_f - \alpha_f e_f) - r_f^T G_f r_f + \tilde{\phi}_f{}^T\left[-\dot{\hat{\phi}}_f + Y_f^T r_f\right] \\ & + r_f^T\left(\frac{1}{2}\dot{M}_p - V_p\right) r_f\end{aligned} \tag{3.61}$$

where (3.51), time derivative of (3.55) and (3.58) are utilized.

If the adaptive compensation $\hat{\phi}_f$ is updated according to the following rule

$$\dot{\hat{\phi}}_f = Y_f^T r_f \tag{3.62}$$

and the skew-symmetry property in (3.49) are utilized, (3.61) can be upper bounded as

$$\dot{V}_f \leq -\beta_f \|z_e\| \tag{3.63}$$

where $\beta_f \in \mathbb{R}$ denotes the positive constant defined as

$$\beta_f \triangleq -\min\left\{\left[\lambda_{min}(\alpha_f) - \frac{1}{2}\right], \left[\lambda_{min}(G_f) - \frac{1}{2}\right]\right\} \tag{3.64}$$

and the fact that $\frac{1}{2}\|e_f\|^2 + \frac{1}{2}\|r_f\|^2 \geq \|e_f\|\|r_f\|$ is utilized. The vector of combined error $z_f \in \mathbb{R}^{10}$ is (3.66) is defined as

$$z_f \triangleq \begin{bmatrix} e_f^T & r_f^T \end{bmatrix}^T. \tag{3.65}$$

The boundedness of $V_f(e_f, r_f, \tilde{\phi}_f)$ can be reached from (3.60) and (3.63) and it can be utilized to guarantee the boundedness of $z_f(t)$ and its elements (i.e., $z_f(t)$, $e_f(t)$ and $r_f(t) \in \mathcal{L}_\infty$). Standard signal chasing arguments can be utilized to show the boundedness of the all of the remaining closed loop operation signals. The boundedness of $r_f(t)$ and $e_f(t)$ can be utilized along with (3.51) to show the

boundedness of $\dot{e}_f(t)$ (i.e., $\dot{e}_f(t) \in \mathcal{L}_\infty$) and this results can be used to shown that $e_f(t)$ is a uniformly continuous signal. Finally, it can be shown that $z_f(t) \in \mathcal{L}_2$ from the integration of both sides of (3.63) and it proves that $e_f(t)$ and $z_f(t) \in \mathcal{L}_2$. The asymptotic tracking result in Theorem 3 can be obtained when all of these boundedness statements are considered with the Barbalat's Lemma [61].

3.2.1.5 Simulation Results

The following link lengths and masses that were selected in accordance with the experimental setup were used in the dynamic model in (2.34) for the simulation studies

$$\begin{gathered} l_p = 0.1m, d_2 = 0.12m, d_3 = 0.19m, \\ m_{p1} = m_{p2} = m_{p3} = m_{p4} = 0.25kg, \\ m_{p5} = 1kg, m_6 = 0.136kg, m_7 = 0.364kg, \end{gathered} \tag{3.66}$$

At this point it should be noted that the dimensions given in (3.66) are the same for both side of 5 DoF parallel robot manipulator. The desired trajectory of the robot manipulator denoted by $\theta_{p_d} \in \mathbb{R}^5$ was determined in the joint space as

$$\theta_{p_d} = \begin{bmatrix} 0.39206t^3 - 2.9415t^2 + 142 \\ 0.036t^3 - 0.2255t^2 + 32.25 \\ -0.000195t^3 + 0.0015t^2 + 0.07075 \\ \theta_{p'_{d_1}} \\ \theta'_{p_{d_2}} \end{bmatrix} \begin{bmatrix} \text{deg} \\ \text{deg} \\ \text{m} \\ \text{deg} \\ \text{deg} \end{bmatrix} \tag{3.67}$$

The desired trajectory of $\theta'_{p_{d_1}}, \theta'_{p_{d_2}}$ is a trajectory determined according to the positions of the end effector of the first side of parallel manipulator system ($\theta_{p_1}, \theta_{p_2}$ and d_1). The initial position of the five bar is $\theta_p(0) = [131.5 \;\; 29 \;\; 0.073 \;\; 43 \;\; 150]^T$. Control gains were selected as follows via trial-and-error method

$$\begin{gathered} \alpha_f = diag\{10, 10, 1, 10, 10\} \\ G_f = diag\{0.33, 0.3, 5, 0.36, 0.36\} \end{gathered} \tag{3.68}$$

Desired trajectories and actual positions are shown in Figure 3.37. Tracking errors are shown in Figure 3.38. From Figures 3.37 and 3.38, it can be seen that the control

objective was met. Control input torques are shown in Figure 3.39. Adaptive compensation is shown in Figures 3.40.

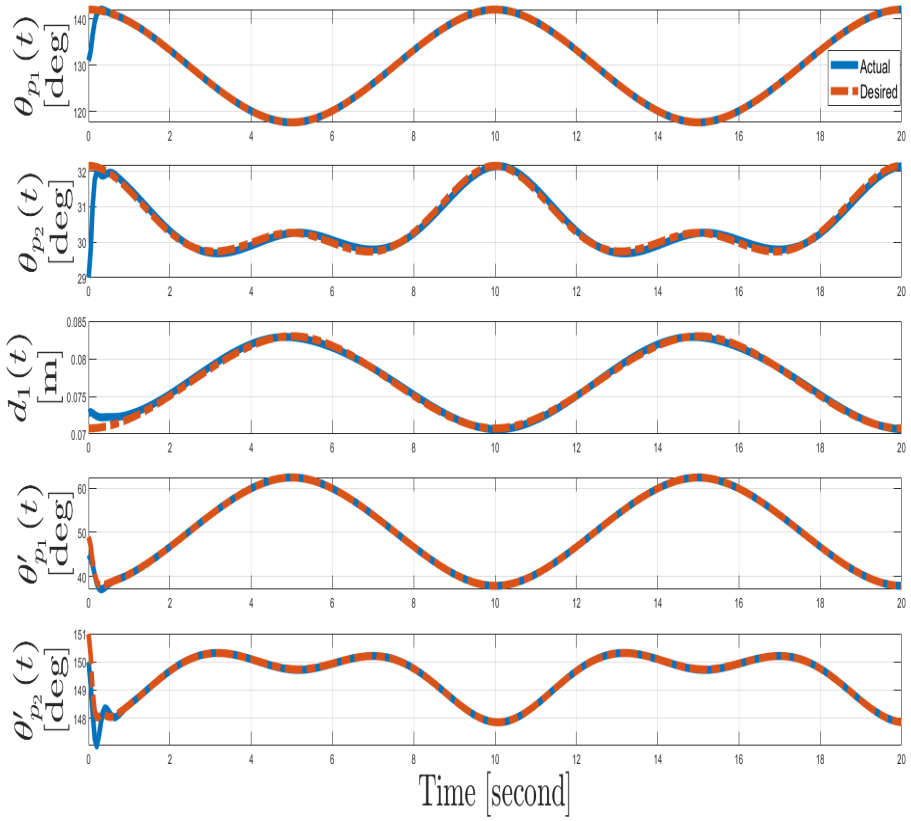

Figure 3.37: Desired vs. actual positions of the parallel manipulator's joints

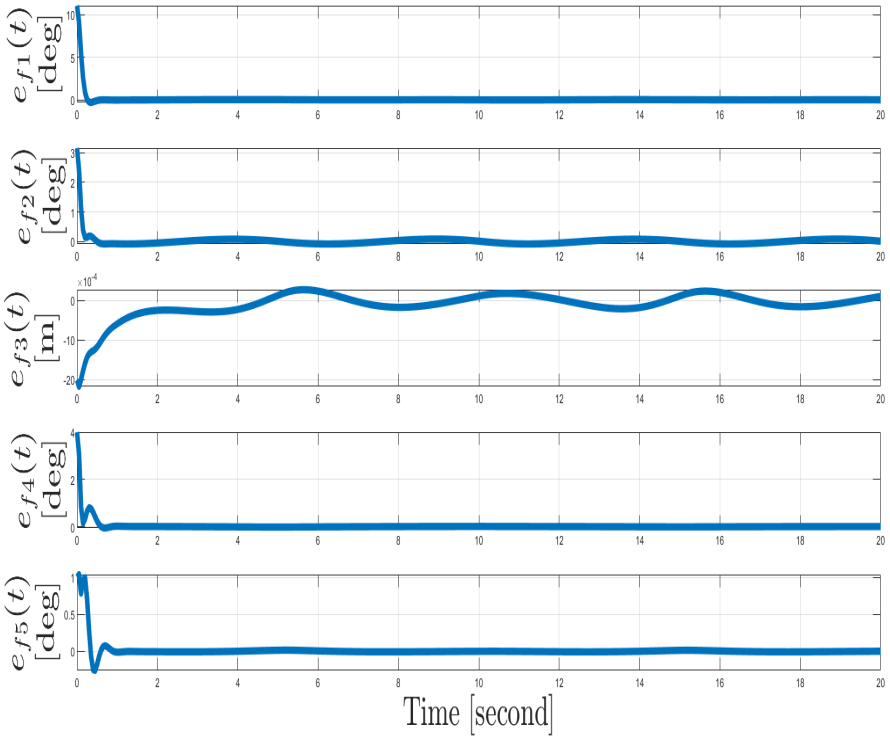

Figure 3.38: Tracking error of the parallel manipulator's joints

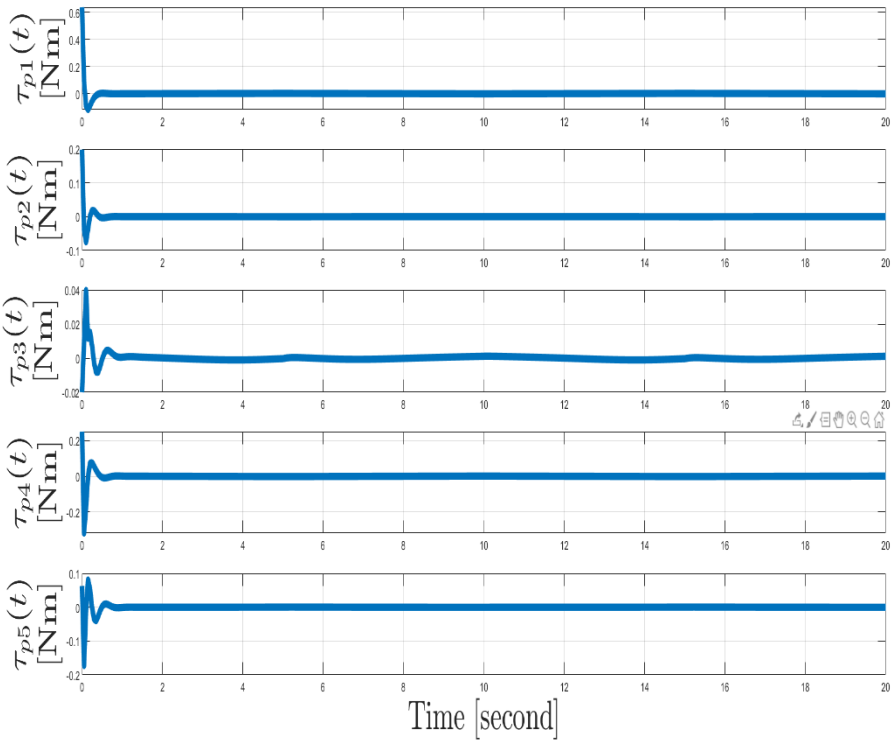

Figure 3.39: Control input torques for the parallel manipulator's joints

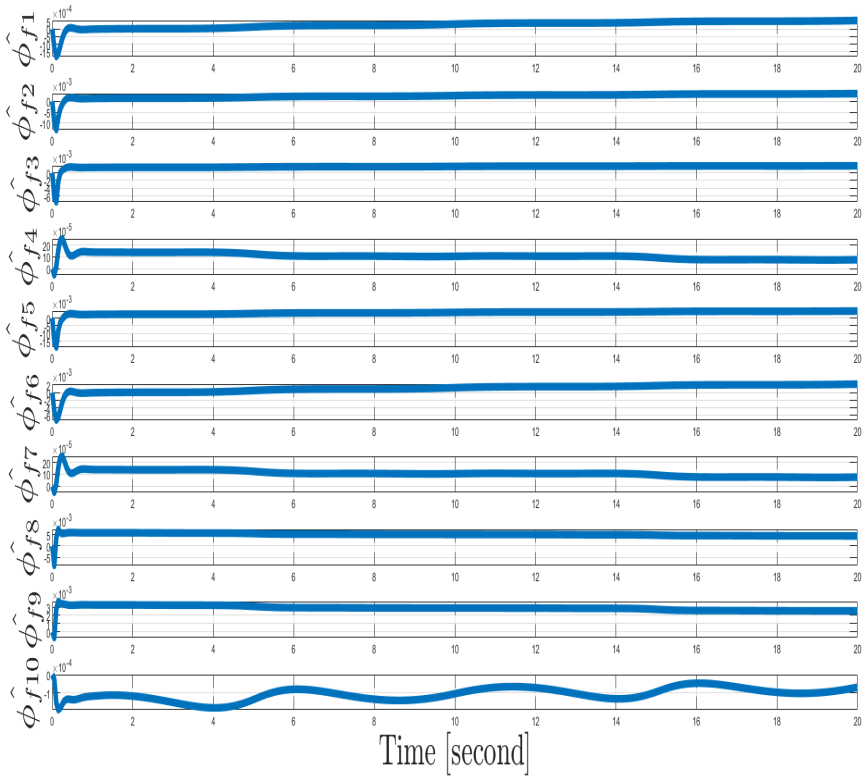

Figure 3.40: Adaptive compensation terms of parallel manipulator system

3.2.1.6 Experimental Results

Performance of the designed controller was tested on the experimental setup by keeping the desired trajectory, control gains identical with the simulation studies presented in Chapter 3.2.1.5. The initial position of the five bar is $\theta_p(0) = [131.5 \;\; 29 \;\; 0.073 \;\; 43 \; 150]^T$.

Desired trajectories and actual positions are shown in Figure 3.41. Tracking errors are shown in Figure 3.42. From Figures 3.41 and 3.42, it can be seen that the control objective was met. Control input torques are shown in Figure 3.43. Adaptive compensation is shown in Figures 3.44.

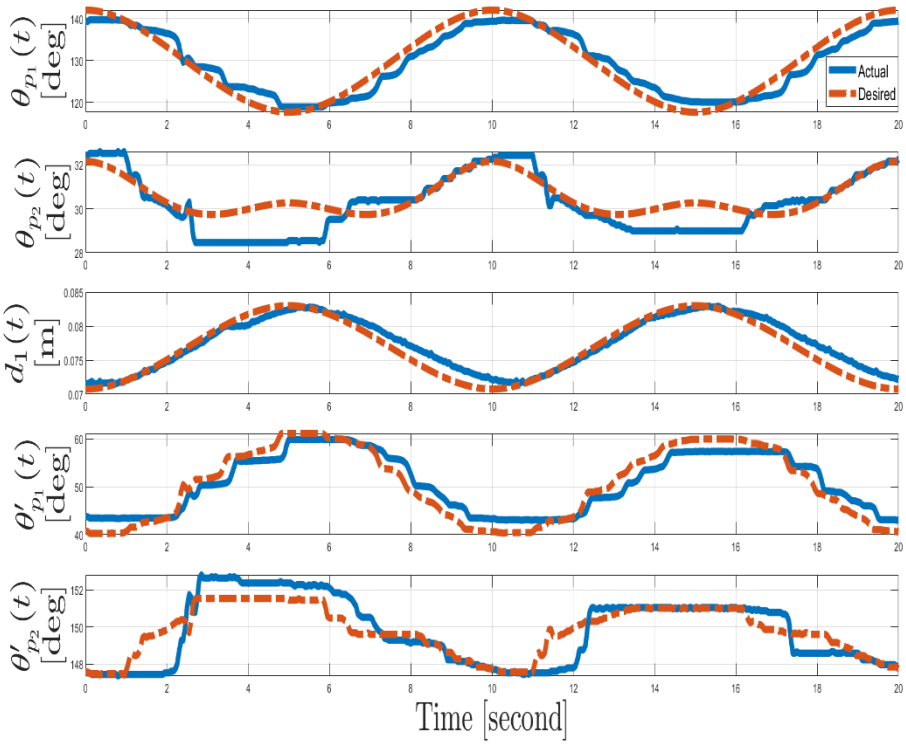

Figure 3.41: Desired vs. actual positions of the parallel manipulator's joints

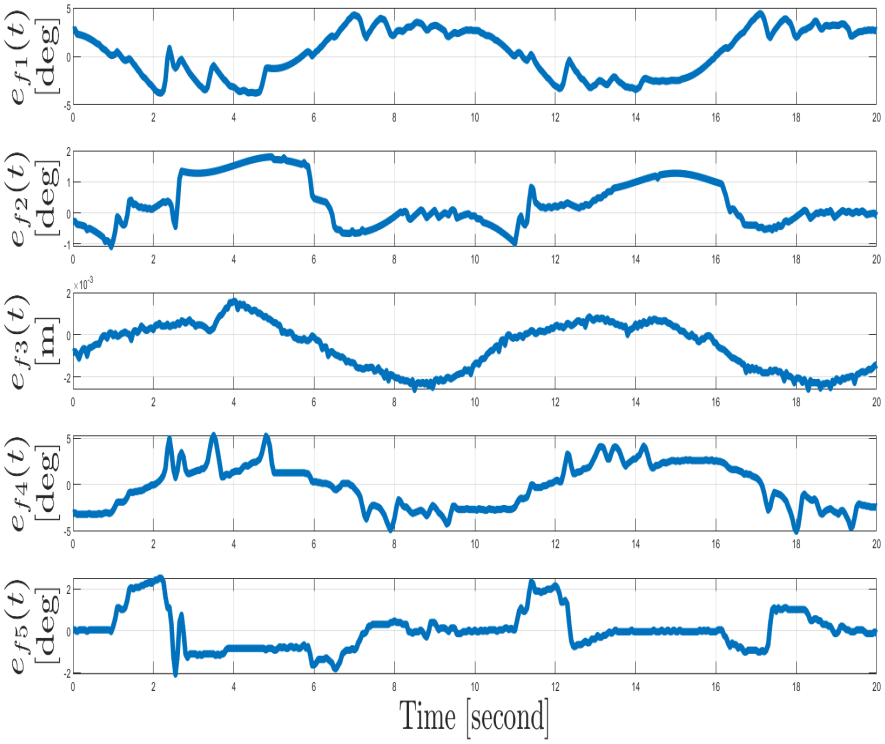

Figure 3.42: Tracking error of the parallel manipulator's joints

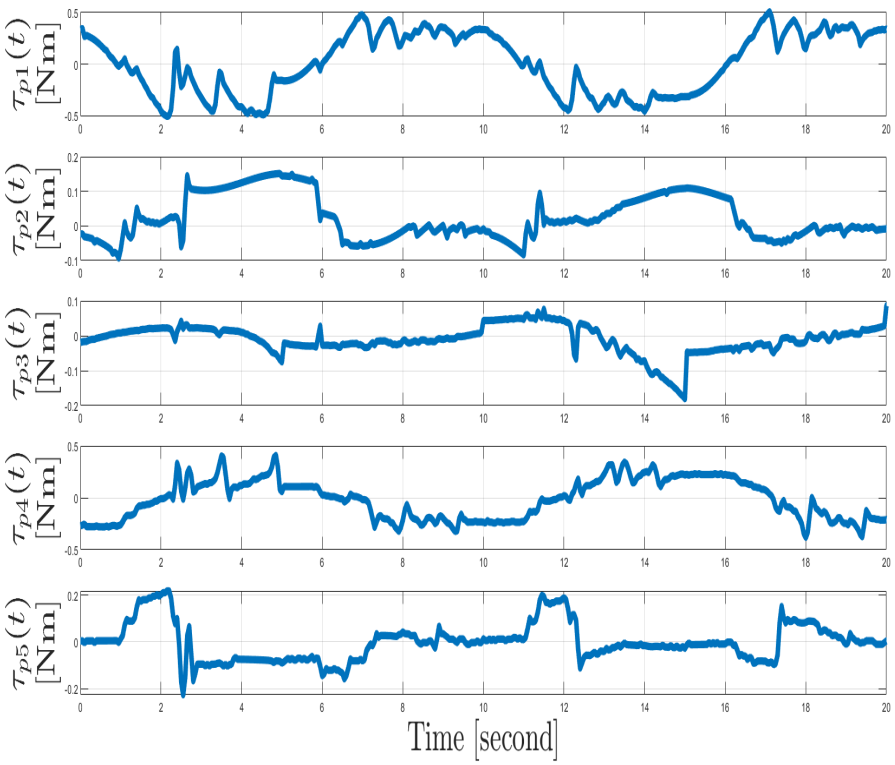

Figure 3.43: Control input torques for the parallel manipulator's joints

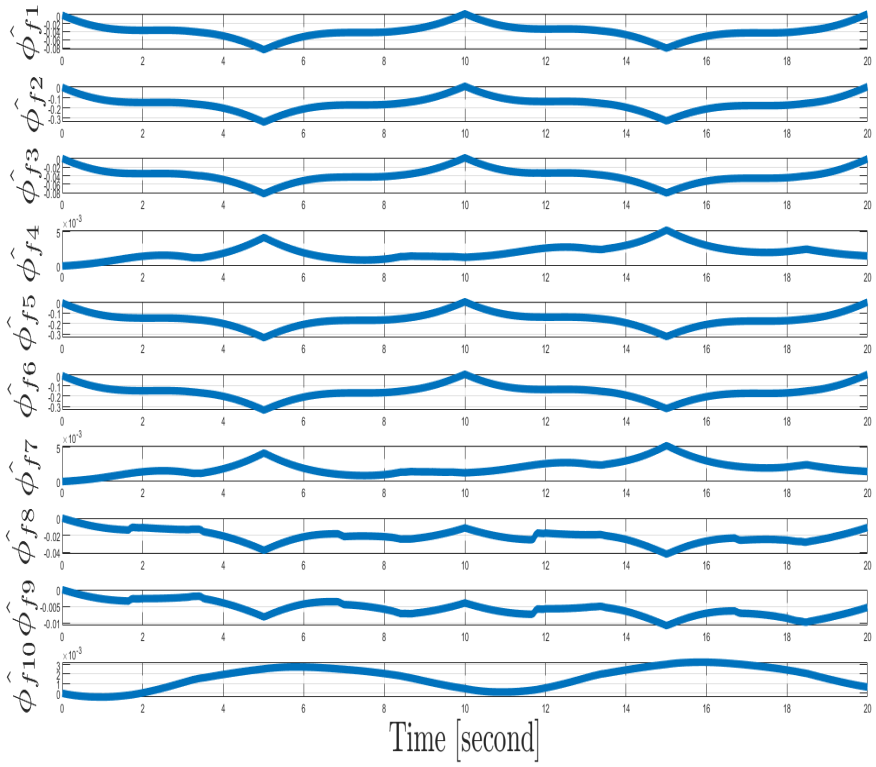

Figure 3.44: Adaptive compensation terms of parallel manipulator system

3.2.2 Task Space Control of 5 DoF Parallel Robot Manipulator

Different from the joint space control the desired trajectory of the robot manipulator can directly be determined in terms of the position of the end effector. Owing to this issue, inverse kinematic can be avoided and the control purpose can directly be determined in the space where the main study is realized. To determine the control purpose in the task space, the task space must also be included in the dynamic model. This situation is possible by using a two-stage model whose first stage is the dynamic model given in (2.34) and second stage is another dynamic equation that gives the transition between joint and task spaces. In this chapter, the dynamic model of the 5 DoF robot manipulator is rearranged and in the final form a dynamic model that both incudes the task space and joint space and provides an opportunity to determine the control objective in the task space is obtained. Then, the control objective is tried to be reached via the newly defined dynamic model. The non-square structure of the Jacobian matrix of the robot manipulator controlled in this part of the study is the main reason of the mentioned rearrangement.

3.2.2.1 System Model and Properties of Parallel Manipulator

The main property that separates the system model given in this chapter from the system model given in the previous control design is included of the forward kinematics model in the design.

$$x_p = f(\theta_p) \tag{3.69}$$

where $x_p \in \mathbb{R}^6$ denotes the end effector position in the cartesian coordinate system and forward kinematics model is given the function denoted as $f: \mathbb{R}^5 \rightarrow \mathbb{R}^6$. Time derivative of (3.69) can be expressed with Jacobian matrix $J_p(\theta_p) \in \mathbb{R}^{6\times5}$ as

$$\dot{x}_p = J_p(\theta_p)\dot{\theta}_p \tag{3.70}$$

where the Jacobian matrix of the robot manipulator is defined as

$$J_p(\theta_p) \triangleq \begin{bmatrix} -l_p \sin\theta_{p1} & -l_p \sin\theta_{p2} & 0 & 0 & 0 \\ l_p \cos\theta_{p1} & l_p \cos\theta_{p2} & 0 & 0 & 0 \\ Z_7 \sin\phi_p & Z_8 \sin\phi_p & Z_9 \sin\phi_p & 0 & 0 \\ 0 & 0 & 0 & -l_p \sin\theta'_{p1} & -l_p \sin\theta'_{p2} \\ 0 & 0 & 0 & l_p \cos\theta'_{p1} & l_p \cos\theta'_{p2} \\ 0 & 0 & Z_{10} \sin\phi'_p & Z_{11} \sin\phi'_p & Z_{12} \sin\phi'_p \end{bmatrix} \quad (3.71)$$

All other properties and definitions related to the model are used as given in the relevant subsection of the previous controller design of parallel manipulator.

An additional assumption used for the control design in this part is the invertibility of the Jacobian matrix related term $J_p^T J_p$ for all angular values. By using this assumption, (3.70) can be rearranged as

$$A\dot{x}_p = \dot{\theta}_p \quad (3.72)$$

where the newly defined matrix denoted by $A \in \mathbb{R}^{5\times 6}$ is defined as $A \triangleq \left(J_p^T J_p\right)^{-1} J_p^T$. The following result can be obtained by substituting (3.72) and its time derivative into (2.34)

$$M_p A\ddot{x}_p + M_p \dot{A}\dot{x}_p + V_p A\dot{x}_p = \tau_p. \quad (3.73)$$

At this point it should be noted that availability of the Jacobian matrix makes the matrix A an available matrix and structure of this matrix makes $A^T A$ an invertible matrix. After that point the following system state can be defined

$$x_N \triangleq A\dot{x}_p \quad (3.74)$$

and the following first order dynamic model, which will form the main of the controller design, can be obtained by utilizing (3.74) into (3.73)

$$M_p \dot{x}_N + V_p x_N = \tau_p. \quad (3.75)$$

From (3.75) it is clear that after that point the control objective $x_p \to x_{p_d}$ can be determined in terms of x_N as long as $x_{N_d} \in \mathbb{R}^5$ is selected properly and $x_N \to x_{N_d}$ result is obtained. Appendix D can be examined to seek the detailed information

about this issue. At this point it should be noted that into the mentioned control objective x_{N_d} denotes the desired trajectory for x_N.

3.2.2.2 Error System Development

The tracking error is defined as

$$e_d \triangleq x_{N_d} - x_N \tag{3.76}$$

where $\mathrm{x}_{\mathrm{N}_d}$ a first order differentiable and sufficiently smooth desired trajectory.

Time derivative of (3.76) is premultiplied with *M* to obtain the following result

$$M_p \dot{e}_d = f_{g_d} - \tau_p - V_p e_d \tag{3.77}$$

where (3.75) and (3.76) are utilized and $V_p e_d$ is added to both sides of the resulting equation. The auxiliary term $f_{g_d}(\theta_p, \dot{\theta}_p, x_{N_d}, \dot{x}_{N_d}) \in \mathbb{R}^6$ is defined as

$$f_g = M_p \dot{x}_{N_d} + V_p x_N + V_p e_d \tag{3.78}$$

For the following steps of the controller design and analysis, this auxiliary can be decomposed as

$$f_{g_d} = Y_d(\theta_p, \dot{\theta}_p, x_{N_d}, \dot{x}_{N_d})\phi_d \tag{3.79}$$

where $\mathrm{Y_d}(\theta_\mathrm{p}, \dot{\theta}_p, \mathrm{x_{N_d}}, \dot{\mathrm{x}}_{\mathrm{N_d}}) \in \mathbb{R}^{6\times k}$ denotes the regression matrix containing the certain and measurable terms while $\phi_d \in \mathbb{R}^k$ indicates the uncertain constant vector containing the system parameters. To cope with the mentioned uncertainty, an adaptive compensation terms $\hat{\phi}_d \in \mathbb{R}^k$ is utilized and the adaptive compensation error $\tilde{\phi}_d \in \mathbb{R}^k$ is defined as

$$\tilde{\phi}_d \triangleq \phi_d - \hat{\phi}_d \tag{3.80}$$

By substituting (3.79) and (3.80) into (3.77), the open loop error system can be obtained as

$$M_p \dot{e}_d = Y_d(\theta_p, \dot{\theta}_p, x_{N_d}, \dot{x}_{N_d})\tilde{\phi}_d + Y_d(\theta_p, \dot{\theta}_p, x_{N_d}, \dot{x}_{N_d})\hat{\phi}_d - \tau_p - V_p e_d \tag{3.81}$$

3.2.2.3 Control Design

Control input is designed as follows

$$\tau_p = Y_d\hat{\phi}_d - G_d e_d \tag{3.82}$$

where $G_d \in \mathbb{R}^{6\times6}$ denotes the positive definite, constant and diagonal control gain matrix. The closed loop error system required for stability analysis can be obtained as follows by substituting the designed controller in (3.81)

$$M_p\dot{e}_d = -Y_d\left(\theta_p, \dot{\theta}_p, x_{N_d}, \dot{x}_{N_d}\right)\tilde{\phi}_d - G_d e_d - V_p e_d \tag{3.83}$$

After that point the analysis can be continued with the stability analysis.

3.2.2.4 Stability Analysis

Theorem 4: *The global asymptotic stability of the closed loop error system mathematically expressed as*

$$\|e_d(t)\|_{i_\infty} \rightarrow 0 \; as \; t \rightarrow 0 \tag{3.84}$$

can be provided via the control design in (3.82).

Proof: The nonnegative Lyapunov function candidate $V_d\left(e_d, \tilde{\phi}_d\right) \in \mathbb{R}$ is selected as.

$$V_d = \frac{1}{2}\left(e_d^T M_p e_d + \tilde{\phi}_d{}^T\tilde{\phi}_d\right) \tag{3.85}$$

Time derivative of the Lyapunov function can be obtained as

$$\dot{V}_d = -e_d^T G_d\, e_d + \tilde{\phi}_d{}^T\left[\dot{\hat{\phi}}_d - Y_d^T e_d\right] + e_d^T\left(\frac{1}{2}\dot{M}_p - V_p\right)e_d \tag{3.86}$$

where time derivative of (3.80) and (3.84) are utilized. If the adaptive compensation $\hat{\phi}_d$ is updated according to the following rule

$$\dot{\hat{\phi}}_d = Y_d^T e_d \tag{3.87}$$

and skew-symmetry property in (3.49) are utilized, (3.86) can be upper bounded as

$$\dot{V}_d \leq -\lambda_{min}(\mathrm{G_d})\|\mathrm{e_d}\|^2 \tag{3.88}$$

The boundedness of $V_d(e_d, \tilde{\phi}_d)$ can be reached from (3.85) and (3.88) and it can be utilized to guarantee the boundedness of $e_d(t)$ (i.e., $e_d(t) \in \mathcal{L}_\infty$). Standard signal chasing arguments can be utilized to show the boundedness of the all of the remaining closed-loop operation signals. It can be shown that $e_d(t) \in \mathcal{L}_2$ from the integration of both sides of (3.88). The asymptotic tracking result in Theorem 4 can be obtained when all of these boundedness statements are considered with the Barbalat's Lemma [61].

3.2.2.5 Simulation Studies

Dimensions of the robot manipulator were used as given in (3.66). The desired trajectory of the first end effector was determined in the task space as follows, and the second end effector follows the position changes in the first end effector by protecting the distance distance between them

$$x_{p_d} = \begin{bmatrix} -0.000547t^3 + 0.0041t^2 + 0.1258 \\ -0.000388t^3 + 0.0029t^2 + 0.1147 \\ 19.25 \\ C'_{u_d} \\ C'_{v_d} \\ \phi'_{p_d} \end{bmatrix} \tag{3.85}$$

The desired trajectory of $C'_{u_d}, C'_{v_d}$and ϕ'_{p_d} is a trajectory determined according to the positions of the end effector of parallel manipulator system C_u, C_v and ϕ_p. The initial position is selected as $x_p(0) = [0.154 \quad 0.121 \quad 20.1 \quad 0.131 \quad 0.113 \quad 162.5]^T$. Controller gains were selected as follows via trial-and-error method

$$G_d = diag\{0.33, 0.36{,}12{,}0.36{,}0.36\} \tag{3.86}$$

Desired trajectories and actual positions of the first and second end effectors are shown in Figures 3.45 and 3.46 against time, respectively. The movements of the end effectors in Cartesian coordinate system can be seen in Figures 3.47 and 3.48 with their desired movements in Cartesian coordinate system. Tracking errors for the tracking of end effectors are shown in Figures 3.49 and 3.50 for the first and second

end effector, respectively. From Figures 3.45-3.50, it can be seen that the control objective was met. Control input torques are shown in Figure 3.51. Adaptive compensation is shown in Figures 3.52.

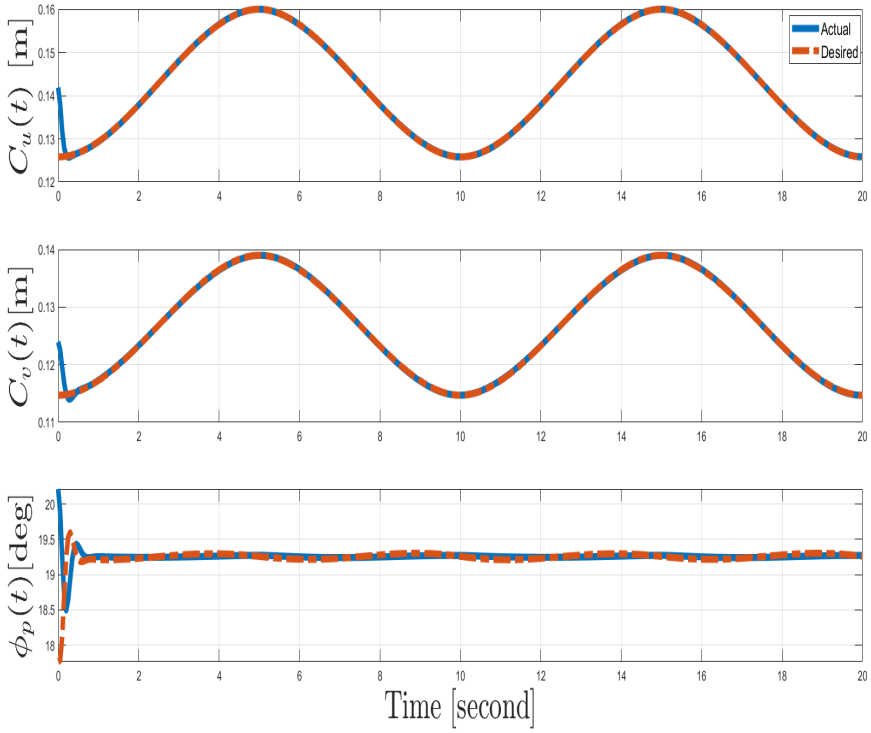

Figure 3.45: Desired vs. actual positions of first end effector of parallel manipulator system

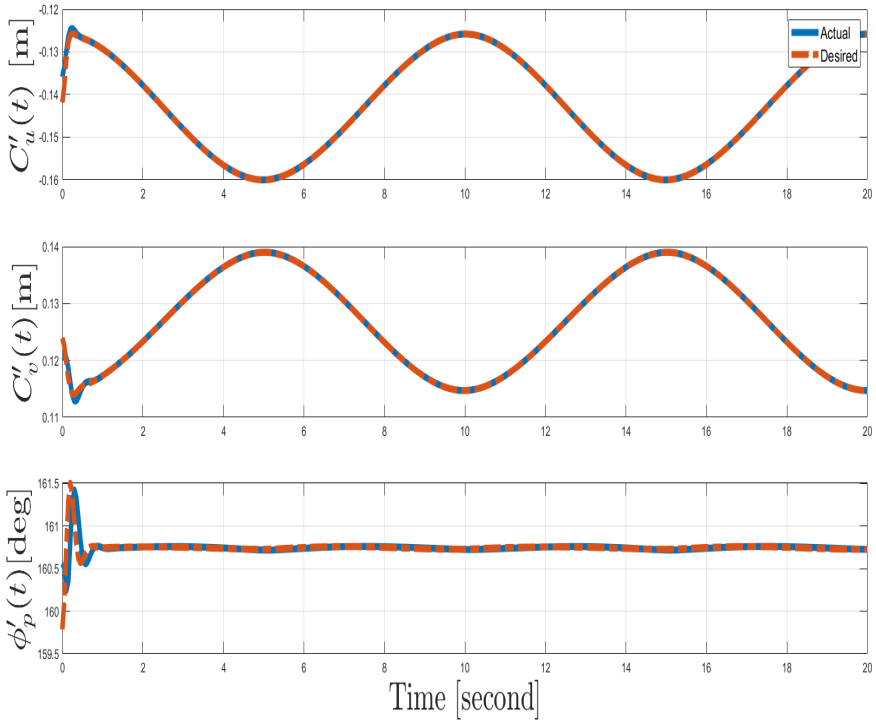

Figure 3.46: Desired vs. actual positions of second end effector of parallel manipulator system

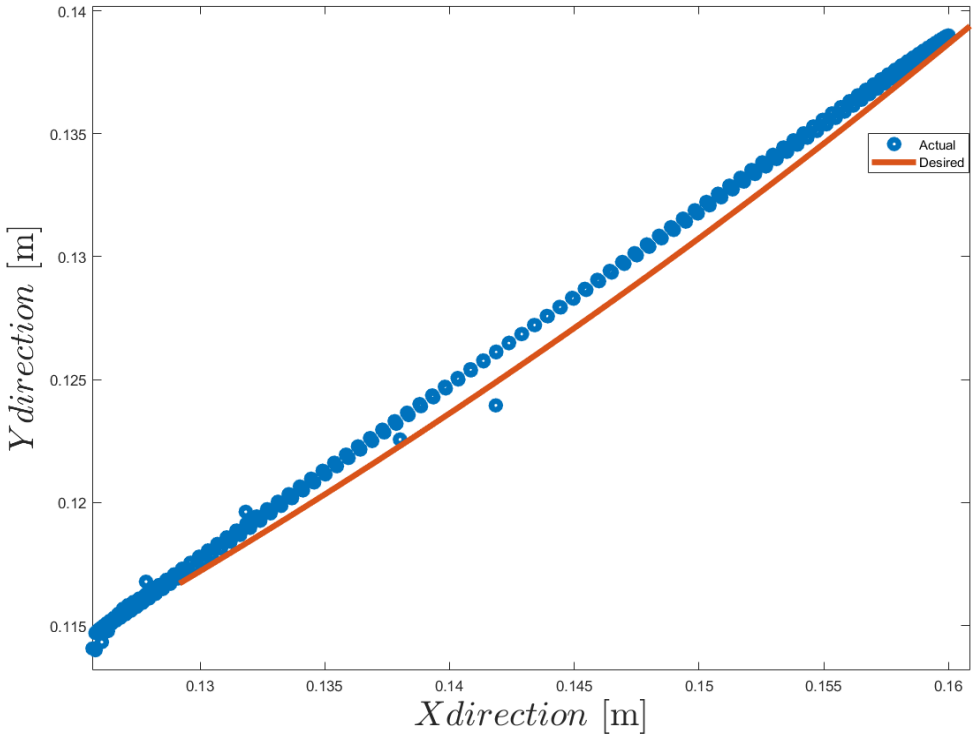

Figure 3.47: Desired vs. actual positions of first end effector of parallel manipulator system

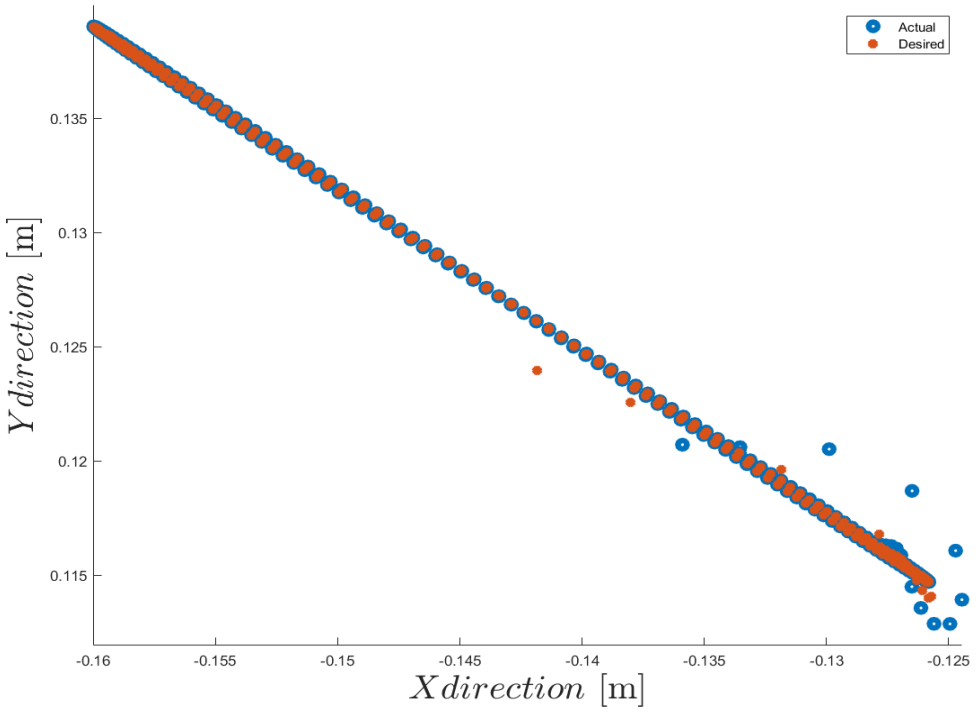

Figure 3.48: Desired vs. actual positions of second end effector of parallel manipulator system

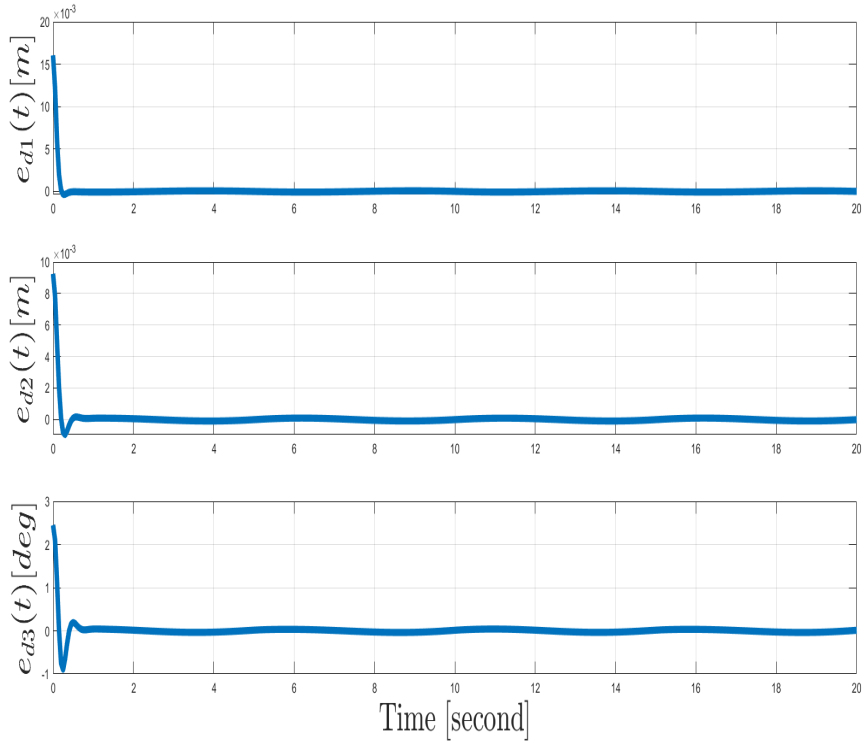

Figure 3.49: Tracking error of first end effector of parallel manipulator system

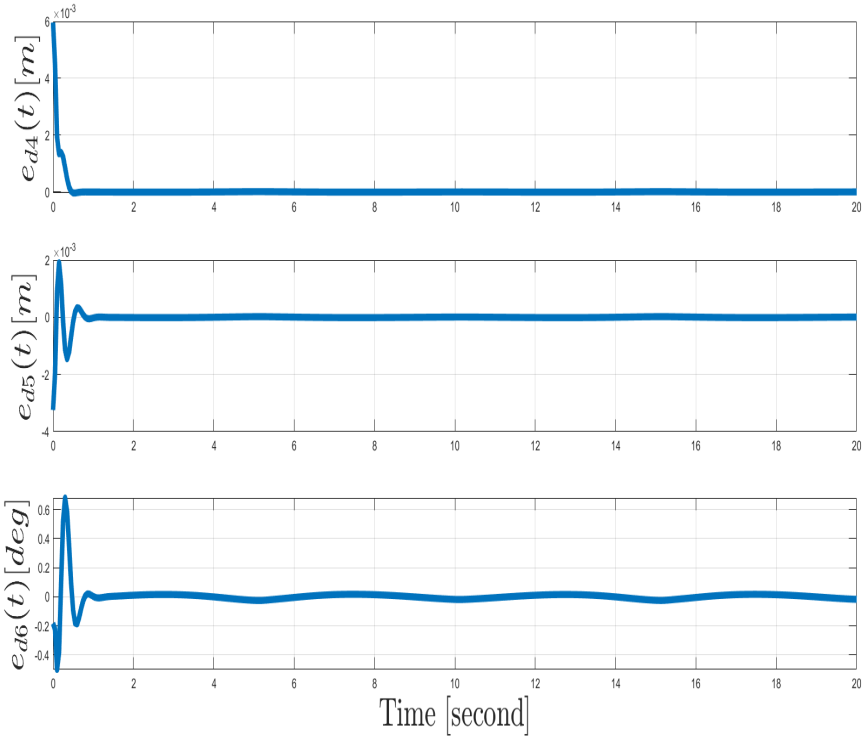

Figure 3.50: Tracking error of second end effector of parallel manipulator system

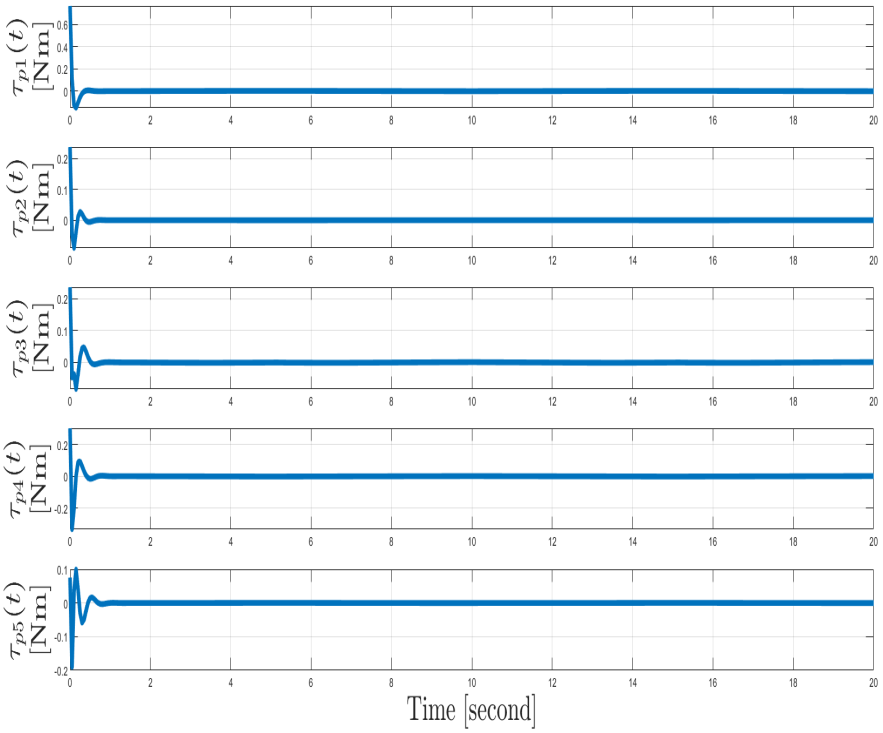

Figure 3.51: Control input torques for the parallel manipulator's joints

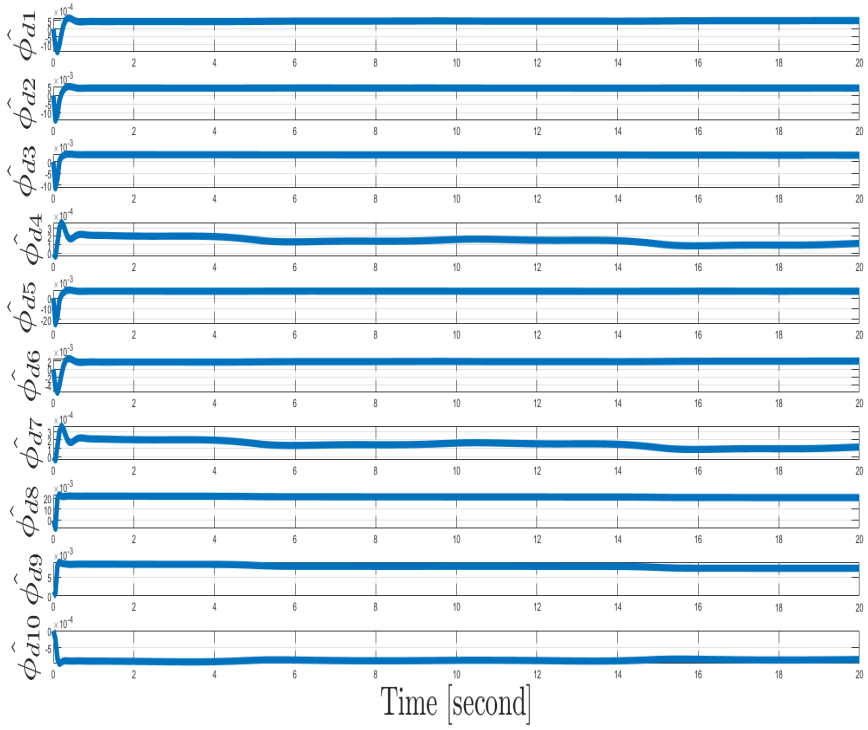

Figure 3.52: Adaptive compensation terms of parallel manipulator system

3.2.2.6 Experimental Results

Performance of the designed controller was tested on the experimental setup by keeping the desired trajectory, control gains identical with the simulation studies presented in Chapter 3.2.2.5. The initial position was selected as $x_p(0) = [0.1543 \quad 0.1215 \quad 18.1 - 0.1309 \quad 0.1133 \quad 162.5]^T$.

Desired trajectories and actual positions of the first and second end effectors are shown in Figures 3.53 and 3.54 against time, respectively. The movements of the end effectors in Cartesian coordinate system can be seen in Figures 3.55 and 3.56 with their desired movements in Cartesian coordinate system. Tracking errors for the tracking of end effectors are shown in Figures 3.57 and 3.58 for the first and second end effector, respectively. From Figures 3.53-3.58, it can be seen that the control objective was met. Control input torques are shown in Figure 3.59. Adaptive compensation is shown in Figures 3.60.

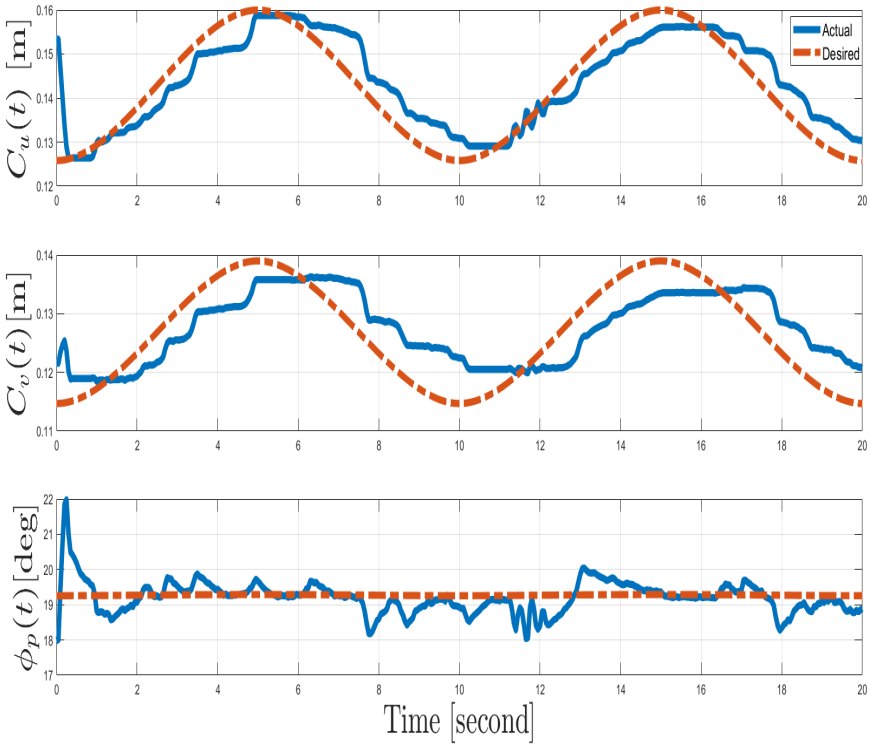

Figure 3.53: Desired vs. actual positions of first end effector of parallel manipulator system

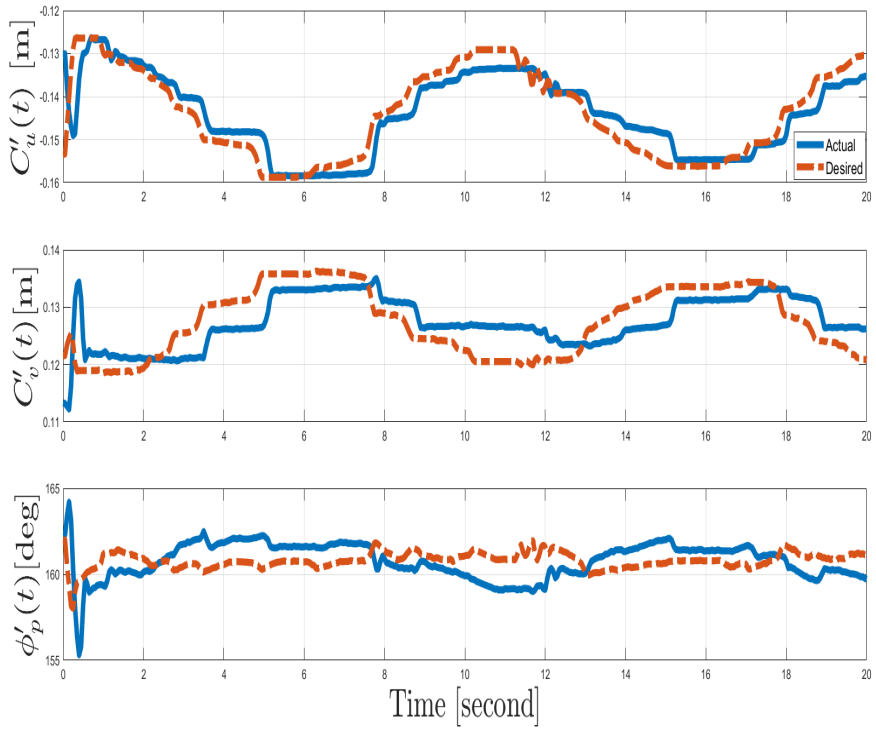

Figure 3.54: Desired vs. actual positions of second end effector of parallel manipulator system

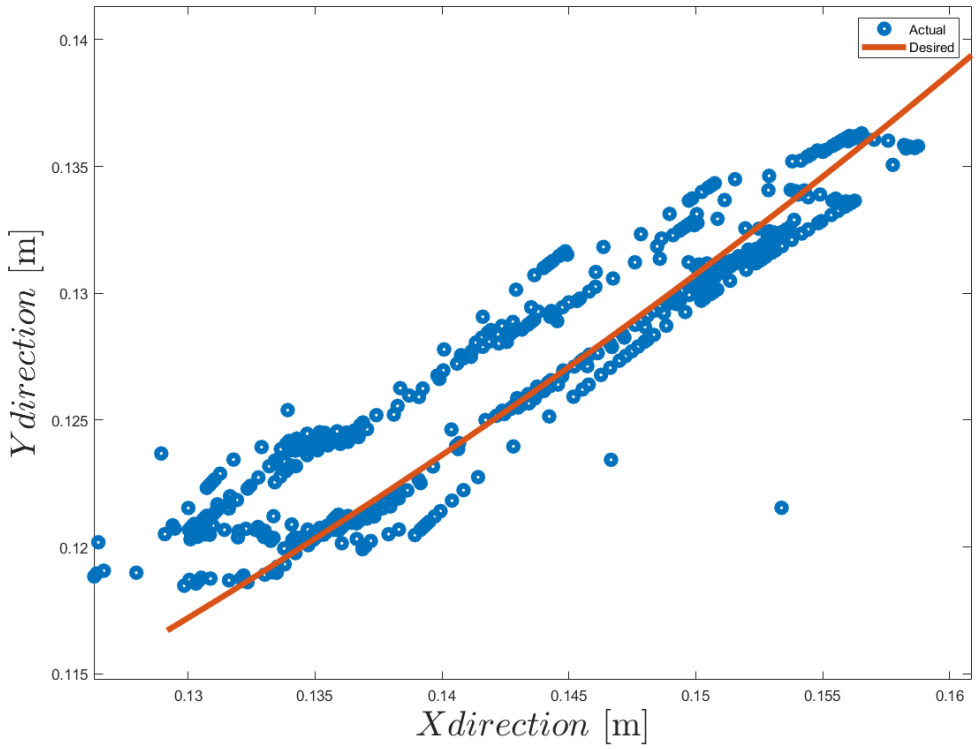

Figure 3.55: Desired vs. actual positions of first end effector of parallel manipulator system

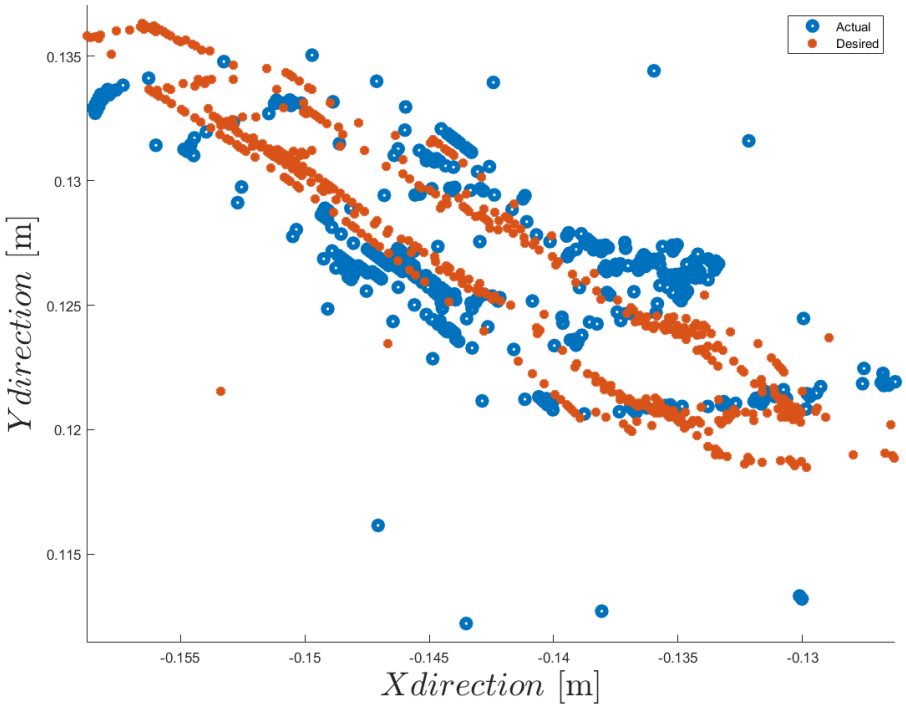

Figure 3.56: Desired vs. actual positions of second end effector of parallel manipulator system

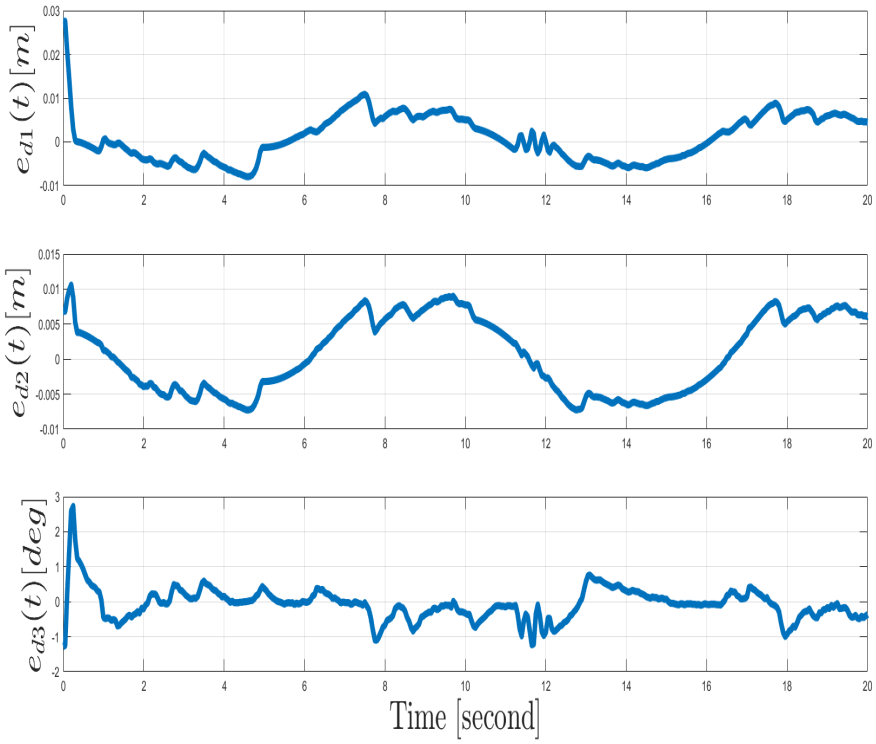

Figure 3.57: Tracking error of first end effector of the parallel manipulator system

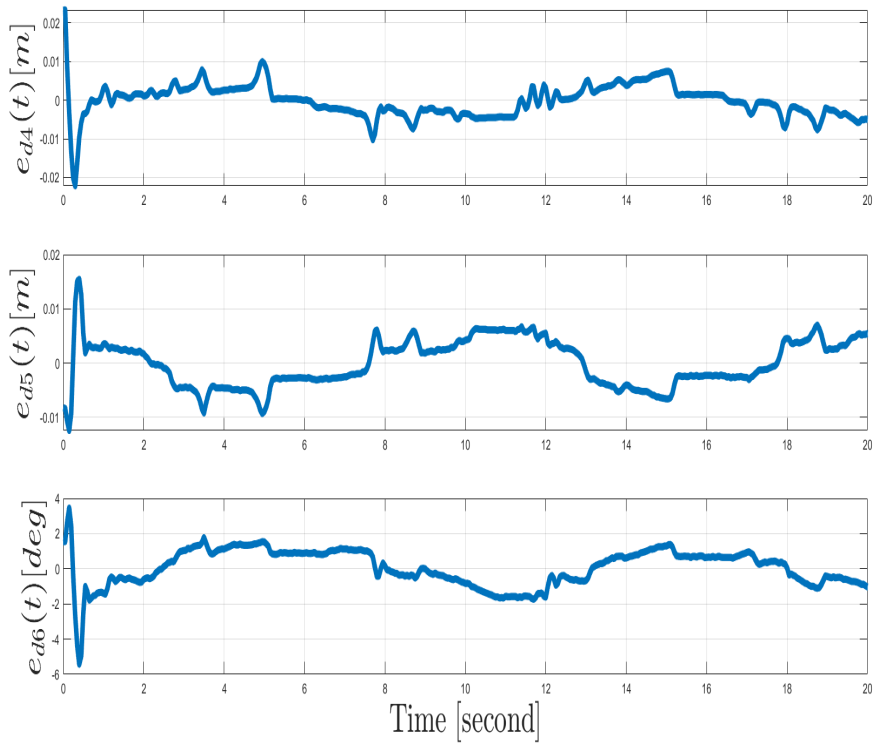

Figure 3.58: Tracking error of second end effector of the parallel manipulator system

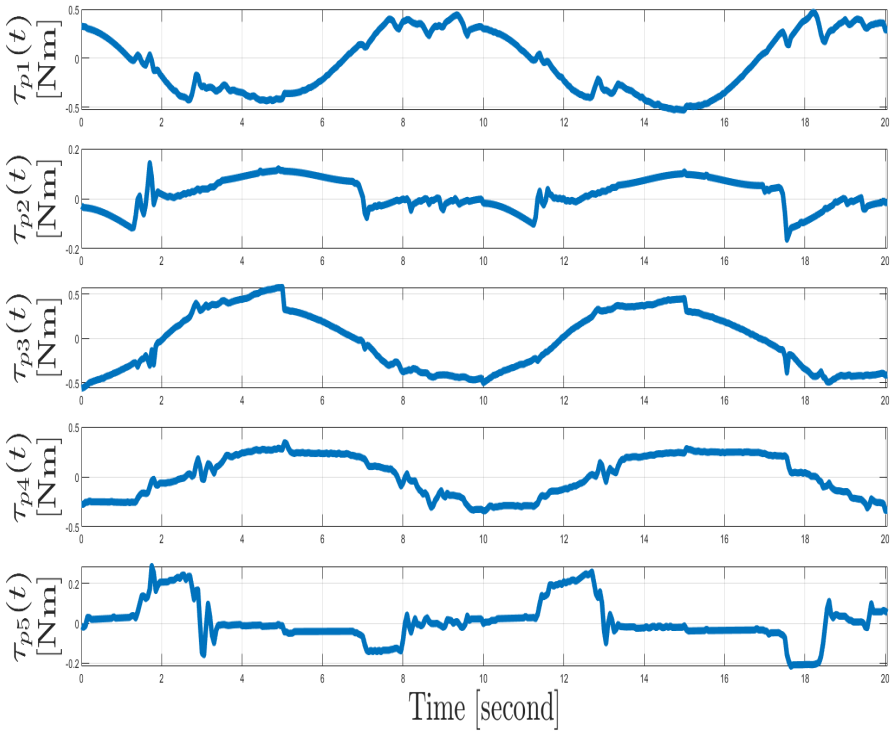

Figure 3.59: Control input torques for the parallel manipulator's joints

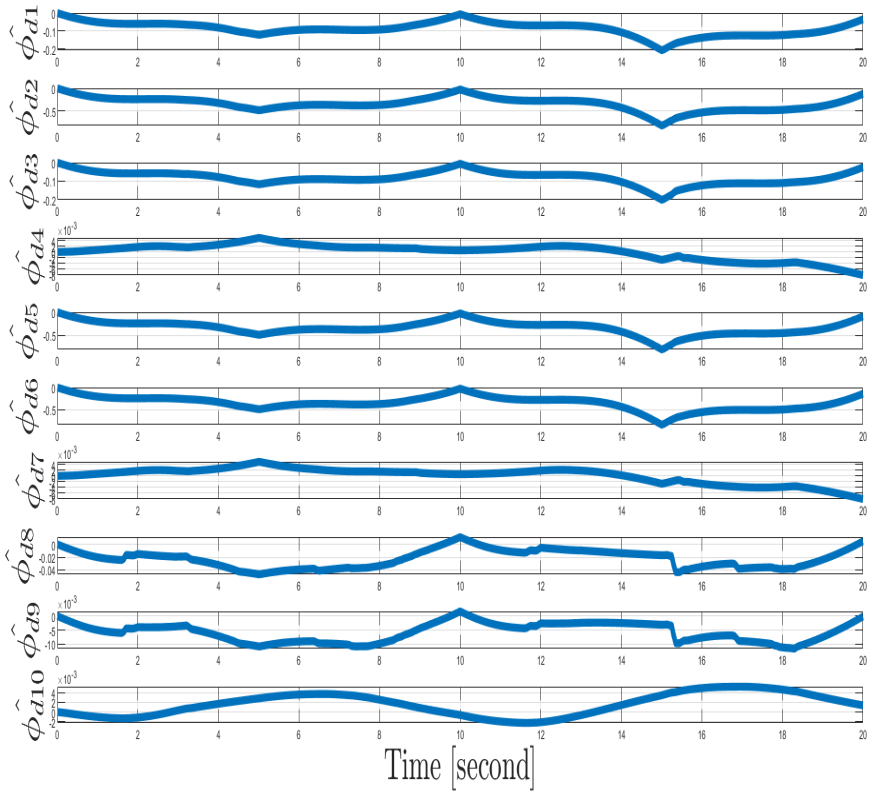

Figure 3.60: Adaptive compensation terms of parallel manipulator

Chapter 4

Conclusion

The control of supportive robotic systems that designed to provide the use of medical microrobots in cochlear workspaces was aimed and realized in this study. Intended to use in medical microrobot operations in the cochlear work area, the system consists of a macro-micro robot manipulator structure that provides to untethered movement within the cochlea ducts. This study includes two different robotic systems serving same aim, one of which contains two identical serial RRR 3 DoF robot manipulators while other one contains a revolute-prismatic joint 5 DoF parallel robot manipulator. The main purpose of these systems were to control the position of the microrobot in the cochlear work area using the magnetic field generated by the help of magnets located in the end effectors of the robot manipulators. To achieve this goal, the main control objective was set that one of the end effectors of the robot manipulator follows the desired trajectory, and the other end effector works in synchronize with the first end effector, and determines and follows its own tracking trajectory. The second end effector calculates the desired trajectory based on orientation of first end effector, workspace limit in the cochlear working area and the distance between the first end effector and the cochlea.

The high precision need of cochlear microrobot operations was met by controlling the system used in these operations. Two robust adaptive nonlinear controllers were designed for each of the robotic systems to provide the high precision required by cochlear microrobot operations. The robust control design was proposed as it can cope with possible changes in experimental systems, parametric uncertainties and external disturbances. However, to cope with the possible need for high control effort of robust controllers, this structure was supported with adaptive compensations and robust adaptive control design was realized for the systems. One of the controllers

was designed for the joint space, while the other was designed for the task space for each robotic system. Owing to the task space control, the burden of reaching the desired trajectory in the joint space was avoided by using inverse kinematics in the joint space control.

The theoretical analysis of each designed controller was proved through Lyapunov-based methods. Dynamic models of each of the robotic systems planned to be used as supporting systems in cochlear operation were obtained via recursive Newton-Euler and Lagrangian formulations. Obtained dynamic models were used to observe the performance of the designed controllers in the simulation environment. After the performance demonstration of the control designs were realized via simulation studies, their experimental performances were observed. The experiments on each of the robotic system verify the function of the adaptive terms and the robustness for model uncertainties.

Instead of using adaptive compensations neural network term can be used to cope with parametric uncertainties. Owing to this issue performances of robust adaptive and neural network based controllers can be observed in a comparative manner. Designing neural network based controllers to reach the control purposes mentioned in this study is considered as a future work. Moreover, to decrease the possible negative effects caused due to sensor precision problems, designing output feedback versions of the designed controllers is also aimed.

References

[1] Hollander KW and Thomas GS. A robust control concept for robotic ankle gait assistance. 2007 IEEE 10th international conference on rehabilitation robotic 2007; 119-123.

[2] Queirós P, Cortesão R and Sousa C. Haptic tele-manipulation for robotic-assisted minimally invasive surgery with explicit posture control. 18th Mediterranean Conference on Control and Automation, MED'10, Ieee 2010; 808-814.

[3] Li Z, Su CY, Wang L, Chen Z , Chai T. Nonlinear Disturbance Observer-Based Control Design for a Robotic Exoskeleton Incorporating Fuzzy Approximation. IEEE Transactions on Industrial Electronics 62.9 2015; 5763-5775

[4] Guzmán CH, Blanco A, Brizuelac J A, Gómez FA. Robust control of a hip–joint rehabilitation robot. Biomedical Signal Processing and Control 35 2017; 100-109.

[5] Le-Tien L, Albu-Schäffer A. Adaptive friction compensation in trajectory tracking control of DLR medical robots with elastic joints. International Conference on Intelligent Robots and Systems. IEEE 2012; 1149-1154

[6] Karar ME. A Simulation Study of Adaptive Force Controller for Medical Robotic Liver Ultrasound Guidance. Arab J Sci Eng 43 2018; 4229–4238 doi.org/10.1007/s13369-017-2893-4.

[7] Kolbari H, Sadeghnejad S, Bahrami M, Kamali EA. Adaptive control of a robot-assisted tele-surgery in interaction with hybrid tissues. Journal of Dynamic Systems, Measurement, and Control 2018; 140(12).

[8] Cortesão R, Zarrad W, Poignet P, Company O and Dombre E. Haptic control design for robotic-assisted minimally invasive surgery. IEEE/RSJ International Conference on Intelligent Robots and Systems 2006; 454-459.

[9] Ali SS, Raafat SM, Al-Khazraji A. Improving the performance of medical robotic system using H∞ loop shaping robust controller. International Journal of Modelling, Identification and Control 2020; 34(1): 3-12.

[10] Jayaswal K, Palwalia DK and Kumar S. Analysis of robust control method for the flexible manipulator in reliable operation of medical robots during COVID-19 pandemic. Microsystem Technologies 27 2021; 2103-2116

[11] Wang Z, Wang T, Zhao B, He Y, Hu Y, Li B, et al. Hybrid adaptive control strategy for continuum surgical robot under external load. IEEE Robotics and Automation Letters 2021; *6*(2), 1407-1414.

[12] Ka H, Ding D and Cooper RA. Three dimentional computer vision-based alternative control method for assistive robotic manipulator. Symbiosis 2016; 1.1.

[13] Dalvand M and Shirinzadeh B. Motion control analysis of a parallel robot assisted minimally invasive surgery/microsurgery system (PRAMiSS). Robotics and Computer-Integrated Manufacturing 2013; 29.2: 318-327

[14] Porto RA, Nageotte F, Zanne P and Mathelin M. Position control of medical cable-driven flexible instruments by combining machine learning and kinematic analysis. International Conference on Robotics and Automation 2019; 7913-7919

[15] Ozkul F and Barkana DE. Design of an admittance control with inner robust position control for a robot-assisted rehabilitation system RehabRoby. Ieee/Asme International Conference on Advanced Intelligent Mechatronics 2011;104-109

[16] Guo J, Yang S, Guo S, Meng C. and Qi, L. Study on robust control for the vascular interventional surgical robot. IEEE International Conference on Mechatronics and Automation 2019; 1361-1366

[17] Ma W, Li J, Niu F Ji Hand Sun, D. Robust control to manipulate a microparticle with electromagnetic coil system. IEEE Transactions on Industrial Electronics 2017; 64(11) :8566-8577

[18] Qin F, Zhao H, Zhen S, Sun H and Zhang Y. Lyapunov based robust control for tracking control of lower limb rehabilitation robot with uncertainty. International Journal of Control, Automation and Systems, 2020, 18.1: 76-84

[19] Sajadi SM, Mahdioun SH and Ghavifekr AA. Design of mechanical structure and tracking control system for 5 DOF surgical robot.. 21st Iranian Conference on Electrical Engineering (ICEE). IEEE; 2013; p. 1-6

[20] Kang H and Wang J. Adaptive Robust Control of 5 DOF Upper-limb Exoskeleton Robot. International Journal of Control, Automation, and Systems 2015; 13(3):733-741.

[21] Yang S, Han J, Xia L and Chen YH. An optimal fuzzy-theoretic setting of adaptive robust control design for a lower limb exoskeleton robot system. Mechanical Systems and Signal Processing 2020; 141: 106706.

[22] Zhang L, Xie J and Lu D. Adaptive Robust Control of One-link Joint Actuated by Pneumatic Artificial Muscles. 1st International Conference on Bioinformatics and Biomedical Engineering 2007; 1185-1189.

[23] Jayaswal K, Palwalia DK and KumarS. Performance investigation of PID controller in trajectory control of two-link robotic manipulator in medical robots. Journal of Interdisciplinary Mathematics, 2021; 24.2: 467-478.

[24] Seyfi NS and Khalaji AK. Robust control of a cable-driven rehabilitation robot for lower and upper limbs. ISA transactions, 2021.

[25] Golovin V, Arkhipov M and Zhuravlev V. Force training for position/force control of massage robots. New trends in medical and service robots 2014; 95-107.

[26] Verma V, Gupta A, Gupta MK and Chauhan P. Performance estimation of computed torque control for surgical robot application. Journal of Mechanical Engineering and Sciences 2020; 14.3: 7017-7028.

[27] Moreira P, Liu C, Zemiti N and Poignet P. Force control for robotic-assisted surgery based on viscoelastic tissue model. In: BIO Web of Conferences. EDP Sciences2011; 00066.

[28] Lee C and Oh S. Robust assistive force control of leg rehabilitation robot. IEEE international conference on advanced intelligent mechatronics (AIM) 2017; 634-638.

[29] Raafat SM ans Ali HA. Robust Controller Analysis and Design of Medical Haptic Control System. Engineering and Technology Journal 2017; 35.4 Part A: 318-326

[30] Verma V, Chauhan P and Gupta MK. Disturbance Observer-assisted Trajectory Tracking Control for Surgical Robot Manipulator. Journal Européen des Systèmes Automatisés 2019; 52.4: 355-362

[31] Shang Wand Cong S. Robust nonlinear control of a planar 2-DOF parallel manipulator with redundant actuation. Robotics and Computer-Integrated Manufacturing 2014; 30.6: 597-604.

[32] Fateh MM. Robust control of flexible-joint robots using voltage control strategy. Nonlinear Dynamics 2012; 67.2: 1525-1537.

[33] Salah M, Al-Jarrah A, Tatlicioglu E and Banihani S. Robust backstepping control for a four-bar linkage mechanism driven by a DC Motor. Journal of Intelligent & Robotic Systems 2019; 94.2: 327-338.

[34] Okur B, Aksoy O, Zergeroglu E and Tatlicioglu E. Nonlinear robust control of tendon–driven robot manipulators. Journal of Intelligent & Robotic Systems 2015; 80.1: 3-14.

[35] Soltanpour MR and Siahi M. Robust control of robot manipulator in task space. International Journal of Applied and Computational Mathematics 2009; 8.2: 227-238.

[36] Karayaman G, Gezgin E, Çetin L, Bıdıklı B, Cerrahi Mikrorobot Operasyonlarında Yardımcı Sistem Olarak Kullanılan Çift Robot Kollu Sistem için Lyapunov Tabanlı Görev Uzayı Denetimi Tasarımı ,TOK 2021;240-245.

[37] Kim H S, Cho Y M and Lee KI. Robust nonlinear task space control for 6 DoF parallel manipulator. Automatica 2005; 41.9: 1591-1600.

[38] Jin M, Kang SH and Chang PH. Robust compliant motion control of robot with nonlinear friction using time-delay estimation. IEEE Transactions on Industrial Electronics 2008; 55.1: 258-269.

[39] Lee D, Burg TC, Dawson DM, Shu D, Xian B and Tatlicioglu E. Robust tracking control of an underactuated quadrotor aerial-robot based on a parametric uncertain model.IEEE international conference on systems, man and cybernetics IEEE 2009; 3187-3192.

[40] Ren B, Wang Y, Liu L, Tu X and Lozano R. An adaptive robust control for trajectory tracking of a robotic manipulator system. Matrix 2018; 1: 2

[41] Achili B, Daachi B, Amirat Yand Ali-Cherif A. A robust adaptive control of a parallel robot. International Journal of control 2010; 83.10: 2107-2119

[42] Yin X and Pan L. Enhancing trajectory tracking accuracy for industrial robot with robust adaptive control. Robotics and Computer-Integrated Manufacturing 2018; 51: 97-102

[43] Chen Q, Chen H, Wang Y and Woo P. Robust adaptive trajectory tracking independent of models for robotic manipulators. Journal of Robotic Systems 2001; 18.9: 545-551

[44] Yao B and Tomizuka M. Comparative experiments of robust and adaptive control with new robust adaptive controllers for robot manipulators.

Proceedings of 1994 33rd IEEE Conference on Decision and Control 1994; 1290-1295

[45] Dou H and Wang S. Robust adaptive motion/force control for motion synchronization of multiple uncertain two-link manipulators. Mechanism and Machine Theory 2013; 67:77-93.

[46] Yin X and Pan, L. Direct adaptive robust tracking control for 6 DOF industrial robot with enhanced accuracy. ISA transactions 2018; 72: 178-184

[47] Barambones O and Etxebarria V. Robust adaptive control for robot manipulators with unmodelled dynamics. Cybernetics and Systems 2000; 31.1: 67-86

[48] Xiao B, Cao L, Xu S and Liu L. Robust tracking control of robot manipulators with actuator faults and joint velocity measurement uncertainty. IEEE/ASME Transactions on Mechatronics 2020; 25.3: 1354-1365

[49] Ahanda JJBM, Mbede JB, Melingui A and Zobo BE. Robust adaptive command filtered control of a robotic manipulator with uncertain dynamic and joint space constraints. Robotica 2018; 36.5: 767-786

[50] Tsai L. W. Robot analysis: the mechanics of serial and parallel manipulators. John Wiley & Sons 1999.

[51] Craig, John J. Introduction to robotics: mechanics and control. Pearson Education, 2005.

[52] Sharon A., Neville H., and David E. H. The macro/micro manipulator: An improved architecture for robot control. Robotics and computer-integrated manufacturing 10.3 1993; 209-222.

[53] Yu H. Modeling and control of hybrid machine systems — a five-bar mechanism case. International Journal of Automation and Computing 3 2006**;** 235–243. doi.org/10.1007/s11633-006-0235-1

[54] Arcese L, Fruchard M and Ferreira A. Adaptive controller and observer for a magnetic microrobot. IEEE Transactions on Robotics 2013; 29(4), 1060-1067.

[55] Mannani, A., & Talebi, H. A. A fuzzy Lyapunov-based control strategy for a macro–micro manipulator: Experimental results. IEEE transactions on control systems technology 2007; 15(2), 375-383.

[56] Chen Y, Mei, G, Ma, G, Lin, S and Gao J. Robust adaptive inverse dynamics control for uncertain robot manipulator. International Journal of Innovative Computing, Information and Control 2014; 10.2: 575-587.

[57] Ahmed S, Wang H and Tian Y. Robust adaptive fractional-order terminal sliding mode control for lower-limb exoskeleton. Asian Journal of Control 2019; 21.1: 473-482.

[58] Azizi S, Soleimani R, Ahmadi M, Malekan A, Abueligah L and Ahangar FD. Performance enhancement of an uncertain nonlinear medical robot with optimal nonlinear robust controller. Computers in Biology and Medicine 2022; 105567.

[59] Harandi MRJ, Khalilpour, SA, Taghirad HD and Romero JG. Adaptive control of parallel robots with uncertain kinematics and dynamics. Mechanical Systems and Signal Processing 2021; 157: 107693.

[60] Liu JF, Abdel-Malek K. Robust control of planar dual-arm cooperative manipulators. Robotics and Computer-Integrated Manufacturing 2000; 16.2-3: 109-119.

[61] Khalil HK. Nonlinear Systems, 3rd Edition. New York, NY, USA: Prentice Hall 2002.

Appendices

Appendix A

The open form of $W_{1,2}$ and Z_j for j=1,⋯,12

The open form of $W_{1,2}$ and Z_j for $j = 1, \cdots, 12$ defined in (2.28) can be obtained as

$$W_1 = 2l_p^2 cos(\theta_{p1} - \theta_{p2}) + d_1^2 + d_2^2 + 2l_p^2 - 2d_1 l_p\ (sin\theta_{p1} + sin\theta_{p2}) + 2d_2 l_p(cos\theta_{p1} + cos\theta_{p2}) \quad (A.1)$$

$$W_2 = 2l_p^2 cos(\theta'_{p1} - \theta'_{p2}) + d_1^2 + d_2^2 + 2l_p^2 + 2d_2 l_p(cos\theta'_{p1} + cos\theta'_{p2}) - 2l_p d_1(\sin\theta'_{p1} + \sin\theta'_{p2}) \quad (A.2)$$

$$Z_1 = l_p^2\, cos(\theta_{p1} - \theta_{p2}) + l^2 + d_2 l_p \cos\theta_{p1} - d_1 l_p \sin\theta_{p1} \quad (A.3)$$

$$Z_2 = l_p^2\, cos(\theta_{p1} - \theta_{p2}) + l_p^2 + d_2 l_p \cos\theta_{p2} - d_1 l_p \sin\theta_{p2} \quad (A.4)$$

$$Z_3 = l_p^2\, cos(\theta'_{p1} - \theta'_{p2}) + l_p^2 - d_2 l_p \cos\theta'_{p1} - d_1 l_p \sin\theta'_{p1} \quad (A.5)$$

$$Z_4 = l_p^2\, cos(\theta'_{p1} - \theta'_{p2}) + l_p^2 - d_2 l_p \cos\theta'_{p2} - d_1 l_p \sin\theta'_{p2} \quad (A.6)$$

$$Z_5 = -d_2 - l_p \cos\theta_{p1} - d_1 l_p \sin\theta_{p2} \quad (A.7)$$

$$Z_6 = d_2 - l_p \cos\theta'_{p1} - d_1 l_p \sin\theta'_{p2} \quad (A.8)$$

$$Z_7 = -\frac{1}{2} d_3 (l_p^2 \cos(\theta_{p1} - \theta_{p2}) + l_p^2 + d_2 l_p \cos\theta_{p1} - d_1 l_p \sin\theta_{p1}) / (2l_p^2 cos(\theta_{p1} - \theta_{p2}) + d_1^2 + d_2^2 + 2l_p^2 + 2d_2 l_p(cos\theta_{p1} + cos\theta_{p2}) - 2d_1 l_p(sin\theta_{p1} + sin\theta_{p2})) \quad (A.9)$$

$$Z_8 = -\frac{1}{2}d_3(l_p^2\cos(\theta_{p1} - \theta_{p2}) + l_p^2 + d_2 l_p \cos\theta_{p2} - d_1 l_p \sin\theta_{p2})/(2l_p^2\cos(\theta_{p1} - \theta_{p2}) + d_1^2 + d_2^2 + 2l_p^2 + 2d_2 l_p(\cos\theta_{p1} + \cos\theta_{p2}) - 2d_1 l_p(\sin\theta_{p1} + \sin\theta_{p2})) \quad \text{(A.10)}$$

$$Z_9 = \frac{1}{2}d_3(d_2 + l_p\cos\theta_{p1} + d_1 l_p \sin\theta_{p2})/(2l_p^2\cos(\theta_{p1} - \theta_{p2}) + d_1^2 + d_2^2 + 2l_p^2 + 2d_2 l_p(\cos\theta_{p1} + \cos\theta_{p2}) - 2d_1 l_p(\sin\theta_{p1} + \sin\theta_{p2})) \quad \text{(A.11)}$$

$$Z_{10} = \frac{1}{2}d_3(d_2 - l_p\cos\theta'_{p1} - d_1 l_p \sin\theta'_{p2})/(2l_p^2\cos(\theta'_{p1} - \theta'_{p2}) + d_1^2 + d_2^2 + 2l_p^2 + 2d_2 l_p(\cos\theta'_{p1} + \cos\theta'_{p2}) - 2l_p d_1(\sin\theta'_{p1} + \sin\theta'_{p2})) \quad \text{(A.12)}$$

$$Z_{11} = \frac{1}{2}d_3(l_p^2\cos(\theta'_{p1} - \theta'_{p2}) + l_p^2 - d_2 l_p \cos\theta'_{p1} - d_1 l_p \sin\theta'_{p1})/(2l_p^2\cos(\theta'_{p1} - \theta'_{p2}) + d_1^2 + d_2^2 + 2l_p^2 + 2d_2 l_p(\cos\theta'_{p1} + \cos\theta'_{p2}) - 2l_p d_1(\sin\theta'_{p1} + \sin\theta'_{p2})) \quad \text{(A.13)}$$

$$Z_{12} = \frac{1}{2}d_3(l_p^2\cos(\theta'_{p1} - \theta'_{p2}) + l_p^2 - d_2 l_p \cos\theta'_{p2} - d_1 l_p \sin\theta'_{p2})/(2l_p^2\cos(\theta'_{p1} - \theta'_{p2}) + d_1^2 + d_2^2 + 2l_p^2 + 2d_2 l_p(\cos\theta'_{p1} + \cos\theta'_{p2}) - 2l_p d_1(\sin\theta'_{p1} + \sin\theta'_{p2})) \quad \text{(A.14)}$$

Appendix B

Elements of $V_p(\theta_p, \dot{\theta}_p)$

The open form of elements of $V_p(\theta_p, \dot{\theta}_p)$ can be obtained as

$$
\begin{aligned}
V_{p11} = \dot{\theta}_{p2}\Big(&\tfrac{1}{4}(l_p^2 m_{p2} + l_p^2 m_{p3} + 2l_p^2 m_{p5})\sin(\theta_{p1} - \theta_{p2}) + \\
&Z_2 l_p\big((m_{p7} d_3^2 + 4I_{p_5} + 4I_{p_7})(d_1 \cos\theta_{p1} + d_2 \sin\theta_{p1} + \\
&l_p \sin(\theta_{p1} - \theta_{p2}))(d_1^2 - 2\, l_p d_1 \sin\theta_{p2} + d_2^2 + \\
&2 l_p d_2 \cos\theta_{p2}))/2W_1^3\big) - \dot{d}_1\big((3Z_1 l_p(m_{p7} d_3^2 + 4I_{p_5} + \\
&4I_{p_7})(d_2^2 \sin\theta_{p1} - d_1^2 \sin\theta_{p1} - l_p^2 \sin\theta_{p1} - 2l_p^2 \sin\theta_{p2} + \\
&2d_1 l_p + l_p^2 \sin(\theta_{p1} - 2\theta_{p2}) + 2d_1 l_p \cos(\theta_{p1} - \theta_{p2}) + \\
&2d_2 l_p \sin(\theta_{p1} - \theta_{p2}) + 2d_1 d_2 \cos\theta_{p1}) - \\
&l_p(d_1 \cos\theta_{p1} + d_2 \sin\theta_{p1} + \\
&l_p \sin(\theta_{p1} - 2\theta_{p2}))(Z_5 m_{p7} d_3^2 + 2W_1 m_{p7} \cos\phi_p\, d_3 + \\
&4I_{p_5} Z_5 + 4I_{p_7} Z_5)(d_1^2 - 2l_p d_1 \sin\theta_{p2} + d_2^2 + \\
&2l_p d_2 \cos\theta_{p2})/8W_1^3\big) - \dot{\theta}_{p1}\Big(Z_1 l_p(m_{p7} d_3^2 + 4I_{p_5} + \\
&4I_{p_7})(d_1 \cos\theta_{p1} + d_2 \sin\theta_{p1} + l_p \sin(\theta_{p1} - 2\theta_{p2}))(d_1^2 - \\
&2l_p\, d_1 \sin(\theta_{p2}) + d_2^2 + 2\, l_p d_2 \cos\theta_{p2})\Big)/4W_1^3
\end{aligned}
\tag{B.1}
$$

$$
\begin{aligned}
V_{p12} = \dot{\theta}_{p2}\Big(&\tfrac{1}{2}(l_p^2 m_{p2} + l_p^2 m_{p3} + 2l_p^2 m_{p5})\, sin(\theta_{p1} - \theta_{p2}) - \\
&(Z_1 l_p(m_{p7} d_3^2 + 4I_{p_5} + 4I_{p_7})(d_1\, cos\,\theta_{p1} + d_2\, sin\,\theta_{p1} - \\
&l_p\, sin(\theta_{p1} - 2\theta_{p2}))(d_1^2 - 2l_p\, d_1 sin(\theta_{p1}) + d_2^2 + \\
&2\, l_p d_2 cos(\theta_{p1}))/W_1^3)) - \dot{\theta}_{p1}(\tfrac{1}{4}(l_p^2 m_2 + l_p^2 m_3 + \\
&2l_p^2 m_5)\, sin(\theta_{p1} - \theta_{p2}) - (Z_1 l_p^2(m_{p7} d_3^2 + 4I_{p_5} + \\
&4I_{p_7})(d_2^2\, sin(\theta_{p1} + \theta_{p2}) - d_1^2\, sin(\theta_{p1} + \theta_{p2}) + \\
&2l_p d_1 cos\theta_{p1} + 2l_p d_1 cos\theta_{p2} + 2l_p d_2 sin\theta_{p1} + \\
&2l_p d_2 sin\theta_{p2} + 2d_2 d_1 cos(\theta_{p1} + \theta_{p2}))/2W_1^3) + \\
&Z_2 l_p((m_{p7} d_3^2 + 4I_{p_5} + 4I_{p_7})(d_1\, cos(\theta_{p1}) + \\
&d_2\, sin(\theta_{p1}) + l_p\, sin(\theta_{p1} - \theta_{p2}))(d_1^2 - 2\, l_p d_1 sin\,\theta_{p2} + \\
&d_2^2 + 2l_p d_2\, cos\,\theta_{p2}))/2W_1^3))) - \dot{d}_1((l_p(m_{p7} d_3^2 + 4I_{p_5} + \\
&4I_{p_7})(Z_1 d_2^2 sin\theta_{p2} - Z_2 d_1^2\, sin\,\theta_{p1} - Z_1 d_1^2 sin\theta_{p2} + \\
&Z_2 d_2^2 sin\theta_{p1} - 2Z_1 l_p^2 sin\theta_{p1} - Z_1 l_p^2 sin\theta_{p2} - \\
&Z_2 l_p^2 sin\theta_{p1} - 2Z_2 l_p^2 sin\theta_{p2} + 2d_1 l_p Z_1 + 2d_1 l_p Z_2 + \\
&Z_2 l_p^2 sin(\theta_{p1} - 2\theta_{p2}) - Z_1 l_p^2 sin(2\theta_{p1} - \theta_{p2}) + \\
&2Z_1 d_1 d_2 cos\theta_{p2} + 2Z_2 d_1 d\_2 cos\theta_{p1} + 2Z_1 d_1 l_p cos(\theta_{p1} -
\end{aligned}
\tag{B.2}
$$

$$\theta_{p2}) + 2Z_2 d_1 l_p cos(\theta_{p1} - \theta_{p2}) - 2Z_1 d_2 l_p sin(\theta_{p1} - \theta_{p2}) + 2Z_2 d_2 l_p sin(\theta_{p1} - \theta_{p2}))/4W_1^3) + (Z_5 l_p^2 (m_{p7} d_3^2 + 4I_{p_5} + 4I_{p_7})(d_2^2 \, sin(\theta_{p1} + \theta_{p2}) - d_1^2 \, sin(\theta_{p1} + \theta_{p2}) + 2l_p d_1 cos\theta_{p1} + 2l_p d_1 cos\theta_{p2} + 2l_p d_2 sin\theta_{p1} + 2l_p d_2 sin\theta_{p2} + 2d_2 d_1 cos(\theta_{p1} + \theta_{p2})/2W_1^3) - Z_2 l_p((m_{p7} d_3^2 + 4I_{p_5} + 4I_{p_7})(d_2^2 \, sin(\theta_{p1}) - d_1^2 \, sin(\theta_{p1}) - l_p^2 \, sin(\theta_{p1}) - 2l_p^2 \, sin(\theta_{p2}) + 2d_1 l_p + l_p^2 \, sin(\theta_{p1} - 2\theta_{p2}) + 2d_1 l_p \, cos(\theta_{p1} - \theta_{p2}) + 2d_2 l_p \, sin(\theta_{p1} - \theta_{p2}) + 2d_1 d_2 \, cos\theta_{p1})/2W_1^3) + d_3 m_7 l_p^2 \, cos \, \phi_p \, (d_2^2 \, sin(\theta_{p1} + \theta_{p2}) - d_1^2 \, sin(\theta_{p1} + \theta_{p2}) + 2l_p d_1 cos\theta_{p1} + 2l_p d_1 cos\theta_{p2} + 2l_p d_2 sin\theta_{p1} + 2l_p d_2 sin\theta_{p2} + 2d_2 d_1 cos(\theta_{p1} + \theta_{p2})))$$

$$V_{p13} = \dot{\theta}_{p2}((l_p^2(Z_5 m_{p7} d_3^2 + 2W_1 m_{p7} \cos\phi_p d_3 + 4I_{p_5} Z_5 + 4I_{p_7} Z_5)(d_2^2 \sin(\theta_{p1} + \theta_{p2}) - d_1^2 \sin(\theta_{p1} + \theta_{p2})) + 2d_1 l_p cos\theta_{p1} + 2d_1 l_p cos\theta_{p2} + d_2 l_p sin\theta_{p1} + d_2 l_p sin\theta_{p2} + 2d_1 d_2 \cos(\theta_{p1} + \theta_{p2})))/4W_1^3 - (\tfrac{1}{4} Z_5 l_p^2 (\mathrm{d}_3^2 \mathrm{m}_{\mathrm{p7}} + 4I_{p_5} + 4I_{p_7})(d_2^2 \sin(\theta_{p1} + \theta_{p2})) - d_1^2 sin(\theta_{p1} + \theta_{p2})) + 2d_1 l_p cos\theta_{p1} + 2d_1 l_p cos\theta_{p2} + d_2 l_p sin\theta_{p1} + d_2 l_p sin\theta_{p2} + + 2d_1 d_2 cos(\theta_{p1} + \theta_{p2})))/2W_1^3 + (\tfrac{1}{4} Z_2 l_p (\mathrm{d}_3^2 \mathrm{m}_{\mathrm{p7}} + 4I_{p_5} + 4I_{p_7})(d_2^2 sin\theta_{p1} - d_1^2 sin\theta_{p1} - l_p^2 sin\theta_{p1} - l_p^2 sin\theta_{p2} + 2d_1 l_p + l_p^2 sin(\theta_{p1} - 2\theta_{p2}) + 2d_1 l_p \cos(\theta_{p1} - \theta_{p2}) + d_2 l_p \sin(\theta_{p1} - \theta_{p2}) + 2d_1 d_2 cos\theta_{p1}))/2W_1^3 + (Z_1 l_p (\mathrm{m}_{\mathrm{p7}} \mathrm{d}_3^2 + 4I_{p_5} + 4I_{p_7})(d_1^2 sin\theta_{p2} - d_2^2 sin\theta_{p2} + 2l_p^2 sin\theta_{p1} + l_p^2 sin\theta_{p2} - 2d_1 l_p + l_p^2 sin(2\theta_{p1} - \theta_{p2}) - 2d_1 l_p \cos(\theta_{p1} - \theta_{p2}) + d_2 l_p sin(\theta_{p1} - \theta_{p2}) - 2d_1 d_2 cos\theta_{p2}))/4W_1^3 - (d_3 l_p^2 m_{p7} \cos\phi_p (\mathrm{d}_2^2 \sin(\theta_{p1} + \theta_{p2})) - \mathrm{d}_1^2 \sin(\theta_{p1} + \theta_{p2})) + 2d_1 l_p cos\theta_{p1} + 2d_1 l_p cos\theta_{p2} + 2d_2 l_p sin\theta_{p1} + 2d_2 l_p sin\theta_{p2} + 2d_1 d_2 cos(\theta_{p1} + \theta_{p2})))/4W_1^2) - \dot{\theta}_{p1}((Z_1 l_p (d_3^2 m_{p7} + 4I_{p_5} + 4I_{p_7})(d_2^2 sin\theta_{p1} - d_1^2 sin\theta_{p1} - l_p^2 sin\theta_{p1} - l_p^2 sin\theta_{p2} + 2d_1 l_p + l_p^2 sin(\theta_{p1} - 2\theta_{p2}) + 2d_1 l_p cos(\theta_{p1} - \theta_{p2})) + d_2 l_p sin(\theta_{p1} - \theta_{p2}) + 2d_1 d_2 cos\theta_{p1}))/8W_1^3 + (l_p(d_1 cos\theta_{p1} + d_2 sin\theta_{p1} + l_p sin(\theta_{p1} - \theta_{p2}))(d_1^2 - 2l_p d_1 sin\theta_{p2} + d_2^2 + 2l_p d_2 cos\theta_{p2})(4I_{p_5} Z_5 + 4I_{p_7} Z_5 + Z_5 m_{p7} d_3^2 + 2W_1 m_{p7} cos\phi_p d_3))/8W_1^3) - \dot{d}_1(Z_1(d_2 + l_p cos\theta_{p1} + l_p cos\theta_{p2})(m_{p7} d_3^2 + 4I_{p_5} + 4I_{p_7})(l_p sin\theta_{p1} - d_1 + l_p sin\theta_{p2}))/2W_1^3 \tag{B.3}$$

$$V_{p14} = V_{p15} = 0 \tag{B.4}$$

$$
\begin{aligned}
V_{p21} = {} & \dot{\theta}_{p2}((l_p^2\, m_{p2}\, sin(\theta_{p1}-\theta_{p2}))/4 + (l_p^2 m_{p3} sin(\theta_{p1}- \\
& \theta_{p2}))/4 + (l_p^2 m_{p5}\, sin(\theta_{p1}-\theta_{p2}))/2 + (Z_2 l_p^2 (m_{p7} d_3^2 + \\
& 4I_{p_5} + 4I_{p_7})(d_2^2\, sin(\theta_{p1}+\theta_{p2}) - d_1^2\, sin(\theta_{p1}+\theta_{p2}) + \\
& 2d_1 l_p cos\theta_{p1} + 2d_1 l_p cos\theta_{p2} + 2d_2 l_p sin\theta_{p1} + \\
& 2d_2 l_p sin\theta_{p2} + 2d_1 d_2 cos(\theta_{p1}+\theta_{p2})))/8W_1^3 - \\
& (Z_1 l_p (m_{p7} d_3^2 + 4I_{p_5} + 4I_{p_7})(d_1 cos\theta_{p2} + d_2 sin\theta_{p2} - \\
& l_p\, sin(\theta_{p1}-\theta_{p2}))(d_1^2 - 2l_p sin\theta_{p1} d_1 + d_2^2 + \\
& 2l_p cos\theta_{p1} d_2))/W_1^3) - \dot{\theta}_{p1}((l_p^2 m_{p2} sin(\theta_{p1}-\theta_{p2}))/2 + \\
& (l_p^2 m_{p3} sin(\theta_{p1}-\theta_{p2}))/2 + (l_p^2 m_{p5} sin(\theta_{p1}-\theta_{p2})) + \\
& (Z_2 l_p (m_{p7} d_3^2 + 4I_{p_5} + 4I_{p_7})(d_1 cos\theta_{p1} + d_2 sin\theta_{p1} + \\
& l_p sin(\theta_{p1}-\theta_{p2}))(d_1^2 - 2l_p d_1 sin\theta_{p2} + d_2^2 + \\
& 2l_p d_2 cos\theta_{p2}))/4W_1^3) - \dot{d}_1((l_p(m_{p7} d_3^2 + 4I_{p_5} + \\
& 4I_{p_7})(Z_1 d_2^2 sin\theta_{p2} - Z_2 d_1^2 sin\theta_{p1} - Z_1 d_1^2 sin\theta_{p2} + \\
& Z_2 d_2^2 sin\theta_{p1} - 2Z_1 l_p^2 sin\theta_{p1} - Z_1 l_p^2 sin\theta_{p2} - Z_2 l_p^2 sin\theta_{p1} - \\
& 2Z_2 l_p^2 sin\theta_{p2} + 2Z_1 d_1 l_p + 2Z_2 d_1 l_p + Z_2 l_p^2 sin(\theta_{p1} - \\
& 2\theta_{p2}) - Z_1 l_p^2 sin(2\theta_{p1}-\theta_{p2}) + 2Z_1 d_1 d_2 cos\,\theta_{p2} + \\
& 2Z_2 d_1 d_2 cos\theta_{p1} + 2Z_1 d_1 l_p cos(\theta_{p1}-\theta_{p2}) + \\
& 2Z_2 d_1 l_p cos(\theta_{p1}-\theta_{p2}) - 2Z_1 d_2 l_p sin(\theta_{p1}-\theta_{p2}) + \\
& 2Z_2 d_2 l_p sin(\theta_{p1}-\theta_{p2})))/4W_1^3 + (l_p^2(Z_5 m_{p7} d_3^2 + \\
& 2W_1 m_{p7} cos\emptyset_p d_3 + 4I_{p_5} Z_5 + 4I_{p_7} Z_5)(d_2^2 sin(\theta_{p1} + \\
& \theta_{p2}) - d_1^2 sin(\theta_{p1}+\theta_{p2}) + 2d_1 l_p cos\theta_{p1} + \\
& 2d_1 l_p cos\theta_{p2} + 2d_2 l_p sin\theta_{p1} + \\
& 2d_2 l_p sin\theta_{p2} + 2d_1 d_2 cos(\theta_{p1}+\theta_{p2})))/8W_1^3 + \\
& (Z_1 l_p (m_{p7} d_3^2 + 4I_{p_5} + 4I_{p_7})(d_1^2 sin\theta_{p2} - d_2^2 sin\theta_{p2} + \\
& 2l_p^2 sin\theta_{p1} + l_p^2 sin\theta_{p2} - 2d_1 l_p + l_p^2 sin(2\theta_{p1}-\theta_{p2}) - \\
& 2d_1 l_p cos(\theta_{p1}-\theta_{p2}) + 2d_2 l_p sin(\theta_{p1}-\theta_{p2}) - \\
& 2d_1 d_2 cos\theta_{p2}))/8W_1^3)
\end{aligned}
\tag{B.5}
$$

$$
\begin{aligned}
V_{p22} = {} & \dot{d}_1((Z_2 l_p (m_{p7} d_3^2 + 4I_{p_5} + 4I_{p_7})(d_1^2 sin\theta_{p2} - \mathrm{d}_2^2 \sin\theta_{p2} + \\
& 2l_p^2 \sin\theta_{p1} + l_p^2 sin\theta_{p2} - 2\mathrm{d}_1 l_p + l_p^2 \sin(2\theta_{p1}-\theta_{p2}) - \\
& 2\mathrm{d}_1 l_p \cos(\theta_{p1}-\theta_{p2}) + 2d_2 l_p \sin(\theta_{p1}-\theta_{p2}) - \\
& 2\mathrm{d}_1 \mathrm{d}_2 \cos\theta_{p2}))/2W_1^3 - Z_2 l_p((m_{p7} d_3^2 + 4I_{p_5} + \\
& 4I_{p_7})(d_1^2 sin\theta_{p2} - \mathrm{d}_2^2 \sin\theta_{p2} + 2l_p^2 \sin\theta_{p1} + l_p^2 sin\theta_{p2} - \\
& 2\mathrm{d}_1 l_p + l_p^2 \sin(2\theta_{p1}-\theta_{p2}) - 2\mathrm{d}_1 l_p \cos(\theta_{p1}-\theta_{p2}) + \\
& 2d_2 l_p \sin(\theta_{p1}-\theta_{p2}) - 2\mathrm{d}_1 \mathrm{d}_2 \cos\theta_{p2}))/8W_1^3 + \\
& (Z_5 l_p (m_{p7} d_3^2 + 4I_{p_5} + 4I_{p_7})(d_1 cos\theta_{p2} + d_2 sin\theta_{p2} - \\
& l_p \sin(\theta_{p1}-\theta_{p2}))(d_1^2 - 2l_p d_1 sin\theta_{p1} + d_2^2 + \\
& 2l_p d_2 cos\theta_{p1}))/8W_1^3 + \\
& (d_3 l_p m_{p7} cos\phi_p (d_1 cos\theta_{p2} + d_2 sin\theta_{p2} - l_p \sin(\theta_{p1}- \\
& \theta_{p2}))(d_1^2 - 2l_p d_1 sin\theta_{p1} + d_2^2 + 2l_p d_2 cos\theta_{p1}))/4W_1^2) - \\
& \dot{\theta}_{p1}((l_p^2 m_2 sin(\theta_{p1}-\theta_{p2}))/4 + (l_p^2 m_3 \sin(\theta_{p1}- \\
& \theta_{p2}))/4 + (l_p^2 m_5 \sin(\theta_{p1}-\theta_{p2}))/2 - (Z_2 l_p^2 (m_{p7} d_3^2 + \\
& 4I_{p_5} + 4I_{p_7})(d_2^2 \sin(\theta_{p1}+\theta_{p2}) - \mathrm{d}_1^2 \sin(\theta_{p1}+\theta_{p2}) +
\end{aligned}
\tag{B.6}
$$

$$
\begin{aligned}
&2d_1 l_p cos\theta_{p1} + 2d_1 l_p cos\theta_{p2} + 2d_2 l_p sin\theta_{p1} + \\
&2d_2 l_p sin\theta_{p2} + 2d_1 d_2 cos(\theta_{p1} + \\
&\theta_{p2})))/2W_1^3 + (\mathrm{Z}_2 l_p^2 (m_{p7} d_3^2 + 4I_{p_5} + 4I_{p_7}) d_2^2 \sin(\theta_{p1} + \\
&\theta_{p2}) - \mathrm{d}_1^2 \sin(\theta_{p1} + \theta_{p2}) + 2d_1 l_p cos\theta_{p1} + \\
&2d_1 l_p cos\theta_{p2} + 2d_2 l_p sin\theta_{p1} + \\
&2d_2 l_p sin\theta_{p2} + 2d_1 d_2 cos(\theta_{p1} + \\
&\theta_{p2}))/8W_1^3 - (\mathrm{Z}_1 l_p (m_{p7} d_3^2 + 4I_{p_5} + \\
&4I_{p_7})(d_1 cos\theta_{p2} + d_2 sin\theta_{p2} - l_p \sin(\theta_{p1} - \theta_{p2}))(d_1^2 - \\
&2l_p d_1 sin\theta_{p1} + d_2^2 + \\
&2l_p d_2 cos\theta_{p1}))/8W_1^3) - \dot{\theta}_{p2} (Z_2 l_p (m_{p7} d_3^2 + 4I_{p_5} + \\
&4I_{p_7})(d_1 cos\theta_{p2} + d_2 sin\theta_{p2} - l_p \sin(\theta_{p1} - \theta_{p2}))(d_1^2 - \\
&2l_p d_1 sin\theta_{p1} + d_2^2 + 2l_p d_2 cos\theta_{p1}))/4W_1^3
\end{aligned}
$$

$$
\begin{aligned}
V_{p23} = &-\dot{\theta}_{p1} ((\tfrac{1}{8} l_p^2 (Z_5 m_{p7} d_3^2 + 2W_1 m_{p7} d_3 cos\phi_p + 4I_{p_5} Z_5 + \\
&4I_{p_7} Z_5)(d_2^2 sin(\theta_{p1} + \theta_{p2}) - d_1^2 sin(\theta_{p1} + \theta_{p2}) + \\
&2d_1 l_p cos\theta_{p1} + 2d_1 l_p cos\theta_{p2} + 2d_2 l_p sin\theta_{p1} + \\
&2d_2 l_p sin\theta_{p2} + 2d_1 d_2 cos(\theta_{p1} + \theta_{p2})))/W_1^3 + \\
&(Z_1 l_p (m_{p7} d_3^2 + 4I_{p_5} + 4I_{p_7})(d_1^2 sin\theta_{p2} - d_2^2 sin\theta_{p2} + \\
&2l_p^2 sin\theta_{p1} + l_p^2 sin\theta_{p2} - 2d_1 l_p + l_p^2 sin(2\theta_{p1} - \theta_{p2}) - \\
&2d_1 l_p cos(\theta_{p1} - \theta_{p2}) + 2d_2 l_p sin(\theta_{p1} - \theta_{p2}) - \\
&2d_1 d_2 cos\theta_{p2}))/8W_1^3 + (Z_2 l_p (m_{p7} d_3^2 + 4I_{p_5} + \\
&4I_{p_7})(d_2^2 sin(\theta_{p1} + \theta_{p2}) - d_1^2 sin(\theta_{p1} + \theta_{p2}) + \\
&2d_1 l_p cos\theta_{p1} + 2d_1 l_p cos\theta_{p2} + 2d_2 l_p sin\theta_{p1} + \\
&2d_2 l_p sin\theta_{p2} + 2d_1 d_2 cos(\theta_{p1} + \\
&\theta_{p2}))/4W_1^3 - (Z_5 l_p^2 (m_{p7} d_3^2 + 4I_{p_5} + 4I_{p_7})(d_2^2 sin(\theta_{p1} + \\
&\theta_{p2}) - d_1^2 sin(\theta_{p1} + \theta_{p2}) + 2d_1 l_p cos\theta_{p1} + \\
&2d_1 l_p cos\theta_{p2} + 2d_2 l_p sin\theta_{p1} + \\
&2d_2 l_p sin\theta_{p2} + 2d_1 d_2 cos(\theta_{p1} + \\
&\theta_{p2})))/4W_1^3 - (d_3 l_p^2 m_{p7} cos\phi_p (d_2^2 sin(\theta_{p1} + \theta_{p2}) - \\
&d_1^2 sin(\theta_{p1} + \theta_{p2}) + 2d_1 l_p cos\theta_{p1} + 2d_1 l_p cos\theta_{p2} + \\
&2d_2 l_p sin\theta_{p1} + 2d_2 l_p sin\theta_{p2} + 2d_1 d_2 cos(\theta_{p1} + \\
&\theta_{p2})))/2W_1^2) - \dot{\theta}_{p2} ((Z_5 l_p (m_{p7} d_3^2 + 4I_{p_5} + \\
&4I_{p_7})(d_1 cos\theta_{p2} - l_p sin(\theta_{p1} - \theta_{p2}) + d_2 sin\theta_{p2})(d_1^2 - \\
&2l_p d_1 sin\theta_{p1} + d_2^2 + 2l_p d_2 cos\theta_{p1}))/8W_1^3 - \\
&(Z_2 l_p (m_{p7} d_3^2 + 4I_{p_5} + 4I_{p_7})(d_1^2 sin\theta_{p2} - d_2^2 sin\theta_{p2} + \\
&2l_p^2 sin\theta_{p1} + l_p^2 sin\theta_{p2} - 2d_1 l_p + l_p^2 sin(2\theta_{p1} - \theta_{p2}) - \\
&2d_1 l_p cos(\theta_{p1} - \theta_{p2}) + 2d_2 l_p sin(\theta_{p1} - \theta_{p2}) - \\
&2d_1 d_2 cos\theta_{p2}))/8W_1^3 + (d_3 l_p m_{p7} cos\phi_p (d_1 cos\theta_{p2} - \\
&l_p sin(\theta_{p1} - \theta_{p2}) + d_2 sin\theta_{p2})(d_1^2 - 2l_p d_1 sin\theta_{p1} + d_2^2 + \\
&2l_p d_2 cos\theta_{p1}))/4W_1^3) - \dot{d}_1 (Z_2 (m_{p7} d_3^2 + 4I_{p_5} + \\
&4I_{p_7})(l_p^2 sin(2\theta_{p1}) - 2d_1 d_2 + l_p^2 sin(2\theta_{p2}) + \\
&2l_p^2 sin(\theta_{p1} + \theta_{p2})) - 2d_1 l_p cos\theta_{p1} - 2d_1 l_p cos\theta_{p2} + \\
&2d_2 l_p sin\theta_{p1} + 2d_2 l_p sin\theta_{p2}))/8W_1^3
\end{aligned}
\tag{B.7}
$$

$$V_{p24} = V_{p25} = 0 \tag{B.8}$$

$$\begin{aligned}
V_{p31} = \dot{\theta}_{p2}((l_p(m_{p7}d_3^2 + 4I_{p_5} + 4I_{p_7})(Z_1 d_2^2 sin\theta_{p2} - \\
Z_2 d_1^2 sin\theta_{p1} - Z_1 d_1^2 sin\theta_{p2} + 2Z_2 d_1 l_p + \\
Z_2 d_2^2 sin\theta_{p1} - 2Z_1 l_p^2 sin\theta_{p1} - Z_1 l_p^2 sin\theta_{p2} - \\
Z_2 l_p^2 sin\theta_{p1} - 2Z_2 l_p^2 sin\theta_{p2} + 2Z_1 d_1 l_p + Z_2 l_p^2 sin(\theta_{p1} - \\
2\theta_{p2}) - Z_1 l_p^2 sin(2\theta_{p1} - \theta_{p2}) + 2Z_1 d_1 d_2 cos\theta_{p2} + \\
2Z_2 d_1 d_2 cos\theta_{p1} + 2Z_1 d_1 l_p cos(\theta_{p1} - \theta_{p2}) + \\
2Z_2 d_1 l_p cos(\theta_{p1} - \theta_{p2}) - 2Z_1 d_2 l_p sin(\theta_{p1} - \theta_{p2}) + \\
2Z_2 d_2 l_p sin(\theta_{p1} - \theta_{p2})))/8W_1^3) + (l_p^2(Z_5 m_{p7} d_3^2 + \\
2W_1 m_{p7} d_3 cos\phi_p + 4I_{p_5} Z_5 + 4I_{p_7} Z_5)(d_2^2 sin(\theta_{p1} + \\
\theta_{p2}) - d_1^2 sin(\theta_{p1} + \theta_{p2}) + 2d_1 l_p cos\theta_{p1} + \\
2d_1 l_p cos\theta_{p2} + 2d_2 l_p sin\theta_{p1} + \\
2d_2 l_p sin\theta_{p2} + 2d_1 d_2 cos(\theta_{p1} + \theta_{p2})))/4W_1^3 + \\
(Z_1 l_p(m_{p7} d_3^2 + 4I_{p_5} + 4I_{p_7})(d_1^2 sin\theta_{p2} - d_2^2 sin\theta_{p2} + \\
2l_p^2 sin\theta_{p1} + l_p^2 sin\theta_{p2} - 2d_1 l_p + l_p^2 sin(2\theta_{p1} - \theta_{p2}) - \\
2d_1 l_p cos(\theta_{p1} - \theta_{p2}) + 2d_2 l_p sin(\theta_{p1} - \theta_{p2}) - \\
2d_1 d_2 cos\theta_{p2}))/4W_1^3) - \dot{d}_1((l_p(Z_5 m_{p7} d_3^2 + \\
2W_1 m_{p7} d_3 cos\phi_p + 4I_{p_5} Z_5 + 4I_{p_7} Z_5)(d_2^2 sin\theta_{p1} - \\
d_1^2 sin\theta_{p1} - l_p^2 sin\theta_{p1} - 2l_p^2 sin\theta_{p2} + 2d_1 l_p + \\
l_p^2 sin(\theta_{p1} - 2\theta_{p2}) + 2d_1 l_p cos(\theta_{p1} - \theta_{p2}) + \\
2d_1 d_2 cos\theta_{p1}))/8W_1^3 + (Z_1(d_2 + l_p cos\theta_{p1} + \\
l_p cos\theta_{p2})(m_{p7} d_3^2 + 4I_{p_5} + 4I_{p_7})(-d_1 + l_p sin\theta_{p1} + \\
l_p sin\theta_{p2})/4W_1^3 - \dot{\theta}_{p1}(l_p(d_1 cos\theta_{p1} + d_2 sin\theta_{p1} + \\
l_p sin(\theta_{p1} - \theta_{p2}))(d_1^2 - 2l_p d_1 sin\theta_{p2} + d_2^2 + \\
2d_2 l_p cos\theta_{p2})(Z_5 m_{p7} d_3^2 + 2W_1 m_{p7} d_3 cos\phi_p + 4I_{p_5} Z_5 + \\
4I_{p_7} Z_5))/4W_1^3
\end{aligned} \tag{B.9}$$

$$\begin{aligned}
V_{p32} = \dot{\theta}_{p1}((l_p(m_{p7} d_3^2 + 4I_{p_5} + 4I_{p_7})(Z_1 d_2^2 sin\theta_{p2} - \\
Z_2 d_1^2 \sin\theta_{p1} - Z_1 d_1^2 sin\theta_{p2} + Z_2 d_2^2 \sin\theta_{p1} - \\
2Z_1 l_p^2 \sin\theta_{p1} - Z_1 l_p^2 sin\theta_{p2} - Z_2 l_p^2 \sin\theta_{p1} - \\
2Z_2 l_p^2 sin\theta_{p2} + 2Z_1 d_1 l_p + 2Z_2 d_1 l_p + Z_2 l_p^2 \sin(\theta_{p1} - \\
2\theta_{p2}) - Z_1 l_p^2 sin(2\theta_{p1} - \theta_{p2}) + 2Z_1 d_1 d_2 cos\theta_{p2} + \\
2Z_2 d_1 d_2 \cos\theta_{p1} + 2Z_1 d_1 l_p \cos(\theta_{p1} - \theta_{p2}) + \\
2Z_2 d_1 l_p \cos(\theta_{p1} - \theta_{p2}) - 2Z_1 d_2 l_p \sin(\theta_{p1} - \theta_{p2}) + \\
2Z_2 d_2 l_p sin(\theta_{p1} - \theta_{p2})))/8W_1^3 + (Z_5 l_p^2(m_{p7} d_3^2 + 4I_{p_5} + \\
4I_{p_7})(d_2^2 si\, n(\theta_{p1} + \theta_{p2}) - d_1^2 si\, n(\theta_{p1} + \theta_{p2}) + \\
2d_1 l_p cos\theta_{p1} + 2d_1 l_p cos\theta_{p2} + 2d_2 l_p sin\theta_{p1} + \\
2d_2 l_p sin\theta_{p2} + 2d_1 d_2 \cos(\theta_{p1} + \theta_{p2})))/4W_1^3 - \\
(Z_2 l_p(m_{p7} d_3^2 + 4I_{p_5} + 4I_{p_7})(d_2^2 sin\theta_{p1} - d_1^2 sin\theta_{p1} - \\
l_p^2 sin\theta_{p1} - 2l_p^2 sin\theta_{p2} + 2d_1 l_p + l_p^2 sin(\theta_{p1} - \\
2\theta_{p2}) + 2d_1 l_p \cos(\theta_{p1} - \theta_{p2}) + 2d_2 l_p sin(\theta_{p1} -
\end{aligned} \tag{B.10}$$

$$
\begin{aligned}
&\theta_{p2})+2d_1d_2cos\theta_{p1}))/4W_1^3 + \\
&(d_3l_p^2m_{p7}cos\phi_p(d_2^2\sin(\theta_{p1}+\theta_{p2}) - \mathrm{d}_1^2\sin(\theta_{p1}+ \\
&\theta_{p2}) + 2d_1l_pcos\theta_{p1} + 2d_1l_pcos\theta_{p2} + 2d_2l_psin\theta_{p1} + \\
&2d_2l_psin\theta_{p2}+2d_1d_2cos(\theta_{p1}+\theta_{p2})))/2\mathrm{W}_1^2) + \\
&\dot{d}_1((Z_2(2d_1 - 2(sin\theta_{p1}+sin\theta_{p2})l_p)(m_{p7}d_3^2 + 4I_{p_5} + \\
&4I_{p_7})(d_2 + l_pcos\theta_{p1} + l_pcos\theta_{p2}))/8W_1^3 + \\
&(Z_5l_p(m_{p7}d_3^2 + 4I_{p_5} + 4I_{p_7})(d_1^2sin\theta_{p2} - d_2^2sin\theta_{p2} + \\
&2l_p^2sin\theta_{p1} + l_p^2sin\theta_{p2} - 2d_1l_p + l_p^2sin(2\theta_{p1}-\theta_{p2}) - \\
&2d_1l_p\cos(\theta_{p1}-\theta_{p2}) + 2d_2l_psin(\theta_{p1}-\theta_{p2}) - \\
&2d_1d_2cos\theta_{p2}))/(8W_1^3) + (d_3l_pm_{p7}cos\phi_p(d_1^2sin\theta_{p2} - \\
&d_2^2sin\theta_{p2} + 2l_p^2sin\theta_{p1} + l_p^2sin\theta_{p2} - 2d_1l_p + \\
&l_p^2\sin(2\theta_{p1}-\theta_{p2}) - 2d_1l_p\cos(\theta_{p1}-\theta_{p2}) + \\
&2d_2l_p\sin(\theta_{p1}-\theta_{p2}) - \\
&2d_1d_2cos\theta_{p2}))/2\mathrm{W}_1^2) - \dot{\theta}_{p2}(((Z_5l_p(m_{p7}d_3^2 + \\
&4I_{p_5}4I_{p_7})(d_1cos\theta_{p2}+d_2sin\theta_{p2} - l_psi\,n(\theta_{p1}- \\
&\theta_{p2}))(d_1^2 - 2l_psin\theta_{p1}d_1 + d_2^2 + 2l_pcos\theta_{p1}d_2))/W_1^3 + \\
&d_3l_pm_{p7}cos\phi_p(d_1cos\theta_{p2}+d_2sin\theta_{p2} - l_p\,sin(\theta_{p1}- \\
&\theta_{p2}))(d_1^2 - 2l_psin\theta_{p1}d_1 + d_2^2 + 2l_pcos\theta_{p1}d_2))/(2W_1^2))
\end{aligned}
$$

$$
\begin{aligned}
V_{p33} = {} & \dot{\theta}'_{p2}((((l_psin\theta'_{p2})/W_2 - (l_p(2l_psin\theta'_{p1} - 2d_1 + \\
&2l_psin\theta'_{p2})(l_p - d_2cos\theta'_{p2} - d_1sin\theta'_{p2} + l_pcos(\theta'_{p1}- \\
&\theta'_{p2})))/W_2^2)(Z_6m_{p7}d_3^2 + 2W_1m_{p7}cos\phi'_pd_3 + 4I_{p_5}Z_6 + \\
&4I_{p_7}Z_6))/8W_1 + (Z_4(m_{p7}d_3^2 + 4I_{p_5} + 4I_{p7})(l_pcos\theta'_{p1} - \\
&d_2 + l_pcos\theta'_{p2})(l_psin\theta'_{p1} - d_1 + l_psin\theta'_{p2}))/4W_2^3 + \\
&(l_p(Z_6m_{p7}d_3^2 + 2W_1m_{p7}cos\phi'_pd_3 + 4I_{p_5}Z_6 + \\
&4I_{p_7}Z_6)(d_1^2sin\theta'_{p2} + 3d_2^2sin\theta'_{p2} + 2l_p^2sin\theta'_{p1} + \\
&l_p^2sin\theta'_{p2} - 2d_1l_p + l_p^2sin(2\theta'_{p1}-\theta'_{p2}) - \\
&2d_1l_pcos(\theta'_{p1}-\theta'_{p2}) - 2d_2l_psin(\theta'_{p1}-\theta'_{p2}) + \\
&2d_1d_2cos\theta'_{p2}))/(2W_1W_2^2)) + \dot{\theta}'_{p1}(((l_psin\theta'_{p1}/W_2 - \\
&(l_p(2l_psin\theta'_{p1} - 2d_1 + 2l_psin\theta'_{p2})(l_p - d_2cos\theta'_{p1} - \\
&d_1sin\theta'_{p1} + l_pcos(\theta'_{p1}-\theta'_{p2})))/W_2^2)(Z_6m_{p7}d_3^2 + \\
&2W_1m_{p7}cos\phi'_pd_3 + 4I_{p_5}Z_6 + 4I_{p_7}Z_6))/8W_1 + \\
&(l_p(Z_6m_{p7}d_3^2 + 2W_1m_{p7}cos\phi'_pd_3 + 4I_{p_5}Z_6 + \\
&4I_{p_7}Z_6)(d_1^2sin\theta'_{p1} + 3d_2^2sin\theta'_{p1} + l_p^2sin\theta'_{p1} + \\
&2l_p^2sin\theta'_{p2} - 2d_1l_p - l_p^2sin(\theta'_{p1} - 2\theta'_{p2}) - \\
&2d_1l_pcos(\theta'_{p1}-\theta'_{p2}) + 2d_2l_psin(\theta'_{p1}-\theta'_{p2}) + \\
&2d_1d_2cos\theta'_{p1}))/(2W_1W_2^2) + (Z_3(m_{p7}d_3^2 + 4I_{p_5} + \\
&4I_{p_7})(l_pcos\theta'_{p1} - d_2 + l_pcos\theta'_{p2})(l_psin\theta'_{p1} - d_1 + \\
&l_psin\theta'_{p2})/(4W_2^3)) - \dot{\theta}_{p2}((Z_2(2d_1 - 2l_p(sin\theta_{p1} + \\
&sin\theta_{p2}))(m_{p7}d_3^2 + 4I_{p_5} + 4I_{p_7})(d_2 + l_pcos\theta_{p1} + \\
&l_pcos\theta_{p2}))/8W_1^3) + \dot{d}_1((Z_5(m_{p7}d_3^2 + 4I_{p_5} + \\
&4I_{p_7})(2d_1 - 2l_p(sin\theta_{p1} + sin\theta_{p2}))(d_2 + l_pcos\theta_{p1} + \\
&l_pcos\theta_{p2}))/4W_1^3 + (d_3m_{p7}cos\phi'_p(2d_1 - 2l_p(sin\theta'_{p1} +
\end{aligned}
\tag{B.11}
$$

$$sin\theta'_{p2}))(l_p cos\theta'_{p1} - d_2 + l_p cos\theta'_{p2}))/2W_2^2 + (d_3 m_{p7} cos\phi_p (2d_1 - 2l_p(sin\theta_{p1} + sin\theta_{p2}))(d_2 + l_p cos\theta_{p1} + l_p cos\theta_{p2}))/2W_1^2 + ((m_{p7} d_3^2 + 4I_{p_5} + 4I_{p_7}) Z_6 (2d_1 - 2l_p(sin\theta'_{p1} + sin\theta'_{p2}))(l_p cos\theta'_{p1} - d_2 + l_p cos\theta'_{p2}))/(4W_1 W_2^2)) - \dot{\theta}_{p1}((3l_p(Z_5 m_{p7} d_3^2 + 2W_1 m_{p7} cos\phi_p d_3 + 4I_{p_5} Z_5 + I_{p_7} Z_5)(d_2^2 sin\theta_{p1} - d_1^2 sin\theta_{p1} - l_p^2 sin\theta_{p1} - 2l_p^2 sin\theta_{p2} + 2d_1 l_p + l_p^2 sin(\theta_{p1} - 2\theta_{p2}) + 2d_1 l_p cos(\theta_{p1} - \theta_{p2}) + 2d_2 l_p sin(\theta_{p1} - \theta_{p2}) + 2d_1 d_2 cos\theta_{p1}))/8W_1^3 - (Z_1(d_2 + l_p cos\theta_{p1} + l_p cos\theta_{p2})(m_{p7} d_3^2 + 4I_{p_5} + 4I_{p_7})(l_p sin\theta_{p1} - d_1 + l_p sin\theta_{p2}))/4W_1^3)$$

$$V_{p34} = \dot{\theta}_{p1}((Z_3 l_p(m_{p7} d_3^2 + 4I_{p_5} + 4I_{p_7})(d_1^2 sin\theta'_{p1} + 3d_2^2 sin\theta'_{p1} + l_p^2 sin\theta'_{p1} + 2l_p^2 sin\theta'_{p2} - 2d_1 l_p - l_p^2 sin(\theta'_{p1} - 2\theta'_{p2}) - 2d_1 l_p cos(\theta'_{p1} - \theta'_{p2}) + 2d_2 l_p sin(\theta'_{p1} - \theta'_{p2}) + 2d_1 d_2 cos\theta'_{p1}))/4W_2^3 - (((l_p(d_1 cos\theta'_{p1} - d_2 sin\theta'_{p1} + l_p sin(\theta'_{p1} - \theta'_{p2})))/W_2 - (2l_p^2(d_1 cos\theta'_{p1} + d_2 sin\theta'_{p1} + l_p sin(\theta'_{p1} - \theta'_{p2}))(l_p - d_2 cos\theta'_{p1} - d_1 sin\theta'_{p1} + l_p cos(\theta'_{p1} - \theta'_{p2})))/W_2^2)(Z_6 m_{p7} d_3^2 + 2W_1 m_{p7} cos\phi'_p d_3 + 4I_{p_5} Z_6 + 4I_{p_7} Z_6))/4W_1 + (Z_3 l_p(m_{p7} d_3^2 + 4I_{p_5} + 4I_{p_7})(2d_1 l_p - 2l_p^2 sin\theta'_{p1} - 2l_p^2 sin\theta'_{p2} - 2d_1^2 sin\theta'_{p1} + W_2 sin\theta'_{p1} - 2l_p^2 sin(\theta'_{p1} - 2\theta'_{p2}) + 2d_1 l_p cos(\theta'_{p1} - \theta'_{p2}) + d_2 l_p sin(2\theta_{p1}) + 2d_1 l_p sin^2\theta'_{p1} - 2d_1 d_2 cos\theta'_{p1} + 2d_2 l_p cos\theta'_{p1} sin\theta'_{p2} + 2d_1 l_p sin\theta'_{p1} sin\theta'_{p2}))/4W_2^3) - \dot{d}_1((((l_p sin\theta'_{p1})/W_2 - (l_p(2l_p sin\theta'_{p1} - 2d_1 + 2l_p sin\theta'_{p2})(l_p - d_2 cos\theta'_{p1} - d_1 sin\theta'_{p1} + l_p cos(\theta'_{p1} - \theta'_{p2})))/W_2^2)(Z_6 m_{p7} d_3^2 + 2W_1 m_{p7} cos\phi'_p d_3 + 4I_{p_5} Z_6 + 4I_{p_7} Z_6))/8W_1 + (Z_3(m_{p7} d_3^2 + 4I_{p_5} + 4I_{p_7})(l_p cos\theta'_{p1} - d_2 + l_p cos\theta'_{p2})(l_p sin\theta'_{p1} - d_1 + l_p sin\theta'_{p2}))/4W_2^3) + \dot{\theta}_{p2}((l_p^2(Z_5 m_{p7} d_3^2 + 2W_1 m_{p7} cos\phi_p d_3 + 4I_{p_5} Z_5 + 4I_{p_7} Z_5)(d_2^2 sin(\theta_{p1} + \theta_{p2}) - d_1^2 sin(\theta_{p1} + \theta_{p2}) + 2d_1 l_p cos\theta_{p1} + 2d_1 l_p cos\theta_{p2} + 2d_2 l_p sin\theta_{p1} + 2d_2 l_p sin\theta_{p2} + 2d_1 d_2 cos(\theta_{p1} + \theta_{p2})))/4W_1^3 + (Z_1 l_p(m_{p7} d_3^2 + 4I_{p_5} + 4I_{p_7})(d_1^2 sin\theta_{p2} - d_2^2 sin\theta_{p2} + l_p^2 sin\theta_{p1} + l_p^2 sin\theta_{p2} - 2d_1 l_p + l_p^2 sin(2\theta_{p1} - \theta_{p2}) - 2d_1 l_p cos(\theta_{p1} - \theta_{p2}) + 2d_2 l_p sin(\theta_{p1} - \theta_{p2}) - 2d_1 d_2 cos\theta_{p2}))/4W_1^3) + \dot{\theta}_{p2}((((l_p^2 sin(\theta'_{p1} - \theta'_{p2}))/W_2 + (2l_p^2(d_1 cos\theta'_{p2} + d_2 sin\theta'_{p2} - l_p sin(\theta'_{p1} - \theta'_{p2}))(l_p - d_2 cos\theta'_{p1} - d_1 sin\theta'_{p1} + l_p cos(\theta'_{p1} - \theta'_{p2})))/W_2^2)(Z_6 m_{p7} d_3^2 + 2W_1 m_{p7} cos\phi'_p d_3 + 4I_{p_5} Z_6 + 4I_{p_7} Z_6))/4W_1 + (l_p(m_{p7} d_3^2 + 4I_{p_5} + 4I_{p_7})(2Z_3 d_1 l_p - 2Z_4 d_1^2 sin\theta'_{p1} - 2Z_3 l_p^2 sin\theta'_{p1} - 2Z_3 l_p^2 sin\theta'_{p2} - \quad (B.12)$$

$$2Z_4l_p^2sin\theta'_{p1} - 2Z_4l_p^2sin\theta'_{p2} - 2Z_3d_1^2sin\theta'_{p2} + 2Z_4d_1l_p + W_2Z_3sin\theta'_{p2} + W_2Z_4sin\theta'_{p1} - 2Z_3d_1d_2cos\theta'_{p2} - 2Z_4d_1d_2cos\theta'_{p1} - 2Z_3l_p^2cos(\theta'_{p1} - \theta'_{p2})sin\theta'_{p1} - 2Z_3l_p^2cos(\theta'_{p1} - \theta'_{p2})sin\theta'_{p2} - 2Z_4l_p^2cos(\theta'_{p1} - \theta'_{p2})sin\theta'_{p1} - 2Z_4l_p^2cos(\theta'_{p1} - \theta'_{p2})sin\theta'_{p2} + 2Z_3d_1l_pcos(\theta'_{p1} - \theta'_{p2}) + 2Z_4d_1l_pcos(\theta'_{p1} - \theta'_{p2}) + Z_3d_2l_psin(2\theta'_{p2}) + Z_4d_2l_psin(2\theta_{p1}) + 2Z_3d_1l_psin^2\theta'_{p2} + 2Z_4d_1l_psin^2\theta'_{p1} + 2Z_3d_2l_pcos\theta'_{p2}sin\theta'_{p1} + 2Z_4d_2l_pcos\theta'_{p1}sin\theta'_{p2} + 2Z_3d_1l_psin\theta'_{p1}sin\theta'_{p2} + 2Z_4d_1l_psin\theta'_{p1}sin\theta'_{p2}))/8W_2^3 + (Z_3l_p(m_{p7}d_3^2 + 4I_{p_5} + 4I_{p_7})(d_1^2sin\theta'_{p2} + 3d_2^2sin\theta'_{p2} + 2l_p^2sin\theta'_{p1} + l_p^2sin\theta'_{p2} - 2d_1l_p + l_p^2sin(2\theta'_{p1} - \theta'_{p2}) - 2d_1l_pcos(\theta'_{p1} - \theta'_{p2}) - 2d_2l_psin(\theta'_{p1} - \theta'_{p2}) + 2d_1d_2cos\theta'_{p2}))/4W_2^3)$$

$$V_{p35} = \dot{\theta}_{p2}((((l_p(d_2sin\theta'_{p2} - d_1cos\theta'_{p2} + l_psin(\theta'_{p1} - \theta'_{p2})))/W_2 + (2l_p^2(d_1cos\theta'_{p2} + d_2sin\theta'_{p2} - l_psin(\theta'_{p1} - \theta'_{p2}))(l_p - d_2cos\theta'_{p2} - d_1sin\theta'_{p2} + l_pcos(\theta'_{p1} - \theta'_{p2})))/W_2^2)(Z_6m_{p7}d_3^2 + 2W_1m_{p7}cos\phi'_pd_3 + 4I_{p_5}Z_6 + 4I_{p_7}Z_6))/4W_1 + (Z_4l_p(m_{p7}d_3^2 + 4I_{p_5} + 4I_{p_7})(2d_1l_p - 2l_p^2sin\theta'_{p1} - 2l_p^2sin\theta'_{p2} - 2d_1^2sin\theta'_{p2} + W_2sin\theta'_{p2} - 2l_p^2cos(\theta'_{p1} - \theta'_{p2})sin\theta'_{p1} - 2l_p^2cos(\theta'_{p1} - \theta'_{p2})sin\theta'_{p2} + 2d_1l_pcos(\theta'_{p1} - \theta'_{p2}) + d_2l_psin(2\theta_{p2}) + 2d_1l_psin^2\theta'_{p2} - 2d_1d_2cos\theta'_{p2} + 2d_2l_pcos\theta'_{p2}sin\theta'_{p1} + 2d_1l_psin\theta'_{p1}sin\theta'_{p2}))/4W_2^3 + (Z_4l_p(m_{p7}d_3^2 + 4I_{p_5} + 4I_{p_7})(d_1^2sin\theta'_{p2} + 3d_2^2sin\theta'_{p2} + 2l_p^2sin\theta'_{p1} + l_p^2sin\theta'_{p2} - 2d_1l_p + l_p^2sin(2\theta'_{p1} - \theta'_{p2}) - 2d_1l_pcos(\theta'_{p1} - \theta'_{p2}) - 2d_2l_psin(\theta'_{p1} - \theta'_{p2}) + 2d_1d_2cos\theta'_{p2}))/(4W_2^3)) - \dot{d}_1((((l_psin\theta'_{p2})/W_2 - (l_p(2l_psin\theta'_{p1} - 2d_1 + 2l_psin\theta'_{p2})(l_p - d_2cos\theta'_{p2} - d_1sin\theta'_{p2} + l_pcos(\theta'_{p1} - \theta'_{p2})))/W_2^2)(Z_6m_{p7}d_3^2 + 2W_1m_{p7}cos\phi'_pd_3 + 4I_{p_5Z_6} + 4I_{p_7Z_6}))/(8W_1) + (Z_4(m_{p7}d_3^2 + 4I_{p_5} + 4I_{p_7})(l_pcos\theta'_{p1} - d_2 + l_pcos\theta'_{p2})(l_psin\theta'_{p1} - d_1 + l_psin\theta'_{p2}))/(4W_2^3)) + \dot{\theta}'_{p1}((l_p(m_{p7}d_3^2 + 4I_{p_5} + 4I_{p_7})(2Z_3d_1l_p - 2Z_4d_1^2sin\theta'_{p1} - 2Z_3l_p^2sin\theta'_{p1} - 2Z_3l_p^2sin\theta'_{p2} - 2Z_4l_p^2sin\theta'_{p1} - 2Z_4l_p^2sin\theta'_{p2} - 2Z_3d_1^2sin\theta'_{p2} + 2Z_4d_1l_p + W_2Z_3sin\theta'_{p2} + W_2Z_4sin\theta'_{p1} - 2Z_3d_1d_2cos\theta'_{p2} - 2Z_4\,d_1d_2cos\theta'_{p1} - 2Z_3l_p^2cos(\theta'_{p1} - \theta'_{p2})sin\theta'_{p1} - 2Z_3l_p^2cos(\theta'_{p1} - \theta'_{p2})sin\theta'_{p2} - 2Z_4l_p^2cos(\theta'_{p1} - \theta'_{p2})sin\theta'_{p1} - 2Z_4l_p^2cos(\theta'_{p1} - \theta'_{p2})sin\theta'_{p2} + 2Z_3d_1l_pcos(\theta'_{p1} - \theta'_{p2}) + 2Z_4d_1l_pcos(\theta'_{p1} - \theta'_{p2}) + Z_3d_2l_psin(2\theta'_{p2}) + Z_4d_2l_psin(2\theta'_{p1}) + 2Z_3\,d_1l_p\,sin^2\theta'_{p2} + 2Z_4d_1l_p\,sin^2\,\theta'_{p1} + \quad (B.13)$$

$$2Z_3d_2\,l_pcos\theta'_{p2}sin\theta'_{p1}\ + 2Z_4d_2l_pcos\theta'_{p1}sin\theta'_{p2} + 2Z_3d_1l_psin\theta'_{p1}sin\theta'_{p2} + 2Z_4d_1l_psin\theta'_{p1}sin\theta'_{p2}))/(8W_2^3) - (((l_p^2sin(\theta'_{p1}-\theta'_{p2}))/W_2 - (2l_p^2(d_1cos\theta'_{p1} + d_2sin\theta'_{p1} + l_psin(\theta'_{p1}-\theta'_{p2}))(l_p - d_2cos\theta'_{p2} - d_1sin\theta'_{p2} + l_pcos(\theta'_{p1}-\theta'_{p2})))/W_2^2)(Z_6m_{p7}d_3^2 + 2W_1m_{p7}cos\phi'_pd_3\ + 4I_{p_5}Z_6 + 4I_{p_7}Z_6))/(4W_1) + (Z_4l_p(m_{p7}d_3^2 + 4I_{p_5} + 4I_{p_7})(d_1^2sin\theta'_{p1} + 3d_2^2sin\theta'_{p1} + l_p^2sin\theta'_{p1} + 2l_p^2sin\theta'_{p2} - 2d_1l_p - l_p^2sin(\theta'_{p1}-2\theta'_{p2}) - 2d_1l_pcos(\theta'_{p1}-\theta'_{p2}) + 2d_2l_psin(\theta'_{p1}-\theta'_{p2}) + 2d_1d_2cos\theta'_{p1}))/(4W_2^3))$$

$$V_{p41} = V_{p42} = 0 \tag{B.14}$$

$$\begin{aligned}V_{p43} = \dot{\theta}'_{p2}(((((l_p^2sin(\theta'_{p1}-\theta'_{p2}))/W_2 - (2l_p^2(d_1cos\theta'_{p1} + d_2sin\theta'_{p1} + l_psin(\theta'_{p1}-\theta'_{p2}))(l_p - d_2cos\theta'_{p2} - d_1sin\theta'_{p2} + l_pcos(\theta'_{p1}-\theta'_{p2})))/W_2^2)(Z_6m_{p7}d_3^2 + 2W_1m_{p7}cos\phi'_pd_3 + 4I_{p_5}Z_6 + 4I_{p_7}Z_6))/(8W_1) + (((l_p^2sin(\theta'_{p1}-\theta'_{p2}))/W_2 + (2l_p^2(d_1cos\theta'_{p2} + d_2sin\theta'_{p2} - l_psin(\theta'_{p1}-\theta'_{p2}))(l_p - d_2cos\theta'_{p1} - d_1sin\theta'_{p1} + l_pcos(\theta'_{p1}-\theta'_{p2})))/W_2^2)(Z_6m_{p7}d_3^2 + 2W_1m_{p7}cos\phi'_pd_3 + 4I_{p_5}Z_6 + 4I_{p_7}Z_6))/(4W_1) - (Z_4l_p(m_{p7}d_3^2 + 4I_{p_5} + 4I_{p_7})(d_1^2sin\theta'_{p1} + 3d_2^2sin\theta'_{p1} + l_p^2sin\theta'_{p1} + 2l_p^2sin\theta'_{p2} - 2d_1l_p - l_p^2sin(\theta'_{p1}-2\theta'_{p2}) - 2d_1l_pcos(\theta'_{p1}-\theta'_{p2}) + 2d_2l_psin(\theta'_{p1}-\theta'_{p2}) + 2d_1d_2cos\theta'_{p1}))/(8W_2^3) + (Z_3l_p(m_{p7}d_3^2 + 4I_{p_5} + 4I_{p_7})(d_1^2sin\theta'_{p2} + 3d_2^2sin\theta'_{p2} + 2l_p^2sin\theta'_{p1} + l_p^2sin\theta'_{p2} - 2d_1l_p + l_p^2sin(2\theta'_{p1}-\theta'_{p2}) - 2d_1l_pcos(\theta'_{p1}-\theta'_{p2}) - 2d_2l_psin(\theta'_{p1}-\theta'_{p2}) + 2d_1d_2cos\theta'_{p2}))/(4W_2^3))\end{aligned} \tag{B.15}$$

$$\begin{aligned}V_{p44} = \ \dot{\theta}'_{p2}((l_p^2m_{p2}sin(\theta'_{p1}-\theta'_{p2}))/4 + (l_p^2m_{p3}sin(\theta'_{p1}-\theta'_{p2}))/4 + (l_p^2m_{p5}sin(\theta'_{p1}-\theta'_{p2}))/2 + (Z_3(m_{p7}d_3^2 + 4I_{p_5} + 4I_{p_7})(((l_p^2sin(\theta'_{p1}-\theta'_{p2}))/W_2 - (2l_p^2(d_1cos\theta'_{p1} + d_2sin\theta'_{p1} + l_psin(\theta'_{p1}-\theta'_{p2}))(l_p - d_2cos\theta'_{p2} - d_1sin\theta'_{p2} + l_pcos(\theta'_{p1}-\theta'_{p2})))/W_2^2))/(8W_2) + (Z_4(m_{p7}d_3^2 + 4I_{p_5} + 4I_{p_7})(((l_p(d_1cos\theta'_{p1} - d_2sin\theta'_{p1} + l_psin(\theta'_{p1}-\theta'_{p2})))/W_2 - (2l_p^2(d_1cos\theta'_{p1} + d_2sin\theta'_{p1} + l_psin(\theta'_{p1}-\theta'_{p2}))(l_p - d_2cos\theta'_{p1} - d_1sin\theta'_{p1} + l_pcos(\theta'_{p1}-\theta'_{p2})))/W_2^2))/(8W_2) + (Z_3l_p^2(m_{p7}d_3^2 + 4I_{p_5} + 4I_{p_7})(W_2sin(\theta'_{p1}-\theta'_{p2}) - l_p^2sin(2\theta'_{p1}-2\theta'_{p2}) - 2l_p^2sin(\theta'_{p1}-\theta'_{p2}) + 2d_1l_pcos\theta'_{p2} + 2d_2l_psin\theta'_{p2} - 2d_1^2cos\theta'_{p2}sin\theta'_{p1} - 2d_2^2cos\theta'_{p1}sin\theta'_{p2} + 2d_1l_pcos(\theta'_{p1}-\theta'_{p2})cos\theta'_{p2} + 2d_2l_psin(\theta'_{p1}-\theta'_{p2})cos\theta'_{p1} + 2d_2l_pcos(\theta'_{p1}-\theta'_{p2})sin\theta'_{p2} + 2d_1l_psin(\theta'_{p1}-\theta'_{p2})sin\theta'_{p1} - 2d_1d_2cos(\theta'_{p1}-\end{aligned} \tag{B.16}$$

$$
\begin{aligned}
&\theta'_{p2}))))/2W_2^3) - \dot{d}'_1((Z_3 l_p(m_{p7}d_3^2 + 4I_{p_5} + \\
&4I_{p_7})(d_1^2 sin\theta'_{p1} + 3d_2^2 sin\theta'_{p1} + l_p^2 sin\theta'_{p1} + 2l_p^2 sin\theta'_{p2} - \\
&2d_1 l_p - l_p^2 sin(\theta'_{p1} - 2\theta'_{p2}) - 2d_1 l_p cos(\theta'_{p1} - \theta'_{p2}) + \\
&2d_2 l_p sin(\theta'_{p1} - \theta'_{p2}) + 2d_1 d_2 cos\theta'_{p1}))/(8W_2^3) - \\
&(((l_p(d_1 cos\theta'_{p1} - d_2 sin\theta'_{p1} + l_p sin(\theta'_{p1} - \theta'_{p2})))/W_2 - \\
&(2l_p^2(d_1 cos\theta'_{p1} + d\_2 sin\theta'_{p1} + l_p sin(\theta'_{p1} - \theta'_{p2}))(l_p - \\
&d_2 cos\theta'_{p1} - d_1 sin\theta'_{p1} + l_p cos(\theta'_{p1} - \theta'_{p2})))/ \\
&W_2^2)(Z_6 m_{p7}d_3^2 + 2W_1 m_{p7} cos\phi'_p d_3 + 4I_{p_5}Z_6 + \\
&4I_{p_7}Z_6))/(8W_1) + (Z_3 l_p(m_{p7}d_3^2 + 4I_{p_5} + 4I_{p_7})(2d_1 l_p - \\
&2l_p^2 sin\theta'_{p1} - 2l_p^2 sin\theta'_{p2} - 2d_1^2 sin\theta'_{p1} + W_2 sin\theta'_{p1} - \\
&2l_p^2 cos(\theta'_{p1} - \theta'_{p2}) sin\theta'_{p1} - 2l_p^2 cos(\theta'_{p1} - \theta'_{p2}) sin\theta'_{p2} + \\
&2d_1 l_p cos(\theta'_{p1} - \theta'_{p2}) + d_2 l_p sin(2\theta'_{p1}) + 2d_1 l_p sin^2\theta'_{p1} - \\
&2d_1 d_2 cos\theta'_{p1} + 2d_2 l_p cos\theta'_{p1} sin\theta'_{p2} + \\
&2d_1 l_p sin\theta'_{p1} sin\theta'_{p2}))/2W_2^3) + (Z_3 l_p \dot{\theta}'_{p1}(m_{p7}d_3^2 + 4I_{p_5} + \\
&4I_{p_7})(2l_p^3 sin(\theta'_{p1} - \theta'_{p2}) + l_p^3 sin(2\theta'_{p1} - \theta'_{p2}) - \\
&W_2 l_p sin(\theta'_{p1} - \theta'_{p2}) + 2d_1 l_p^2 cos\theta'_{p1} + 2d_2 l_p^2 sin\theta'_{p1} + \\
&2d_2 l_p^2 sin\theta'_{p2} - 2d_1 d_2 l_p - d_1^2 l_p sin(2\theta'_{p1}) - \\
&d_2^2 l_p sin(2\theta'_{p1}) - W_2 d_1 cos\theta'_{p1} + 2d_1 l_p^2 cos(2\theta'_{p1} - \\
&\theta'_{p2}) + W_2 d_2 sin\theta'_{p1}))/4W_2^3
\end{aligned}
$$

$$
\begin{aligned}
V_{p45} = \; &\dot{\theta}'_{p2}((l_p^2 m_{p2} sin(\theta'_{p1} - \theta'_{p2}))/2 + (l_p^2 m_{p3} sin(\theta'_{p1} - \\
&\theta'_{p2}))/2 + l_p^2 m_{p5} sin(\theta'_{p1} - \theta'_{p2}) + (Z_4(d_3^2 m_{p7} + 4I_{p_5} + \\
&4I_{p_7})((l_p(d_2 sin\theta'_{p2} - d_1 cos\theta'_{p2} + l_p sin(\theta'_{p1} - \\
&\theta'_{p2})))/W_2 + (2l_p^2(d_1 cos\theta'_{p2} + d_2 sin\theta'_{p2} - l_p sin(\theta'_{p1} - \\
&\theta'_{p2}))(l_p - d_2 cos\theta'_{p2} - d_1 sin\theta'_{p2} + l_p cos(\theta'_{p1} - \\
&\theta'_{p2})))/W_2^2))/(4W_2) + (Z_3(d_3^2 m_{p7} + 4I_{p_5} + \\
&4I_{p_7})((l_p(d_2 sin\theta'_{p2} - d_1 cos\theta'_{p2} + l_p sin(\theta'_{p1} - \\
&\theta'_{p2})))/W_2 + (2l_p^2(d_1 cos\theta'_{p2} + d_2 sin\theta'_{p2} - l_p sin(\theta'_{p1} - \\
&\theta'_{p2}))(l_p - d_2 cos\theta'_{p2} - d_1 sin\theta'_{p2} + l_p cos(\theta'_{p1} - \\
&\theta'_{p2})))/W_2^2))/(4W_2) + (Z_4 l_p^2(d_3^2 m_{p7} + 4I_{p_5} + \\
&4I_{p_7})(W_2 sin(\theta'_{p1} - \theta'_{p2}) - l_p^2 sin(2\theta'_{p1} - 2\theta'_{p2}) - \\
&2l_p^2 sin(\theta'_{p1} - \theta'_{p2}) - 2d_1 l_p cos\theta'_{p1} - 2d_2 l_p sin\theta'_{p1} + \\
&2d_1^2 cos\theta'_{p1} sin\theta'_{p2} + 2d_2^2 cos\theta'_{p2} sin\theta'_{p1} - 2l_p cos(\theta'_{p1} - \\
&\theta'_{p2})(d_1 cos\theta'_{p1} + d_2 sin\theta'_{p1}) + 2l_p sin(\theta'_{p1} - \\
&\theta'_{p2})(d_2 cos\theta'_{p2} + d_1 sin\theta'_{p2}) + 2d_1 d_2 \cos(\theta'_{p1} - \\
&\theta'_{p2}))/4W_2^3) - \dot{d}_1((l_p(d_3^2 m_{p7} + 4I_{p_5} + 4I_{p_7})(2Z_3 d_1 l_p - \\
&2Z_4 d_1^2 sin\theta'_{p1} - (2Z_3 l_p^2 + 2Z_4 l_p^2)(sin\theta'_{p1} + sin\theta'_{p2}) - \\
&2Z_3 d_1^2 sin\theta'_{p2} + 2Z_4 d_1 l_p + W_2 Z_3 sin\theta'_{p2} + W_2 Z_4 sin\theta'_{p1} - \\
&2Z_3 d_1 d_2 cos\theta'_{p2} - 2Z_4 d_1 d_2 cos\theta'_{p1} - 2Z_3 l_p^2 cos(\theta'_{p1} - \\
&\theta'_{p2})(sin\theta'_{p1} + sin\theta'_{p2}) - 2Z_4 l_p^2 cos(\theta'_{p1} - \theta'_{p2})(sin\theta'_{p1} + \\
&sin\theta'_{p2}) + 2Z_3 d_1 l_p cos(\theta'_{p1} - \theta'_{p2}) + 2Z_4 d_1 l_p cos(\theta'_{p1} - \\
&\theta'_{p2}) + Z_3 d_2 l_p sin(2\theta'_{p2}) + Z_4 d_2 l_p sin(2\theta'_{p1}) + \\
&2Z_3 d_1 l_p \sin^2\theta'_{p2} + 2Z_4 d_1 l_p sin^2\theta'_{p1} +
\end{aligned}
\tag{B.17}
$$

$$2d_2l_p(Z_3cos\theta'_{p2}sin\theta'_{p1} + Z_4cos\theta'_{p1}sin\theta'_{p2}) + 2(Z_3 + Z_4)d_1l_psin\theta'_{p1}sin\theta'_{p2}))/(4W_2^3) - (((l_p^2sin(\theta'_{p1} - \theta'_{p2}))/W_2 - (2l_p^2(d_1cos\theta'_{p1} + d_2sin\theta'_{p1} + l_psin(\theta'_{p1} - \theta'_{p2}))(l_p - d_2cos\theta'_{p2} - d_1sin\theta'_{p2} + l_pcos(\theta'_{p1} - \theta'_{p2})))/W_2^2)(Z_6m_{p7}d_3^2 + 2W_1m_{p7}cos\phi'_pd_3 + 4I_{p_7}Z_6 + 4I_{p_7}Z_6))/(8W_1) + (Z_4l_p(d_3^2m_{p7} + 4I_{p_5} + 4I_{p_7})(d_1^2sin\theta'_{p1} + 3d_2^2sin\theta'_{p1} - 2d_1l_p + l_p^2sin\theta'_{p1} + 2l_p^2sin\theta'_{p2} - l_p^2sin(\theta'_{p1} - 2\theta'_{p2}) - 2d_1l_pcos(\theta'_{p1} - \theta'_{p2}) + 2d_2l_psin(\theta'_{p1} - \theta'_{p2}) + 2d_1d_2cos\theta'_{p1}))/8W_2^3) - \dot{\theta}'_{p1}((l_p^2m_{p2}sin(\theta'_{p1} - \theta'_{p2}))/4 + (l_p^2m_{p3}sin(\theta'_{p1} - \theta'_{p2}))/4 + (l_p^2m_{p5}sin(\theta'_{p1} - \theta'_{p2}))/2 - (2l_p^2(d_1cos\theta'_{p1} + d_2sin\theta'_{p1} + l_psin(\theta'_{p1} - \theta'_{p2}))(l_p - d_1sin\theta'_{p1} - d_2cos\theta'_{p1} + l_pcos(\theta'_{p1} - \theta'_{p2})))/W_2^2))/(2W_2) + (Z_3(d_3^2m_{p7} + 4I_{p_5} + 4I_{p_7})((l_p^2sin(\theta'_{p1} - \theta'_{p2}))/W_2 - (2l_p^2(d_1cos\theta'_{p1} + d_2sin\theta'_{p1} + l_psin(\theta'_{p1} - \theta'_{p2}))(l_p - d_2cos\theta'_{p2} - d_1sin\theta'_{p2} + l_pcos(\theta'_{p1} - \theta'_{p2})))/W_2^2))/(8W_2) + (Z_4(d_3^2m_{p7} + 4I_{p_5} + 4I_{p_7})((l_p(d_1cos\theta'_{p1} - d_2sin\theta'_{p1} + l_psin(\theta'_{p1} - \theta'_{p2})))/W_2 - (2l_p^2(d_1cos\theta'_{p1} + d_2sin\theta'_{p1} + l_psin(\theta'_{p1} - \theta'_{p2}))(l_p - d_2cos\theta'_{p1} - d_1sin\theta'_{p1} + l_pcos(\theta'_{p1} - \theta'_{p2})))/W_2^2))/(8W_2))$$

$$V_{p51} = V_{p52} = 0 \tag{B.17}$$

$$\begin{aligned} V_{p53} = \; & \dot{\theta}'_{p2}((((l_p(d_2sin\theta'_{p2} - d_1cos\theta'_{p2} + l_psin(\theta'_{p1} - \theta'_{p2})))/W_2 + (2l_p^2(d_1cos\theta'_{p2} + d_2sin\theta'_{p2} - l_psin(\theta'_{p1} - \theta'_{p2}))(l_p - d_2cos\theta'_{p2} - d_1sin\theta'_{p2} + l_pcos(\theta'_{p1} - \theta'_{p2})))/W_2^2)(Z_6m_{p7}d_3^2 + 2W_1m_{p7}cos\phi'_pd_3 + 4I_{p5}Z_6 + 4I_{p_7}Z_6))/(8W_1) + (Z_4l_p(m_{p7}d_3^2 + 4I_{p_5} + 4I_{p_7})(d_1^2sin\theta'_{p2} + 3d_2^2sin\theta'_{p2} + 2l_p^2sin\theta'_{p1} + l_p^2sin\theta'_{p2} - 2d_1l_p + l_p^2sin(2\theta'_{p1} - \theta'_{p2}) - 2d_1l_pcos(\theta'_{p1} - \theta'_{p2}) - 2d_2l_psin(\theta'_{p1} - \theta'_{p2}) + 2d_1d_2cos\theta'_{p2}))/8W_2^3) - \\ & \dot{\theta}'_{p1}((((l_p^2sin(\theta'_{p1} - \theta'_{p2}))/W_2 - (2l_p^2(d_1cos\theta'_{p1} + d_2sin\theta'_{p1} + l_psin(\theta'_{p1} - \theta'_{p2}))(l_p - d_2cos\theta'_{p2} - d_1sin\theta'_{p2} + l_pcos(\theta'_{p1} - \theta'_{p2})))/W_2^2)(Z_6m_{p7}d_3^2 + 2W_1m_{p7}cos\phi'_pd_3 + 4I_{p5}Z_6 + 4I_{p_7}Z_6))/(4W_1) + \\ & (((l_p^2sin(\theta'_{p1} - \theta'_{p2}))/W_2 + (2l_p^2(d_1cos\theta'_{p2} + d_2sin\theta'_{p2} - l_psin(\theta'_{p1} - \theta'_{p2}))(l_p - d_2cos\theta'_{p1} - d_1sin\theta'_{p1} + l_pcos(\theta'_{p1} - \theta'_{p2})))/W_2^2)(Z_6m_{p7}d_3^2 + 2W_1m_{p7}cos\phi'_pd_3 + 4I_{p5}Z_6 + 4I_{p_7}Z_6))/8W_1 - \\ & (Z_4l_p(m_{p7}d_3^2 + 4I_{p_5} + 4I_{p_7})(d_1^2sin\theta'_{p1} + 3d_2^2sin\theta'_{p1} + l_p^2sin\theta'_{p1} + 2l_p^2sin\theta'_{p2} - 2d_1l_p - l_p^2sin(\theta'_{p1} - 2\theta'_{p2}) - 2d_1l_pcos(\theta'_{p1} - \theta'_{p2}) + 2d_2l_psin(\theta'_{p1} - \theta'_{p2}) + 2d_1d_2cos\theta'_{p1}))/(4W_2^3) + (Z_3l_p(m_{p7}d_3^2 + 4I_{p_5} + 4I_{p_7})(d_1^2sin\theta'_{p2} + 3d_2^2sin\theta'_{p2} + 2l_p^2sin\theta'_{p1} + l_p^2sin\theta'_{p2} - \end{aligned} \tag{B.18}$$

$$2d_1l_p + l_p^2sin(2\theta'_{p1} - \theta'_{p2}) - 2d_1l_pcos(\theta'_{p1} - \theta'_{p2}) - 2d_2l_psin(\theta'_{p1} - \theta'_{p2}) + 2d_1d_2cos\theta'_{p2}))/8W_2^3) - \dot{d}_1((((l_psin\theta'_{p2})/W_2 - (l_p(2l_psin\theta'_{p1} - 2d_1 + 2l_psin\theta'_{p2})(l_p - d_2cos\theta'_{p2} - d_1sin\theta'_{p2} + l_pcos(\theta'_{p1} - \theta'_{p2})))/W_2^2)(Z_6m_{p7}d_3^2 + 2W_1m_{p7}cos\phi'_pd_3 + 4I_{p5}Z_6 + 4I_{p_7}Z_6))/(4W_1) + (Z_4(m_{p7}d_3^2 + 4I_{p_5} + 4I_{p_7})(l_pcos\theta'_{p1} - d_2 + l_pcos\theta'_{p2})(l_psin\theta'_{p1} - d_1 + l_psin\theta'_{p2}))/(2W_2^3) + (l_p(Z_6m_{p7}d_3^2 + 2W_1m_{p7}cos\phi'_pd_3 + 4I_{p5}Z_6 + 4I_{p_7}Z_6)(d_1^2sin\theta'_{p2} + 3d_2^2sin\theta'_{p2} + 2l_p^2sin\theta'_{p1} + l_p^2sin\theta'_{p2} - 2d_1l_p + l_p^2sin(2\theta'_{p1} - \theta'_{p2}) - 2d_1l_pcos(\theta'_{p1} - \theta'_{p2}) - 2d_2l_psin(\theta'_{p1} - \theta'_{p2}) + 2d_1d_2cos\theta'_{p2}))/(4W_1W_2^2))$$

$$\begin{aligned}
V_{p54} = {} & \dot{\theta}'_{p2}((l_p^2m_{p2}sin(\theta'_{p1} - \theta'_{p2}))/4 + (l_p^2m_{p3}sin(\theta'_{p1} - \theta'_{p2}))/4 + (l_p^2m_{p5}sin(\theta'_{p1} - \theta'_{p2}))/2 + (Z_4(d_3^2m_{p7} + 4I_{p_5} + 4I_{p_7})((l_p^2sin(\theta'_{p1} - \theta'_{p2}))/W_2 + (2l_p^2(d_1cos\theta'_{p2} + d_2sin\theta'_{p2} - l_psin(\theta'_{p1} - \theta'_{p2}))(l_p - d_2cos\theta'_{p1} - d_1sin\theta'_{p1} + l_pcos(\theta'_{p1} - \theta'_{p2})))/W_2^2))/(8W_2) + (Z_3(d_3^2m_{p7} + 4I_{p_5} + 4I_{p_7})((l_p(d_2sin\theta'_{p2} - d_1cos\theta'_{p2} + l_psin(\theta'_{p1} - \theta'_{p2})))/W_2 + (2l_p^2(d_1cos\theta'_{p2} + d_2sin\theta'_{p2} - l_psin(\theta'_{p1} - \theta'_{p2}))(l_p - d_2cos\theta'_{p2} - d_1sin\theta'_{p2} + l_pcos(\theta'_{p1} - \theta'_{p2})))/W_2^2))/(8W_2)) - \\
& \dot{\theta}'_{p1}((l_p^2m_{p2}sin(\theta'_{p1} - \theta'_{p2}))/2 + (l_p^2m_{p3}sin(\theta'_{p1} - \theta'_{p2}))/2 + l_p^2m_{p5}sin(\theta'_{p1} - \theta'_{p2}) + (Z_3(d_3^2m_{p7} + 4I_{p_5} + 4I_{p_7})((l_p^2sin(\theta'_{p1} - \theta'_{p2}))/W_2 - (2l_p^2(d_1cos\theta'_{p1} + d_2sin\theta'_{p1} + l_psin(\theta'_{p1} - \theta'_{p2}))(l_p - d_2cos\theta'_{p2} - d_1sin\theta'_{p2} + l_pcos(\theta'_{p1} - \theta'_{p2})))/W_2^2))/(4W_2) + (Z_4(d_3^2m_{p7} + 4I_{p_5} + 4I_{p_7})((l_p(d_1cos\theta'_{p1} - d_2sin\theta'_{p1} + l_psin(\theta'_{p1} - \theta'_{p2})))/W_2 - (2l_p^2(d_1cos\theta'_{p1} + d_2sin\theta'_{p1} + l_psin(\theta'_{p1} - \theta'_{p2}))(l_p - d_2cos\theta'_{p1} - d_1sin\theta'_{p1} + l_pcos(\theta'_{p1} - \theta'_{p2})))/W_2^2))/(4W_2) + (Z_3l_p^2(d_3^2m_{p7} + 4I_{p_5} + 4I_{p_7})(W_2sin(\theta'_{p1} - \theta'_{p2}) - l_p^2sin(2\theta'_{p1} - 2\theta'_{p2}) - 2l_p^2sin(\theta'_{p1} - \theta'_{p2}) + 2d_1l_pcos\theta'_{p2} + 2d_2l_psin\theta'_{p2} - 2d_1^2cos\theta'_{p2}sin\theta'_{p1} - 2d_2^2cos\theta'_{p1}sin\theta'_{p2} + 2d_1l_pcos\big(\theta'_{p1} - \theta'_{p2}\big)cos\theta'_{p2} + 2d_2l_psin\big(\theta'_{p1} - \theta'_{p2}\big)cos\theta'_{p1} + 2d_2l_pcos\big(\theta'_{p1} - \theta'_{p2}\big)sin\theta'_{p2} + 2d_1l_psin\big(\theta'_{p1} - \theta'_{p2}\big)sin\theta'_{p1} - 2d_1d_2cos\theta'_{p1}cos\theta'_{p2} - 2d_1d_2sin\theta'_{p1}sin\theta'_{p2}))/(4W_2^3)) - \dot{d}_1((((l_p^2sin(\theta'_{p1} - \theta'_{p2}))/W_2 + (2l_p^2(d_1cos\theta'_{p2} + d_2sin\theta'_{p2} - l_psin(\theta'_{p1} - \theta'_{p2}))(l_p - d_2cos\theta'_{p1} - d_1sin\theta'_{p1} + l_pcos(\theta'_{p1} - \theta'_{p2})))/W_2^2)(Z_6m_{p7}d_3^2 + 2W_1m_{p7}cos\phi'_pd_3 + 4I_5Z_6 + 4I_7Z_6))/(8W_1) + (l_p(d_3^2m_{p7} + 4I_{p_5} + 4I_{p_7})(2Z_3d_1l_p - 2Z_4d_1^2sin\theta'_{p1} - 2Z_3l_p^2sin\theta'_{p1} - 2Z_3l_p^2sin\theta'_{p2} -
\end{aligned} \tag{B.19}$$

$$2Z_4l_p^2sin\theta'_{p1} - 2Z_4l_p^2sin\theta'_{p2} - 2Z_3d_1^2sin\theta'_{p2} + 2Z_4d_1l_p + W_2Z_3sin\theta'_{p2} + W_2Z_4sin\theta'_{p1} - 2Z_3d_1d_2cos\theta'_{p2} - 2Z_4d_1d_2cos\theta'_{p1} - 2Z_3l_p^2cos(\theta'_{p1} - \theta'_{p2})sin\theta'_{p1} - 2Z_3l_p^2cos(\theta'_{p1} - \theta'_{p2})sin\theta'_{p2} - 2Z_4l_p^2cos(\theta'_{p1} - \theta'_{p2})sin\theta'_{p1} - 2Z_4l_p^2cos(\theta'_{p1} - \theta'_{p2})sin\theta'_{p2} + 2Z_3d_1l_pcos(\theta'_{p1} - \theta'_{p2}) + 2Z_4d_1l_pcos(\theta'_{p1} - \theta'_{p2}) + Z_3d_2l_psin(2\theta'_{p2}) + Z_4d_2l_psin(2\theta'_{p1}) + 2Z_3d_1l_psin^2\theta'_{p2} + 2Z_4d_1l_psin^2\theta'_{p1} + 2Z_3d_2l_pcos\theta'_{p2}sin\theta'_{p1} + 2Z_4d_2l_pcos\theta'_{p1}sin\theta'_{p2} + 2Z_3d_1l_psin\theta'_{p1}sin\theta'_{p2} + 2Z_4d_1l_psin\theta'_{p1}sin\theta'_{p2}))/4W_2^3 + (Z_3l_p(d_3^2m_{p7} + 4I_{p_5} + 4I_{p_7})(d_1^2sin\theta'_{p2} + 3d_2^2sin\theta'_{p2} + 2l_p^2sin\theta'_{p1} + l_p^2sin\theta'_{p2} - 2d_1l_p + l_p^2sin(2\theta'_{p1} - \theta'_{p2}) - 2d_1l_pcos(\theta'_{p1} - \theta'_{p2}) - 2d_2l_psin(\theta'_{p1} - \theta'_{p2}) + 2d_1d_2cos\theta'_{p2}))/(8W_2^3))$$

$$V_{p55} = -\dot{d}_1\ ((((l_p(d_2sin\theta'_{p2} - d_1cos\theta'_{p2} + l_psin(\theta'_{p1} - \theta'_{p2})2 + (2l_p^2(d_1cos\theta'_{p2} + d_2sin\theta'_{p2} - l_psin(\theta'_{p1} - \theta'_{p2}))(l_p - d_2cos\theta'_{p2} - d_1sin\theta'_{p2} + l_p\cos(\theta'_{p1} - \theta'_{p2})))/W_2^2)(Z_6m_{p7}d_3^2 + 2W_1m_{p7}cos\phi'_pd_3 + 4I_{p5}Z_6 + 4I_{p_7}Z_6))/(8W_1) + (Z_4l_p(m_{p7}d_3^2 + 4I_{p_5} + 4I_{p_7})(2d_1l_p - 2l_p^2sin\theta'_{p1} - 2l_p^2sin\theta'_{p2} - 2d_1^2sin\theta'_{p2} + W_2sin\theta'_{p2} - 2l_p^2\cos(\theta'_{p1} - \theta'_{p2})\,sin\theta'_{p1} - 2l_p^2\cos(\theta'_{p1} - \theta'_{p2})\,sin\theta'_{p2} + 2d_1l_pcos(\theta'_{p1} - \theta'_{p2}) + d_2l_psin(2\theta'_{p2}) + 2d_1l_psin^2\theta'_{p2} - 2d_1d_2cos\theta'_{p2} + 2d_2l_pcos\theta'_{p2}sin\theta'_{p1} + 2d_1l_psin\theta'_{p1}sin\theta'_{p2}))/(2W_2^3) + (Z_4l_p(m_{p7}d_3^2 + 4I_{p_5} + 4I_{p_7})(d_1^2sin\theta'_{p2} + 3d_2^2sin\theta'_{p2} + 2l_p^2sin\theta'_{p1} + l_p^2sin\theta'_{p2} - 2d_1l_p + l_p^2sin(2\theta'_{p1} - \theta'_{p2}) - 2d_1l_pcos(\theta'_{p1} - \theta'_{p2}) - 2d_2l_psin(\theta'_{p1} - \theta'_{p2}) + 2d_1d_2cos\theta'_{p2}))/(8W_2^3)) - \dot{\theta}'_{p1}((l_p^2m_{p2}sin(\theta'_{p1} - \theta'_{p2}))/4 + (l_p^2m_{p3}sin(\theta'_{p1} - \theta'_{p2}))/4 + (l_p^2m_{p5}sin(\theta'_{p1} - \theta'_{p2}))/2 + (Z_4(m_{p7}d_3^2 + 4I_{p_5} + 4I_{p_7})((l_p^2sin(\theta'_{p1} - \theta'_{p2}))/W_2 + (2l_p^2(d_1cos\theta'_{p2} + d_2sin\theta'_{p2} - l_psin(\theta'_{p1} - \theta'_{p2}))(l_p - d_2cos\theta'_{p1} - d_1sin\theta'_{p1} + l_pcos(\theta'_{p1} - \theta'_{p2})))/W_2^2))/(8W_2) + (Z_3(m_{p7}d_3^2 + 4I_{p_5} + 4I_{p_7})((l_p(d_2sin\theta'_{p2} - d_1cos\theta'_{p2} + l_psin(\theta'_{p1} - \theta'_{p2})))/W_2 + (2l_p^2(d_1cos\theta'_{p2} + d_2sin\theta'_{p2} - l_psin(\theta'_{p1} - \theta'_{p2}))(l_p - d_2cos\theta'_{p2} - d_1sin\theta'_{p2} + l_pcos(\theta'_{p1} - \theta'_{p2})))/W_2^2))/(8W_2) + (Z_4l_p^2(m_{p7}d_3^2 + 4I_{p_5} + 4I_{p_7})(W_2sin(\theta'_{p1} - \theta'_{p2}) - l_p^2sin(2\theta'_{p1} - \theta'_{p2}) - 2l_p^2sin(\theta'_{p1} - \theta'_{p2}) - 2d_1l_pcos\theta'_{p1} - 2d_2l_psin\theta'_{p1} + 2d_1^2cos\theta'_{p1}sin\theta'_{p2} + 2d_2^2cos\theta'_{p2}sin\theta'_{p1} - 2d_1l_pcos(\theta'_{p1} - \theta'_{p2})cos\theta'_{p1} - 2d_2l_pcos(\theta'_{p1} - \theta'_{p2})sin\theta'_{p1} + 2d_2l_psin(\theta'_{p1} - \theta'_{p2})cos\theta'_{p2} + 2d_1l_psin(\theta'_{p1} - \tag{B.20}$$

$$\theta'_{p2}\big)sin\theta'_{p2} + 2d_1d_2cos\theta'_{p1}cos\theta'_{p2} + 2d_1d_2sin\theta'_{p1}sin\theta'_{p2}))/(2W_2^3)) - \dot{\theta}'_{p2}(Z_4l_p(m_{p7}d_3^2 + 4I_{p_5} + 4I_{p_7})(2l_p^3sin(\theta'_{p1} - \theta'_{p2}) + l_p^3sin(2\theta'_{p1} - 2\theta'_{p2}) - W_2l_psin(\theta'_{p1} - \theta'_{p2}) - 2d_1l_p^2cos\theta'_{p2} - 2d_2l_p^2sin\theta'_{p1} - 2d_2l_p^2sin\theta'_{p2} - 2d_1l_p^2cos(\theta'_{p1} - \theta'_{p2}) + 2d_1d_2l_p + d_1^2l_psin(2\theta'_{p2}) + d_2^2l_psin(2\theta'_{p2}) + W_2d_1cos\theta'_{p2} - W_2d_2sin\theta'_{p2}))/(4W_2^3)$$

Appendix C

Motor Torque and Current Relation Experiment Quotes

At this point an important issue about control experiments must be highlighted. As it can be seen from the structures of the control design presented in this chapter all control inputs are designed as torque inputs. However, in the prototype systems current controller motors were used. As a result of this, the relationship between the current and torque was required. This requirement was provided with an experimental data based method. This process is tried to be explained in this chapter.

The data were collected after the motor and torque sensor were fixed as in the Figure (C.1) and (C.2). A linearization was made according to the input and output values of each motors. According to these equations, the characteristic equation of each motors were achieved. These equations are given in the Table C.1.

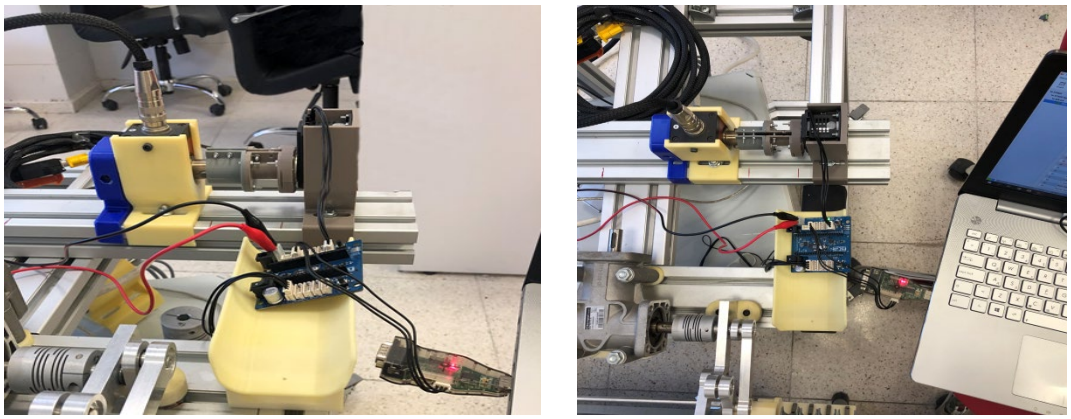

(a) (b)

Figure C.1: Two different view, (A) Front view, (B) Top view.

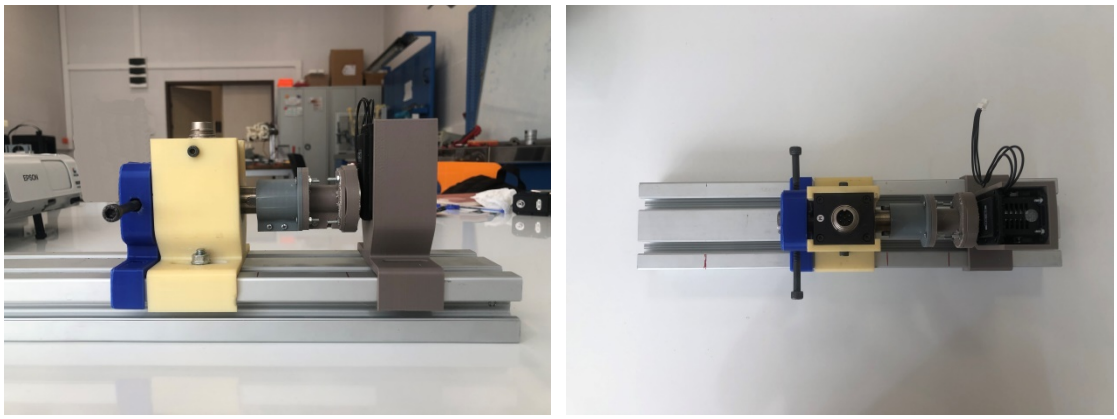

(a) (b)

Figure C.2: Two different view, (A) Front View, (B) Top view.

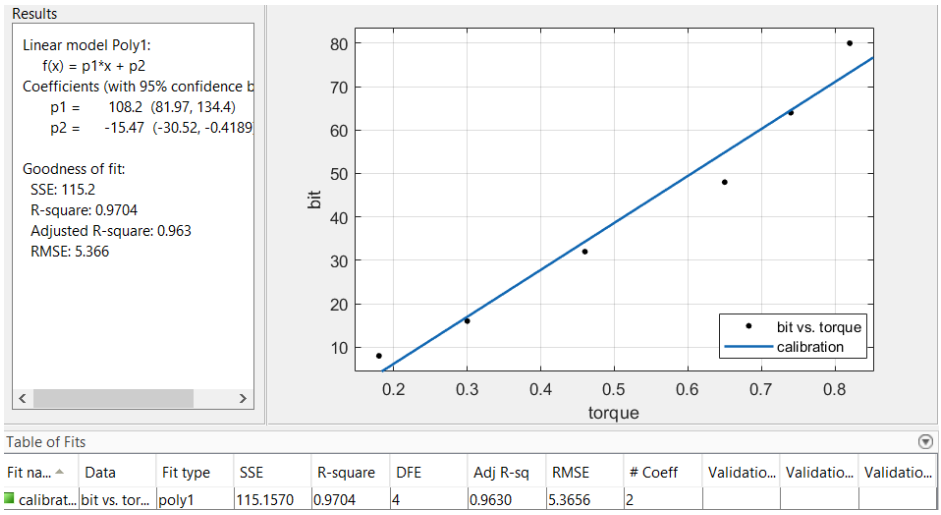

Figure C. 3: Curve fitting for motor calibration

Table C.1: Calibration table showing the linearization of each motor

MX-64	
ID1	$y = 108.2 \times x - 15.47$
ID2	$y = 122.3 \times x - 23.7$
ID3	$y = 122.3 \times x - 23.7$
ID4	$y = 111.9 \times x - 16.8$
ID5	$y = 94.68 \times x - 14.37$
ID6	$y = 116.7 \times x - 25.7$
XM-540	
ID1	$y = 97.2 \times x - 0.567$

Appendix D

Defining the Control Purpose of x_p in Terms of x_N

If the desired trajectory of newly defined state is selected as

$$x_{N_d} = A(\dot{x}_{p_d} - K_p e_p) \tag{D.1}$$

and $x_N \rightarrow x_{N_d}$ condition is satisfied, (3.74) can be rearranged as

$$A\dot{e}_p = -AK_p e_p. \tag{D.2}$$

At this point it should be noted that in the above equations, $e_p \in \mathbb{R}^6$ is a tracking error defined as

$$e_p \triangleq x_{p_d} - x_p \tag{D.3}$$

and $K_p \in \mathbb{R}^{6\times 6}$ denotes positive definite, constant, diagonal gain matrix. If the both sides of the resulting equation is premultiplied with $(A^T A)^{-1}A^T$ it can be reaaranged as

$$\dot{e}_p + K_p e_p = 0 \tag{D.4}$$

and this result mathematically proves that $e_p \rightarrow 0$ exponentially fast. From this result it can be reached that the main control purpose can be reached as long as $x_N \rightarrow x_{N_d}$ condition is satisfied for the selection given above.

Appendix E

Publications from the Thesis

Conference Papers

1. Karayaman G, Gezgin E, Çetin L, Bıdıklı B, Cerrahi Mikrorobot Operasyonlarında Yardımcı Sistem Olarak Kullanılan Çift Robot Kollu Sistem için Lyapunov Tabanlı Görev Uzayı Denetimi Tasarımı ,TOK 2021

Projects

1. Project Fellow in The Scientific and Technological Research Council of Turkey with Project No: 218E055

Curriculum Vitae

Name Surname : Goncagül Karayaman

Education:

2014–2019 İzmir Kâtip Çelebi University, Dept. of Mechatronics Eng.

2020–2022 İzmir Kâtip Çelebi University, Dept. of Robotic Eng.

Publications :

1. Karayaman G., Gezgin E., Çetin L., Bıdıklı B., Cerrahi Mikrorobot Operasyonlarında Yardımcı Sistem Olarak Kullanılan Çift Robot Kollu Sistem için Lyapunov Tabanlı Görev Uzayı Denetimi Tasarımı,TOK 2021

Projects

1. Project Fellow in The Scientific and Technological Research Council of Turkey with Project No: 218E055